Research Square

Preprints are preliminary reports that have not undergone peer review.
They should not be considered conclusive, used to inform clinical practice,
or referenced by the media as validated information.

Henry Gas Solubility Optimization Algorithm: A Systematic Review of Its Variants and Applications

François Xavier Rugema

silisaveri@yahoo.fr

University of Rwanda

Sylvère Mugemanyi

silisaveri1@yahoo.fr

Rwanda Polytechnic, Tumba College

Félicité Pacifique Mutuyimana

Département des Sciences Fondamentales, Université du Québec à Chicoutimi, Québec, QC G7H 2B1, Canada

Emmanuel Mutabazi

Hohai University

Providence Habumuremyi

Fuzhou University

Christophe Bananeza

Hohai University

Clarisse Kagaju

Rwanda Polytechnic, Tumba College

Jennifer Batamuliza

University of Rwanda

Systematic Review

Keywords: Henry gas solubility optimization, Swarm intelligence, Metaheuristic algorithm, Nature-inspired algorithm, Optimization, Hybridization, Variant, Exploration, Exploitation

Posted Date: March 3rd, 2026

DOI: https://doi.org/10.21203/rs.3.rs-9010618/v1

License: This work is licensed under a Creative Commons Attribution 4.0 International License.
Read Full License

Additional Declarations: The authors declare no competing interests.

Henry Gas Solubility Optimization Algorithm: A Systematic Review of Its Variants and Applications

François Xavier Rugema [1], Sylvère Mugemanyi [2], Félicité Pacifique Mutuyimana [3,4,5], Emmanuel Mutabazi [6], Providence Habumuremyi [7], Christophe Bananeza [8], Clarisse Kagaju [2], Jennifer Batamuliza [1]

✉ Sylvère Mugemanyi
silisaveri1@yahoo.fr
François Xavier Rugema
silisaveri@yahoo.fr
Félicité Pacifique Mutuyimana
pacimus@gmail.com
Emmanuel Mutabazi
mutabemma@hhu.edu.cn
Providence Habumuremyi
providenceha@gmail.com
Christophe Bananeza
bananezac@gmail.com
Clarisse Kagaju
kgjclarisse@yahoo.fr
Jennifer Batamuliza
bajelo2000@yahoo.co.uk

[1] Department of Business Information Technology, College of Business and Economics, University of Rwanda, P.O. Box 4285 Kigali, Rwanda
[2] Department of Electronics and Telecommunication Technology, Rwanda Polytechnic, Tumba College, P.O. Box 6638 Rulindo, Rwanda
[3] Département des Sciences Fondamentales, Université du Québec à Chicoutimi, Québec, QC G7H 2B1, Canada
[4] Department of Mathematics, Sciences and Physical Education, College of Education, University of Rwanda, P.O. Box 55 Rwamagana, Rwanda
[5] The African Centre of Excellence for Innovative Teaching and Learning Mathematics and Science (ACEITLMS), College of Education, University of Rwanda, P.O. Box 55 Rwamagana, Rwanda
[6] College of IoT Engineering, Hohai University, Changzhou 310000, China
[7] College of Civil Engineering, Fuzhou University, Fuzhou 350116, Fujian, China

[8] School of Energy and Electrical Engineering, Hohai University, Nanjing 210098, China

Abstract

Henry Gas Solubility Optimizer (HGSO) is a new metaheuristic algorithm which has attracted many researchers due to its supremacy, outstanding results, and its best convergence when applied to several real-world optimization applications. Thanks to much interest from researchers, several variants of HGSO have been proposed and applied in tackling numerous optimization areas in diverse domains. Consequently, this work intends to provide a comprehensive review and analysis of various studies reported in literature concerning HGSO variants. Different applications of HGSO variants are also reviewed. Our methodology is based on identifying and selecting 118 HGSO-related papers from various recognized journals. The HGSO algorithm was examined, and its merits and drawbacks were analyzed. In this study, the performance of the HGSO and its variants has been tested on the benchmark test functions regards to various assessment criteria including convergence behavior, Friedman test, mean absolute error (MAE) test, overall effectiveness test, performance index (PI) analysis and execution time analysis. According to the results, the HHO-HGSO exhibits better convergence behaviors in most of the cases for the dimensions 10, 30, 50 and 100. The Friedman test results show that the HHO-HGSO records the first rank in 30, 50 and 100 dimensions, whilst the MVQIHGSO gets the first rank in 10 dimension. Likewise, the HHO-HGSO attains better MAE test results in 30, 50 and 100 dimensions, whereas the MVQIHGSO surpasses its counterparts in 10 dimension for MAE test results. The comparison demonstrate that the HHO-HGSO accomplishes an overall effectiveness of 71.552% which is the best amidst the HGSO variants. The HHO-HGSO also achieves better PI values in most of the cases. Besides, the simulation results reveals that based on the computational time, the QHGSO is the most rapid algorithm in terms of tackling all the benchmark test functions. Lastly, some future works for the HGSO variants are recommended.

Keywords: Henry gas solubility optimization; Swarm intelligence; Metaheuristic algorithm; Nature-inspired algorithm; Optimization; Hybridization; Variant; Exploration; Exploitation.

1. Introduction

Real-world problems are categorized into static or dynamic, linear or nonlinear, continuous or discrete, constrained or unconstrained, single objective or multi-objective optimization problems [1]. There are many optimization-based strategies used to tackle real world problems. Conventional strategies including gradient descent and Newton's method have difficulties in handling complex optimization problems due to rigorous conditions on search space as well as mediocre searching performance [2]. The metaheuristic algorithms have been developed to alleviate the shortcomings of classical methods [3].

Literature found in [4, 5] provide diverse criteria which are used to classifying metaheuristic algorithms. Amidst these criteria, the mostly utilized is the number of candidate solutions performed per each iteration. Accordingly, the categorization of the metaheuristics falls into two types [6, 7]: population-based (such as genetic algorithm (GA) [8], particle swarm optimization (PSO) [9, 10], cuckoo search algorithm (CSA) [11]) and single solution based (including tabu search (TS) [12], variable neighborhood search (VNS) [13], simulated annealing (SA) [14], vortex search algorithm (VSA) [15]). The optimal or suboptimal solution in population-based algorithms corresponds to the optimum or is located in the neighborhood of the optimum [4]. Only one solution is proceeded by the single solution based algorithm during the optimization process. On the other hand, many solutions are handled by the population-based algorithm over the whole optimization process [4].

The population based metaheuristic algorithms known as P-metaheuristics mimic the natural phenomena and comprise four types [6, 16, 17]: swarm intelligence (SI) algorithms, physics-based, human-based and evolutionary algorithms (EAs). According to references [17-19], EAs emulate the features of biological evolution, namely mutation, recombination as well as selection. Certain examples of EA are GA which emulates the theory of evolution established by Darwin [8], biogeography-based optimization (BBO) algorithm [20], evolutionary strategy (ES) [21], differential evolution (DE) [22] and evolutionary programming (EP) [23].

Based on the works in [16, 17, 24, 25], physics-based algorithms simulate the physical laws. The widely known amidst them are electromagnetism like algorithm (ELA) [26], lightning attachment procedure optimization (LAPO) [16], gravitational search algorithm (GSA) [27], charged system search (CSS) [28] and central force optimization (CFO) [29]. The third class of P-metaheuristics simulate the behaviors of the human beings. Some examples of human-based algorithms are human mental search [17, 30], imperialist competitive algorithm (ICA) [31], teaching-learning based optimization (TLBO) [32], sewing training-based optimization (STBO) [33]. The fourth class of P-metaheuristic algorithms includes the algorithms which are imitating the social conducts of organisms living in herds, flocks, swarms, or shoals [34]. A few examples of them are bat algorithm [35], PSO [9], grey wolf optimizer (GWO) [36], artificial bee colony (ABC) [37], crow search algorithm [38] and ant colony optimization (ACO) [39], etc.

Every metaheuristic algorithm consists of two major phases, namely diversification (exploration) and intensification (exploitation) [6]. During the diversification phase, diverse solutions are yielded by the algorithm so as to widely explore the searching space. On the other hand, the focus of the algorithm in the intensification phase is to perform the local region searching and make certain that the best obtained solution belongs to that particular region. A suitable balance among diversification and intensification is indispensable for the algorithm to circumvent the global optima or local optima entrapments [40, 41]. According to [42], the population-based algorithms

are predominantly diversification oriented whilst the single-solution based algorithms are predominantly intensification oriented.

HGSO is a novel metaheuristic algorithm introduced in 2019 [43], which is inspired by the Henry's gas law. HGSO has been efficiently applied to different kinds of problems in various fields of research.

The objective of this work review is to provide a comprehensive review of the HGSO, its variants, its modifications and their applications in different areas of research. Furthermore, the performance assessment was performed to compare the HGSO variants. At the end, future research directions for the HGSO are suggested.

The major contributions of this review study which makes it different from the previous HGSO surveys [176-178] are to:

- Present the HGSO algorithm in detail
- Present a complete review of the HGSO variants
- Present the current applications of the HGSO variants
- Provide the effectiveness assessment and comparison of the HGSO variants on 29 benchmark functions from CEC 2018
- Provide the statistical analysis in an effort to validate and compare the HGSO along with its variants
- Discuss and suggest future directions of the HGSO variants

Different HGSO-related articles presented in this review work have been sought from various well reputed publishers including Elsevier, Springer, IEEE Xplore, Wiley, Sage, Taylor&Francis, MDPI, etc; and they have been published from 2019 up to May 2025. In fact, the selection of these HGSO-related papers is based on the methodology presented in [44-47]. We have collected 118 HGSO-related papers from various search engines including Google Scholars, Research Gate, Semantic Scholar, etc, by utilizing the keyword "Henry gas solubility optimization algorithm". Among those 118 articles, 108 articles have been published in journals and 10 articles have been published in conferences.

The distribution of the HGSO-based articles according to their respective publishers is shown in Fig. 1. From Fig. 1, the highest numbers of articles (i.e., 31 articles) are published from Elsevier (26%), followed by 25 articles from Springer (24%), etc. Furthermore, the annual distribution of the HGSO-based articles is tabulated in Table 1. According to Table 1, there is a trend of annual

rising for the HGSO-related articles which shows the increasing of its popularity between 2019 and 2023, and a smooth decline from 2024 up to now.

This review study is structured as: In Section 2, a detailed presentation of the HGSO is given. In Section 3, a thorough presentation of the HGSO variants, namely hybridizations, modifications, quantum, chaotic and multi-objective variants of the HGSO are provided. Different applications of the HGSO are illustrated in Section 4. Section 5 gives discussions along with critical analysis of HGSO variants. Ultimately, the conclusion as well as future research trends of the study are drawn in Section 6.

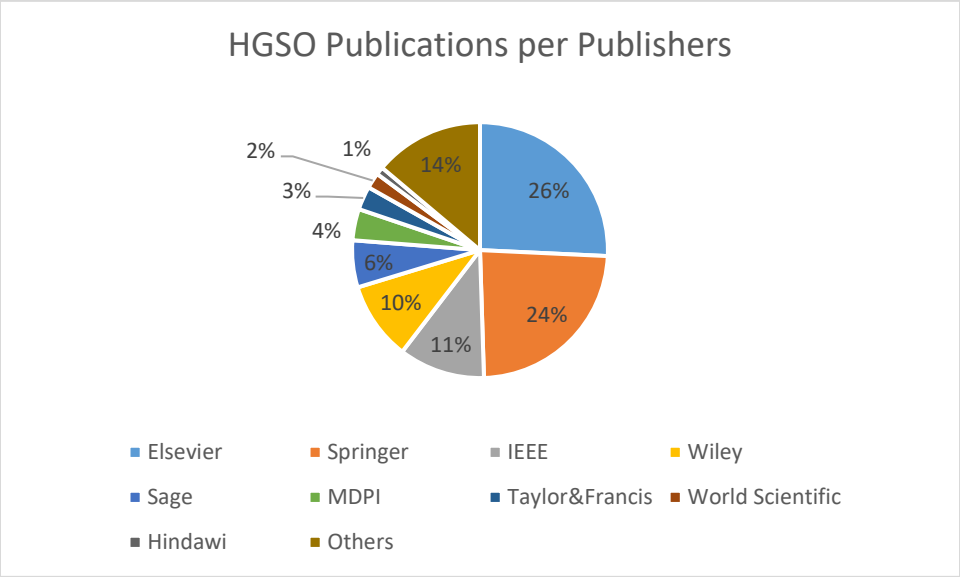


Fig. 1 The distribution of the HGSO-related articles according to the publishers.

Table 1
The annual distribution of the HGSO-based articles

No.	Publisher	Number of HGSO-related articles according to the publisher	Annual number of HGSO-related articles						
			2019	2020	2021	2022	2023	2024	2025
1	Elsevier	31	1	3	5	11	9	2	0
2	Springer	28	0	1	7	12	5	3	0
3	IEEE	13	0	4	0	4	4	1	0
4	Wiley	12	0	0	1	3	5	2	1
5	Sage	7	0	0	0	1	6	0	0

6	MDPI	5	0	0	0	1	3	1	0
7	Taylor&Francis	3	0	0	0	0	3	0	0
8	World Scientific	2	0	0	0	0	1	1	0
9	Hindawi	1	0	0	0	1	0	0	0
10	Others	16	0	2	4	5	4	1	0
Total		118	1	10	17	38	40	11	1

2. Henry Gas Optimization Algorithm

Developed by Hashim in 2019 [43], the HGSO is a new metaheuristic algorithm that has attracted many researchers in recent years.

The HGSO takes inspiration from Henry's gas law, proposed by William Henry in 1803 [43, 48]. The fundamental concept of Henry's law for gas solubility is expressed as [48]: "At a constant temperature, the amount of a given gas that dissolves in a given type and volume of liquid is directly proportional to the partial pressure of that gas in equilibrium with that liquid". Consequently, the reliance of Henry's law on temperature is eminent and advocates/recommends that there is a direct proportion between the solubility of a gas (S_g) and the partial pressure of the gas (P_g) as described through Eq. (1) [49]:

$$S_g = H \times P_g \tag{1}$$

Here S_g, H and P_g are the gas solubility, Henry's constant and gas partial pressure, respectively. Moreover, the reliance of Henry's law on temperature should be considered. Henry's law constant varies with the change of temperature, which may be expressed with the help of the Van't Hoff formula given in Eq. (2) below [43]:

$$\frac{d \ln H}{d(1/T)} = \frac{-\nabla_{sol} E}{R} \tag{2}$$

Where $\nabla_{sol} E$ and R indicate the enthalpy of dissolution and the gas constant, respectively. A and B stands for two factors parameters showing that T varies when H varies. Consequently, the Eq. (1) may be reformulated as Eq. (3) [43]:

$$H(T) = \exp(B/T) \times A \tag{3}$$

Where H is proportional to two coefficients A and B, which show that T will change with the change of H. The following equation describes the relationship between H and the reference temperature ($T^{\theta} = 298.15K$) as in Eq. (4) [49]:

$$H(T) = H^{\theta} \times \exp\left(\frac{-\nabla_{sol} E}{R}\left(1/T - 1/T^{\theta}\right)\right) \tag{4}$$

The validity of Van't Hoff formula is confirmed in case $\nabla_{sol} E$ is a constant, consequently, Eq. (4) may be simplified as Eq. (5) [43]:

$$H(T) = \exp\left(-C \times \left(1/T - 1/T^{\theta}\right)\right) \times H^{\theta} \tag{5}$$

In accordance with the Henry's law of gas solubility, HGSO algorithm may be expressed through eight mathematical steps presented below [50-52]:

2.1. Initialization

The initialization of the number of gases (population size N) along with the locations of gases is described as in Eq. (6):

$$X_i(t+1) = X_{\min} + r \times \left(X_{\max} - X_{\min}\right) \tag{6}$$

Here X_i denotes the initial position for the i^{th} gas within population N, r is the random number within the range [0,1], $X_{\min}$ and $X_{\max}$ signify the lower and upper limits of the problem, and t indicates the iteration time. i, H_j, $P_{i,j}$ and $\nabla_{sol} E/R$ denote the number of gas, the Henry's constant for the cluster j, the partial pressure of gas i within cluster j, and a constant value for each gas particle in the interior of j^{th} cluster, respectively. The initial values of the latter parameters are expressed by Eq. (7):

$$H_j(t) = l_1 \times rand(0,1), P_{i,j} = l_2 \times rand(0,1), C_j = l_3 \times rand(0,1) \tag{7}$$

Here, l_1, l_2, l_3 denote the constants whose values are equal to $5 \times 10^{-2}, 100, 1 \times 10^{-2}$, respectively .

2.2. Clustering

The population of gas particles is grouped into identical clusters approximating to the number of gas types. Every cluster groups the particles of gas with the same properties and hence possesses the identical Henry's constant value (H_j).

2.3. Evaluation

The gas particles in each cluster *j* are evaluated in order to find out the best gas particles that reach the optimal equilibrium state compared with others within its type. On the contrary, the ranking of all the gas is performed to determine the best gas particle within the entire population.

2.4. Update Henry's coefficient

The update of Henry's constant is based on the following Eq. (8):

$$H_j(t+1) = H_j(t) \times \exp\left(-C_j \times \left(\frac{1}{T(t)} - \frac{1}{T^{\theta}}\right)\right), T(t) = (-t/iter) \tag{8}$$

Here H_j, T, T^{θ} and $iter$ are the Henry's coefficient for every cluster j, the temperature, a constant equals to 298.15 as well as the total number of iterations, respectively.

2.5. Update gas solubility

The updating formula of solubility can be expressed by Eq. (9):

$$S_{i,j}(t) = K \times H_j(t+1) \times P_{i,j}(t) \tag{9}$$

Where $S_{i,j}$, K and $P_{i,j}$ denote the solubility of gas i within cluster j, a constant and the partial pressure on gas i within cluster j, respectively.

2.6. Update position

Updating the gas position is performed by using the below Eq. (10):

$$X_{i,j}(t+1) = X_{i,j}(t) + F \times r \times \gamma \times \left(X_{i,best}(t) - X_{i,j}(t)\right) + F \times r \times \alpha \times \left(S_{i,j}(t) \times X_{best}(t) - X_{i,j}(t)\right)$$
$$\gamma = \beta \times \exp\left(-\frac{F_{best}(t) + \varepsilon}{F_{i,j}(t) + \varepsilon}\right), \varepsilon = 0.05 \tag{10}$$

Where the location of gas i within cluster j is represented by $X_{(i,j)}$, t signifies the iteration time and r denotes a random constant. $X_{i,best}(t)$ is the best gas in i in cluster j, while X_{best} represents the best gas in the whole population. Furthermore, γ denotes the ability of gas j within cluster i which interacts with the gases within its cluster, α represents the other gases' effects on gas i within cluster j and its value is 1, and β denotes a constant. $F_{(i,j)}$ indicates the gas fitness i within cluster

j, on the contrary F_{best} represents the best gas fitness in the whole swarm. F signifies the flag whose searching direction varies to offer diversity $= \pm$. $X_{(i,best)}$ along with X_{best} denote the two factors that help to find within the searching space an appropriate balance between the exploration and exploitation phases. Explicitly, $X_{(i,best)}$ denotes the best gas i within cluster j, and X_{best} represents the best gas in the entire population.

2.7. Escape from local optimum

The local optimum is avoided at this stage. Categorize and determine the number of worst agents (N_w) employing the Eq. (11) as:

$$N_w = N \times \left(rand(c_2 - c_1) + c_1\right), c_1 = 0.1 \text{ and } c_2 = 0.2 \tag{11}$$

Here N denotes the number of search agents.

2.8. Update the position of the worst agents

$$G_{(i,j)} = G_{\min(i,j)} + r \times \left(G_{\max(i,j)} - G_{\min(i,j)}\right) \tag{12}$$

Where $G_{(i,j)}$ represents the position of gas i in cluster j, r denotes a random number, $G_{\min}$ and $G_{\max}$ represent the lower and upper limit of the problem, respectively.

The summary of the pseudocode for HGSO algorithm [43] is given as:

Algorithm 1 Pseudo-code of HGSO algorithm

1: Initialization: $X_i(i = 1,2,...,N)$, number of gas types $i, H_j, P_{i,j}, C_j, l_1, l_2$ and l_3.

2: Split up the population agents into cluster (number of gas types) having identical Henry's constant value (H_j)

3: Evaluate every cluster *j*

4: Obtain the best gas $X_{i,best}$ in every cluster, and the best searching agent X_{best}

5: while $t \prec$ maximum number of iterations do

6: for every searching agent do

7: Update the positions for all the searching agents utilizing Eq. (10)

8: end for

9: Update the Henry's coefficient for every gas type employing Eq. (8)

10: Update the solubility for every gas utilizing Eq. (9)

11: Perform the ranking as well as selection of the worst agents number through Eq. (11)

12: Update the position for the worst agents via Eq. (12)

13: Update the best gas $X_{i,best}$, and the best searching agent X_{best}

14: end while

15: $t = t + 1$

16: return X_{best}

3.Variants of HGSO

In July 2019, the classical HGSO algorithm has been published for the first time in [43], and from that time onwards, various variants of HGSO have been presented and applied to diverse optimization problems. The HGSO variants are categorized as binary, hybridizations, modifications, quantum, chaotic and multi-objective versions of the HGSO. Tables 2, 3, 4, 5 and 6 depict various HGSO variants with their respective names. Moreover, a variety of the methods introduced into the classical HGSO, fields of applications, datasets along with benchmark functions employed to examine the HGSO, performance metrics utilized to evaluate them, improvement made on these variants, and the article references, have been presented in these tables. Fig. 2 illustrates the distribution percentages of the HGSO variants. Based on Fig.2, the

highest percentage (51%) belongs to hybridizations of HGSO succeeded by the modifications of HGSO with 23%. The subsequent subsections describe the HGSO variants.

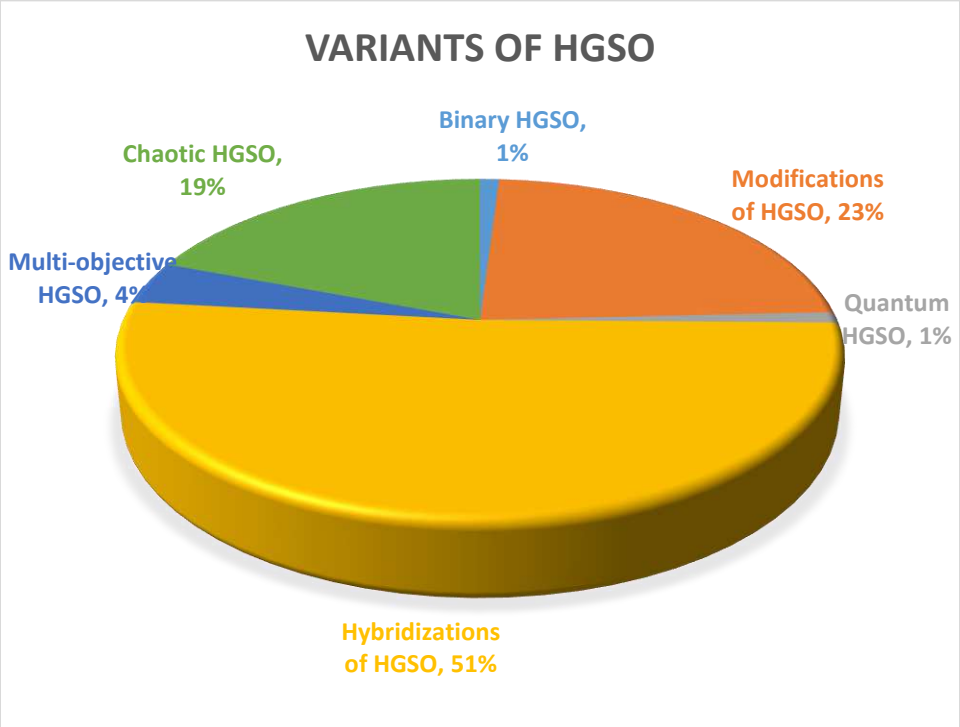


Fig. 2 Distribution percentages of HGSO variants.

3.1. Binary HGSO

In [53], a binary exponential HGSO (bEHGSO) algorithm has been presented for feature selection. Firstly, the data transformation approach based on fast independent component analysis techniques and weighted principal component analysis was employed to transform the original datasets. Subsequently, the proposed bEHGSO incorporated with KNN classifier was used to select the optimal subset of features from the transformed datasets. The effectiveness of the proposed bEHGSO was evaluated on 26 benchmark functions from CEC'17 test suite and 7 datasets from

UCI (University of Carfornia, Irvine). The experimental outcomes showed that the bEHGSO surpassed other compared methods. Table 2 summarizes the features of the bEHGSO.

3.2. Modifications of HGSO algorithm

Table 3 tabulates a variety of variants achieved by performing diverse modifications on the classical HGSO. Their details are presented as follows:

To address the problem of DNA (deoxyribonucleic acid) motif discovery (MD), the study in [54] proposed an approach known as MHGSO which introduced the motif samples into the HGSO. To confirm the proposed MHGSO, six real datasets along with five synthetic datasets have been examined according to diverse evaluation measurements. Furthermore, the MHGSO has been compared with other metaheuristics comprising DREME, MEME, XXmotif, MACS, and PMbPSO. The simulation results demonstrated the outstanding robustness of the MHGSO over other compared algorithms regards to global search ability while dealing with DNA MD problem.

In [55], the authors proposed a HHGSO (hybrid HGSO) algorithm to tackle the fuel consumption vehicle routing problem (FCVRP). In the proposed HHGSO, the neighborhood exchange approach has been utilized to enhance the algorithm performance. To confirm the HHGSO, two data instances having 12 and 22 nodes, respectively, have been investigated by considering the KPL (Kilometers per liter), REP (relative error percentage), fuel consumption and computation time indicator measurements. The simulation results confirmed that the HHGSO yielded better results than HPSO (hybrid PSO), simulated anneal (SA) and tabu search (TS) algorithms in dealing with the FCVRP.

To address the automatic image segmentation problem, the work in [56] presented a novel variant of the HGSO known as RHGSO-FC. Firstly, the randomly generated number has been employed to update the position equation in the conventional HGSO and thereby harmonizes the exploration and exploitation phases. Then, the fuzzy clustering (FC) has been accomplished by the RGHSO-FC on various RGB-D (red, green, blue-depth) features to get the optimal clusters. At last, a segmentation by aggregating super-pixels approach is performed on the optimal clusters to produce final segmented images. The effectiveness of the presented RHGSO-FC approach has been examined on both 47 benchmark functions and NYU-Depth V2 dataset. The performance metrics considered in this work are GCE (Global Consistency Error), PRI (Probability Rand Index), VOI (Variation of Information), SC (Structural Content), NAE (Normalized Absolute Error), SSIM (Structural Similarity Index), MSE (Mean Square Error), AD (Average Difference), PSNR (Peak Signal to Noise Ratio) and MD (Maximum Difference). The experimental results revealed that the RHGSO-FC approach outperforms the CKGSA-FC, HGSO-FC, K-means, J-Segmentation and FCM in offering the best segmentation quality.

The Taylor series have been integrated into the HGSO in [57] to constitute an algorithm named as Taylor HGSO. The developed algorithm was employed to train the Deep Maxout network for detecting the epilepsy seizure through Electroencephalogram (EEG) signal. The effectiveness of the Taylor HGSO-based Deep Maxout network was examined on two datasets, namely TUEP EEG Epilepsy Corpus dataset as well as CHB-MIT Scalp EEG dataset taking into account sensitivity, specificity and accuracy measurements. The experimental results revealed that the Taylor HGSO-based Deep Maxout network was effective in discovering the epilepsy seizures using EEG.

The authors in [58] incorporated the Brown motion operator and Lévy flight operator into the HGSO to tackle the global optimization along with engineering design problems. To confirm the proposed BL-HGSO algorithm, 20 benchmark test functions from IEEE CEC2005 and 20 benchmark test functions from IEEE CEC2017 were employed for global optimization. Furthermore, the pressure vessel design problem and tension/compression spring design problem were examined for the engineering design problems. The simulation results approved the superiority of the proposed BL-HGSO over WOA (whale optimization algorithm), WCA (water cycle algorithm), SCA (sine and cosine algorithm) and LSA (lightning search algorithm) in terms of offering better solutions on the considered problems.

In order to address the problem of identifying the plant leaf diseases, the authors in [59] proposed a mutation-based HGSO algorithm to optimally tune the hyper-parameters of the DenseNet-121 architecture and thereby diminishing the error rate as well as computational complexity of the convolution neural networks (CNN). The effectiveness of the presented MHGSO optimized DenseNet-121 architecture was examined on the PlantVillage and field datasets considering different evaluation measurements. The simulation results confirmed the supremacy of the proposed models over other compared models.

In [60], the fractional calculus (FC) concept was embedded into the HGSO algorithm to train the deep convolution neural networks (DCNN) classifier for electronic waste (E-waste) management. The proposed FHGSO-DCNN model was tested on Gofile dataset and compared with other models. The performance measures taken into account in this work were accuracy, sensitivity, specificity, energy, delay and ROC (Receiving Operating Characteristics). The obtained results from simulations demonstrated the supremacy of the proposed FHGSO-DCNN model over other compared models.

To boost the performance of a 5G-enabled AVS (autonomous vehicle system), a technique combining the CNN and oppositional-based HGSO (CNN-OHGSO) was developed in [61]. The developed CNN-OHGSO integrated the CNN along with opposition-based learning (OBL) strategy into the HGSO. The main task performed by the CNN-OHGSO was to guarantee the safety along with optimal distance variation by diminishing the distance variations within the automated vehicles. The effectiveness of the CNN-OHGSO was evaluated on an AVS considering three performance metrics such as Frechet inception distance (FID), accuracy and remorse function. The results obtained through the simulation affirmed the outperformance of the CNN-OHGSO over the NDRL (new deep reinforcement learning) and NDRL-LSTM-GNN (new deep

reinforcement learning-based long short-term memory with generative adversarial network) techniques.

To regulate the DC (direct current) motor speed, the authors in [62] proposed an OBL-HGSO algorithm which incorporated the OBL strategy into the HGSO. The developed OBL-HGSO was employed to find the optimal gain parameters of a PID (proportional-integral-derivative) controller that controlled the speed of a DC motor. The objective function studied was the minimization of the integral of time multiplied absolute error (ITAE). The performance of the OBL-HGSO-PID was compared with that of other methods such as HGSO-PID, SFS-PID, ACO-PID, SCA-PID and GWO-PID. The experimental results affirmed the supremacy of the OBL-HGSO-PID in accomplishing the best gain parameters of the PID controller utilized to regulate the speed of the DC motor.

Table 2
HGSO variants (binary HGSO)

Name	Incorporated method	Application	Datasets/Benchmark functions	Evaluation metrics	Improvement	References
bEGHSO	Exponential function	Global optimization, Feature selection	26 benchmark functions from CEC'17 test suite, 7 datasets from UCI	Std (standard deviation), average (avg) fitness value Computational time, accuracy, mean number of selected features	Premature convergence reduced, population diversity enhanced	[53]

Table 3
HGSO variants (modifications of HGSO)

Name	Incorporated method	Application	Datasets/Benchmark functions	Evaluation metrics	Improvement	References
MHGSO	Motif samples	Bioinformatics	Six real datasets (CREB, SRF, TBP, SP1, USF and CAAT) Five synthetic datasets	Nucleotide-level correlation coefficient, nucleotide-level positive predictive value, nucleotide-level sensitivity, motif correlation coefficient, precision, recall, F-score, statistical validation, Cohen's Kappa	Execution time shortened, local optima prevented	[54]
HHGSO	Neighborhood exchange approach	Fuel consumption vehicle routing problem	Two data instances having 12 and 22 nodes	KPL, REP, fuel consumption, computation time	Solution quality enhanced	[55]

RHGSO	Randomly generated number	Image processing	47 benchmark functions, NYU-Depth V2 dataset	Mean, std, PRI, GCE, VOI, SC, NAE, SSIM, MSE, AD, PSNR, MD	Global convergence attained, Solution precision enhanced, Local optima escaped, Exploration and exploitation phases harmonized	[56]
Taylor HGSO	Taylor series	Medical	TUEP EEG Epilepsy Corpus dataset, CHB-MIT Scalp EEG dataset	Accuracy, sensitivity, specificity	Local optimal avoided, Global optimal solutions accomplished	[57]
BL-HGSO	Lévy flight operator, Brown motion operator	Global optimization, Engineering design problems	20 Benchmark test functions from IEEE CEC2005, 20 Benchmark test functions from IEEE CEC2017, Pressure vessel design problem, tension/compression spring design problem	Best, avg, std,	Local and global search abilities boosted, local optima prevented, exploration and exploitation phases harmonized, convergence rate speeded up	[58]
MHGSO	Mutation strategy	Agriculture	Plant Village dataset, field dataset	Accuracy, recall, confusion matrix, ROC curve, F1-Score	Global optimal solutions obtained, population diversity enhanced	[59]

FHGSO	FC concept	E-waste management	Gofile dataset	Accuracy, Sensitivity, Specificity, Energy, Delay, ROC	Convergence speed improved, optimal algorithm performance ameliorated	[60]
OHGSO	OBL strategy	Autonomous vehicle system optimization	Autonomous vehicle system	Accuracy, FID, Remorse function	Initial population Ameliorated, exploration phase enhanced	[61]
OBL-HGSO	OBL strategy	DC motor speed control employing PID controller	ITAE objective function, W objective function	Best, avg, worst, std,	Initial population quality enhanced, exploration phase ameliorated, convergence speed improved	[62]
OHGSA	OBL strategy	WSN	Network simulator platform with 400 sensor nodes	Detection rate, accuracy, false alarm rate, network lifetime, throughput, packet delivery ratio	Initial population quality ameliorated, convergence speed increased, local optima avoided, exploration phase improved	[63]
HHGSO	OBL strategy	Power LED driver system design	LED chip packaging along with LED luminaire having thermal aging loading	SPD error norm, CCT, Lumen maintenance, XY[a]	Quality of the initial population ameliorated, exploration and exploitation phases harmonized, convergence speed boosted local optima prevented	[64]

EHGSO	EWMA	Intrusion detection	KDD dataset	Energy, Throughput, Recall, Precision	Local optima prevented, exploration and exploitation phases harmonized	[65]
SFS-HGSO	Three stochastic fractal mechanisms based on Lévy flight, Gaussian walk and Brown movement	Feature selection, engineering optimization	20 standard benchmarks from UCI dataset		Local searching ability ameliorated, convergence speed increased	[66]
βHC-HGSO	βHC strategy	Feature selection	ACS dataset	Accuracy, Feature size	Local searching ability enriched, Balance between exploration and exploitation enhanced	[67]
SAHGSO	Self-adaptive technique	Global optimization, SOFC	10 benchmark functions from IEEE CEC 2024, 96-cell SOFC stack	Mean, Std, MSE	Convergence speed increased	[68]
EHGSO	Random number (difference between current fitness and worst fitness values)	WSN	Objective function: optimizing cluster head selection, optimizing routing path Hybrid MAC protocol (IEEE 802.15.4 protocol and LEACH protocol) considering 50 nodes, 100 nodes and 150 nodes	Distance Delay, PDR, Energy, Throughput	Performance enhanced	[127]

To deal with the problem of DoS attack detection in wireless sensor networks (WSN), the authors in [63] developed a method which combines the mixed kernel extreme learning machine (MKELM) and random forest (RF) with the oppositional-based HGSO (OHGSO) algorithm. In this work, the MKELM-RF classifier is optimized by the OHGSO algorithm. The developed MKELMRF-OHGSA was used for detecting and isolating the attacks in data transmission phase. The feasibility of the MKELMRF-OHGSA method was tested on the network simulator platform with 400 sensor nodes taking into account detection rate, accuracy, network lifetime, throughput, false alarm rate as well as packet delivery ratio evaluation metrics. The simulation results revealed that the developed method outperformed the WSN-FAHN, DLDM, TEHODBN as well as HNWT in accomplishing better results based on the above-mentioned evaluation metrics.

In [64], a hybrid HGSO with deep learning (HHGSO-DL) model was proposed for power light emitting diode (LED) driver system design. In the proposed HHGSO-DL, the opposition-based HGSO has been utilized to optimally tune the bidirectional long short-term memory (BiLSTM) model which investigated the empirical relationship. The effectiveness of the HHGSO-DL was evaluated on the LED chip packaging along with LED luminaire having thermal aging loading. The evaluation metrics utilized in this study are SPD (spectral power distribution) error norm, CCT (correlated color temperature), lumen maintenance, and XY^a. The simulation results illustrated that the presented HHGSO-DL yielded better results than LSTM (long short-term memory) for LED driver system design.

To address the intrusion detection in MANETs (mobile ad hoc networks), the EHGSO-DNFN method was proposed in [65]. In this approach the HGSO was blended with EWMA (exponential weighted moving average) to train the DNFN (deep neuro fuzzy network) model for intrusion detection. The effectiveness of the proposed technique has been evaluated on KDD (knowledge discovery in database) dataset employing various evaluation metrics such as recall, precision, energy and throughput. The experimental results affirmed the outperformance of the EHGSO-DNFN over other compared approaches.

In [66], the HGSO has been blended with three stochastic fractal mechanisms based on Lévy flight, Gaussian walk and Brown movement to address the feature selection along with engineering optimization problem. The proposed SFS (stochastic fractal search)-HGSO algorithm has been applied on 20 standard benchmarks from UCI dataset to examine its performance. The simulation results proved that the developed SFS-HGSO outperformed the HHO (harris hawk optimization algorithm), WOA and HBA (honey badger algorithm) for handling feature selection and engineering optimization problems as well.

In [67], a β-hill climbing (βHC) operator was integrated into the conventional HGSO for enhancing the local search ability along with harmonizing both the exploration and exploitation phases. The newly proposed βHC-HGSO was combined with the RF classifier to construct a feature selection model. This model was investigated on the American Community Survey (ACS) dataset.

Table 4
HGSO variants (hybridizations of HGSO)

Name	Incorporated method	Application	Datasets/Benchmark functions	Evaluation metrics	Improvement	References
HHO-HGSO	HHO	Global optimization, Engineering design problems	23 benchmark test functions from CEC2005, 30 benchmark test functions from CEC2017, 4 real engineering design problems: three-bar truss design problem, tension/compression spring design problem, speed reducer design problem, welded beam design problem	Best, Avg, Std	Local optima prevented, Exploration and exploitation phases harmonized	[49]
LR-HGSO	Modified LR	Economic dispatch for SMES	IEEE 10 units 24-hour test system, Objective function: Minimizing both emission level and operating cost	Best	Global optimal solutions achieved	[69]
MHGSO	SA	PV-BES	IEEE 69-bus system Power loss, voltage profile,	Best	Exploitation phase enhanced	[70]
ExpRHGSO	EWMA, ROA	Agriculture	Rice plant dataset, Rice disease dataset	Accuracy, specificity, sensitivity	Global optimal solutions obtained	[71]
HHGSO	JA, BOA, STOA, OSA, Penalized and reward adaptive probability	Search-based software engineering problem	IMDB dataset, DBLP dataset	Best cost, Average cost, Average time, Number of team members	Local optima prevented, exploration and exploitation phases balanced	[72]

HGSWC	COBL mechanism, WOA	Task scheduling problem in cloud computing	36 benchmark functions, NASA iPSC and HPC2N real workloads	Avg, std, Makespan, PIR, Wilcoxon rank sum test	Local search ability enhanced, exploitation phase ameliorated, global optimal solutions attained, convergence rate boosted	[74]
DHGHHD	HHO, HTDs	Feature selection for drug design and discovery	18 datasets from UCI, 2 real-world datasets for drug design and discovery	Accuracy, Fitness value, Number of selected features	Exploration phase ameliorated	[75]
DOLHGSO	Dynamic OBL strategy, Conversion probability from BOA, Interval contraction strategy, Improved iterative search technique, Sine-cosine operator from SCA,	Global optimization, Engineering design problems	30 benchmark functions from CEC 2017, 3 real-world engineering design problems (speed reducer design problem, gear train design problem, tension/compression spring design)	Best, mean, std, Friedman's test, Wilcoxon signed-rank test	Population diversity ameliorated, local optima prevented, exploration and exploitation phases balanced, convergence rate hastened convergence accuracy enhanced	[76]
DHGSO	Dolphin Echolocation (DE) algorithm	Medical	Lung and Colon Cancer Histopathological Images dataset	Accuracy, sensitivity, specificity	Algorithm performance ameliorated, Global optimal solutions attained	[77]
HGWWO	WWO	Medical	DeepCovid dataset with 5000 CXR images	Accuracy, Sensitivity, Specificity	Global optimal solutions accomplished	[78]
MFABC-ACV-HGS	MFABC, ACV	Medical	Lung cancer dataset	Accuracy, Sensitivity, Specificity	Global optimal solutions achieved, exploration and exploitation phases	[79]

					harmonized	
Ar-HGSO	CAViaR, SFO	Medical	IDRID dataset, DDR dataset	Accuracy, Sensitivity, specificity	Local optima avoided, Computational complexity decreased	[80]
CSHGSO	CSO	Internet of Things	BoT-IoT dataset	Energy, Precision, F-measure, Recall	Exploration and exploitation phases harmonized, global optimal solutions achieved	[81]
EHO	DE, WOA, Lévy flight strategy	MPPT problem in PRO system	PRO system	Accuracy, tracking speed, cost-efficiency	Convergence speed accelerated, Searching ability boosted, exploration and exploitation phases strengthened, local optima escaped, execution time shortened	[73]
HSLnO	SLnO	Medical		Accuracy, Sensitivity, Specificity		[82]
LHGSO-DFC	ALO	Feature extraction for image retrieval	Large-sized image dataset	Recall, Precision, F-measure	Algorithm performance improved	[83]
AQO-HGSO	AQO	Medical	Neurosurgical dataset from Mansoura International Hospital (Egypt)	Recall, F-measure, precision, accuracy, sensitivity	Exploration and exploitation phases balanced	[84]
MVQIHGSO	MVO, QI	Fault diagnosis	23 benchmark functions from CEC2005,	Mean, Std, R^2,	Local optima escaped, Exploration and	[85]

			Data from Xiluodu and Xiangjiaba hydropower reservoirs (China)	RMSE, MAE, MAPE, Friedman's test, Wilcoxon's rank sum test,	exploitation phases harmonized	
MVOHGSO	MVO	Fabric defect detection	Various fabric defect datasets	Accuracy	Local optima averted, Computation time reduced	[86]
HFGSO	FA	Medical	Prostate MRI dataset	Accuracy, Specificity, Sensitivity	Exploration and exploitation phases balanced	[87]
HFCVO	CMVO, Fuzzy concept	Classification	20-Newsgroup dataset, Reuter dataset, Real-time dataset	Accuracy, Precision, FNR, TNR, TPR	Exploration and exploitation phases improved, Searching ability boosted	[88]
HHBGGSO	HBA	Feature extraction	Kannada handwritten character dataset	Accuracy, Precision, Sensitivity, Specificity, F1Score, Negative NPV, MCC, FNR, FPR, FDR	Convergence rate enhanced, Global optimal solutions accomplished	[89]
FHGSO	FAT	Medical	ABIDE dataset	Accuracy, Sensitivity, Specificity	Algorithm efficiency ameliorated	[70]
FrHHGSO	FC concept, HOA	E-waste management	Gofile dataset	Accuracy, Sensitivity, Specificity, Energy Delay, ROC	Global optimal solutions attained	[71]

HGBSO-DCNN	BSA	Medical	BRATS 2018 database, Figshare dataset	Accuracy, Sensitivity, Specificity, ROC	Exploration and exploitation phases harmonized, local optima avoided	[72]
CSHGSO	CSO	Data mining	Heart disease dataset: Cleveland (Database-1), Hungarian (Database-2), Switzerland (Database-3), VA Long beach (Database-4)	Conditional privacy, Accuracy, NMI	Global optimal solution accomplished, Computation complexity minimized, Local optima escaped, Exploration and exploitation phases balanced	[93]
THGSO	TSA	Image classification	Fruits 360 dataset, banana-ripeness classification dataset	Accuracy, Sensitivity, Specificity	Exploration and exploitation phases balanced, local optima averted	[94]
IIWGSO	IIWO	Communication engineering	MANET model	Packet delivery, Jitter, Delay, Throughput, Overhead	Exploration and exploitation phases balanced	[95]
IIWFPO FHGSO	IIWO, FPA	Image segmentation Image classification	Stanford background dataset	Testing accuracy, Sensitivity, Specificity	Exploration and exploitation phases balanced, global solution achieved, premature convergence prevented	[96]

EHHGSO	JA, BOA, STOA, OSA, Penalized and reward adaptive probability, Backtracking technique	Global optimization	Benchmark functions: sphere, Ackley, Rosenberock, Quartic with noise, Rastrigin	Mean	Local optima prevented, exploration and exploitation phases balanced	[97]
RHGSO	ROA	Agriculture	Rice plant dataset, Rice disease dataset	F1-Score, Accuracy, Specificity, Sensitivity	Global optimal solutions obtained	[98]
SHGSO	SSA	Image forgery detection	MISD dataset, Copy-Move Image Forgery database	TNR, TPR, Accuracy	Exploration and exploitation phases balanced, Local optima averted	[99]
EHGSO	Sine-cosine mutualism phase from SOS	Parameter estimation of PV models	RTC France, New objective function integrating the first-order numerical technique known as Berndt-Hall-Hall-Hausman with adaptive damping parameter (AdBHHH)	RMSE, R^2, AE, MBE, TS, CPU-execution time, STD	Population diversity improved, exploration promoted, Computation time reduced, Convergence speed accelerated, Global convergence accomplished	[100]
HGSOEO	EO	Feature selection, Twitter spam detection	Social Honeypot dataset	AUC, Precision, Accuracy, Recall	Exploration ability enhanced, Premature convergence avoided, Solutions quality improved	[101]

FHJO	JS, FAT	Medical	ACERTA-ABIDE dataset (ABIDE-I and ABIDE-II)	Sensitivity, Specificity, Accuracy	Exploration and exploitation phases balanced, Execution time reduced, Local optima averted	[102]

The experimental outcomes showed that the proposed βHC-HGSO achieved better results than the conventional HGSO in terms of accuracy.

In [68], the self-adaptive technique has been introduced into the classical HGSO to boost the convergence speed of the algorithm. Primarily, the proposed SAHGSO has been applied to 10 benchmark functions from IEEE CEC 2014 in order to assess its performance. Afterwards, the presented algorithm has been investigated on 96-cell SOFC (solid oxide fuel cell) stack by considering diverse temperature and pressure conditions. In all cases, the proposed algorithm outperformed other competitive algorithms.

A novel multi-channel medium access control (MAC) protocol for WSN has been designed in [127] by integrating the aspects of both IEEE 802.15.4 and low-energy adaptive clustering hierarchy (LEACH) protocols. Afterward, an enhanced HGSO (EHGSO) updating the random number (i.e the difference between the current fitness and worst fitness values) has been utilized to optimally select the cluster heads for LEACH protocol and routing path for IEEE 802.15.4 protocol. The effectiveness of the proposed EHGSO algorithm was examined on 50, 100 and 150 sensor nodes. The simulation outcomes showed the outperformance of the EHGSO over other compared algorithms concerning enhanced throughput, maximum packet data ratio (PDR), minimum energy consumption, delay and distance.

3.3. Hybridizations of HGSO

Various metaheuristic algorithms have been hybridized with the HGSO algorithm to construct the new hybridized algorithms with new characteristics and applied to solve different problems. These hybridized algorithms have been mostly presented with the aim of enhancing the performance of the conventional HGSO algorithm. Table 4 depicts various hybridized algorithms accomplished with the HGSO algorithm.

In [49], the HHO has been blended with the HGSO to tackle the global optimization and engineering design problems. The efficacy of the presented HHO-HGSO algorithm has been investigated on 23 benchmark test functions from CEC2005, 30 benchmark test functions from CEC2017 as well as 4 real engineering design problems (i.e. three-bar truss design problem, tension/compression spring design problem, welded beam design problem, speed reducer design problem). The simulation outcomes proved that the presented HHO-HGSO yielded better results than HHO, HGSO, WCA, LSA, WOA and MPA algorithms.

To cope with the problem of optimal size allocation for the superconducting magnetic energy storage (SMES) system incorporating IEEE 10-unit 24-hour test system, the authors in [69] proposed a LR-HGSO algorithm. The proposed algorithm introduced the modified Lagrange relaxation (LR) into the HGSO to minimize both emission level and operation cost. The results from the simulation approved that the proposed LR-HGSO outstandingly reduced the emission and cost for economic dispatch of the SMES system.

To optimally allocate PV and BES (battery energy storage) in radial distribution system (RDS) taking into consideration the stochastic PV generation and time-varying load demand, the authors in [70] proposed a MHGSO. The minimization of the power loss is the objective function investigated in this study. The MHGSO algorithm blended the simulated algorithm (SA) with the HGSO in an effort to improve the exploitation phase of the conventional HGSO. The efficacy of the MHGSO has been investigated on the IEEE 69-bus RDS. The simulation outcomes proved that the presented MHGSO outstandingly achieved better results in incorporating the BES along with PV in RDS.

To cope with the problem of detecting the rice plant diseases, the authors in [71] developed a hybrid algorithm known as ExpRHGSO, which blends the EWMA and rider optimization algorithm (ROA) with the HGSO. Initially, the hybridized ExpRHGSO was employed to train the DNFN so as to detect the rice leaf diseases. Lastly, the classification of the rice leaf diseases was accomplished by the deep residual network (DRN). The effectiveness of the proposed ExpRHGSO-based Hybrid Deep Learning method, was ascertained on the two datasets, namely rice disease dataset and rice plant dataset by considering accuracy, specificity as well sensitivity evaluation indicators. The experimental outcomes demonstrated the supremacy of the presented method over PSO-SVM, ADSNN-BO, RHGSO-DNFN, CNN and CNNIR-OWELM.

In [72], the authors proposed a hybridized algorithm known as HHGSO to tackle the search-based software engineering (SBSE) problem. The proposed HHGSO algorithm mingled four metaheuristics, namely sooty tern optimization algorithm (STOA), Jaya algorithm (JA), owl search algorithm (OSA) and butterfly optimization algorithm (BOA) with the HGSO. In addition, the penalized and reward adaptive probability has been utilized to render dynamic the individual mapping of every metaheuristic. The feasibility of the proposed HHGSO has been examined on both DBLP and IMDB datasets utilizing different indicator metrics such as best cost, average cost, average time and number of team members. The simulation results affirmed the supreme performance of the HHGSO algorithm over the modified choice function (MCF), exponential Monte Carlo with counter (EMCC), fuzzy inference selection (FIS) and improvement selection rules (ISR) in handling SBSE problem.

To cope with the MPPT (maximum power point tracking) problem in PRO (pressure retarded osmosis) process, the authors in [73] presented a hybridized algorithm named as EHO. The presented EHO blends the differential evolution (DE), WOA and Lévy flight mechanism with the HGSO to ameliorate the performance of the conventional HGSO. The efficacy of the EHO was ascertained on the PRO system and compared with WOA, DFOA and GWO. The experimental outcomes revealed that EHO offered better results than other algorithms in terms of tracking speed, accuracy and cost-efficiency.

To tackle the problem of task scheduling in cloud computing, a technique known as HGSWC has been proposed in [74] which mingled a comprehensive opposition-based learning (COBL) mechanism and WOA with the HGSO. The key role played by the COBL mechanism in the presented HGSWC approach is to ameliorate the worst solutions whereas WOA is used as a local

search operator to boost the solutions quality as well as convergence rate. The feasibility of the HGSWC has been investigated on the 36 benchmark functions and also on the NASA iPSC and HPC2N real workloads. The simulation results revealed that the proposed HGSWC surpassed MFO, FA, WOA and SSA in terms of the performance improvement rate (PIR) and makespan evaluation metrics.

The authors in [75], proposed the DHGHHD algorithm to handle the problem of feature selection in drug design and discovery. In this work, the HHO algorithm improved by the heavy-tailed distributions (HTDs) was blended with the HGSO to constitute the DHGHHD. The effectiveness of the DHGHHD algorithm was investigated on 18 datasets from UCI along with 2 real-world datasets related to drug design and discovery. The simulation results approved that the DHGHHD is effective for feature selection in drug design and discovery.

To handle engineering design along with global optimization problems, the authors in [76] developed a novel algorithm known as DOLHGSO blending the dynamic OBL strategy, improved iterative search technique, conversion probability from the butterfly optimization algorithm (BOA), interval contraction strategy and sine-cosine operator from sine cosine algorithm (SCA) with the HGSO. The developed DOLHGSO was evaluated on 30 CEC 2017 benchmark functions along with 3 real-world engineering design problems (i.e. gear train design problem, speed reducer design problem, tension/compression spring design). The simulation results affirmed the supremacy of the developed DOLHGSO algorithm over other compared algorithms for the considered problems.

In [77], the hybridized DHGSO algorithm, which blends the dolphin echolocation (DE) algorithm with the HGSO has been employed for lung cancer image classification. Firstly, the Gaussian filter along with region of interest (ROI) extraction are employed to perform the preprocessing of the inputted histopathological images. Afterwards, the fractional rider gradient descent-based U-Net accomplishes the image segmentation. Then, various features are extracted in order to be used by the deep maxout network (DMN). The proposed DHGSO is employed to train the DMN for lung cancer classification. The feasibility of the DHGSO-DMN method was examined on the Lung and Colon Cancer Histopathological Images dataset considering three performance metrics (i.e. sensitivity, accuracy and specificity). The simulation results confirmed the supremacy of the DHGSO-DMN method in comparison with other methods in achieving the best performance.

For detecting COVID-19 from chest X-Ray images, the authors in [78] proposed a new technique named as HGWWO-Deep GAN, which introduces the deep generative adversarial network (GAN) into the hybridized algorithm made by water wave optimization (WWO) algorithm with HGSO (HGWWO). Firstly, the prepreprocessing is performed via media filter along with ROI for de-noising the images. Subsequently, the U-net architecture is utilized to segment the lung lobes and the lung regions are extracted through CNN features. Lastly, the hybridized HGWWO algorithm is employed to train the Deep GAN for COVID-19 detection. The feasibility of the presented technique was examined on the DeepCovid Dataset comprising 5000 CXR images. The evaluation metrics used in this work are accuracy, specificity and sensitivity. The experimental outcomes

confirmed the supremacy of the presented techniques over DeepCoroNet, CoroNet and HGSO-SVM techniques in achieving the best performance based on the considered metrics.

To efficiently detect the lung cancer in a medical IoT (internet-of-things)-based platform, the authors in [79] proposed a model known as MFABC-ACV-HGSO based DMN. In this model, the IoT data routing is firstly accomplished by the multi-objective fractional artificial bee colony (MFABC) which facilitates the optimal transfer of the medical data from the nodes to the sink to which place the lung cancer detection is carried out. The data preprocessing stage is performed by Gaussian filter along with log transformation. Subsequently, the kernel LDA (Linear Discriminant Analysis) and wrapper model are utilized to diminish the dimension of the preprocessed data. The resulted data are fused via RV coefficient. In the last stage, the anti-corona virus optimization (ACVO) is incorporated into the HGSO (ACV-HGSO) to train the DMN so as to detect the lung cancer. The performance of the presented MFABC-ACV-HGSO was evaluated on the lung cancer dataset by using the accuracy, sensitivity and specificity performance metrics. The simulation outcomes proved that the presented model could remarkably detect the lung cancer.

In [80], the authors proposed an Ar-HGSO-based deep learning approach to detect diabetic retinopathy (DR) along with severity level classification. The proposed technique combines the sailfish optimization (SFO), conditional autoregressive value at risk by regression quantiles (CAViaR) and HGSO. The proposed approach performance was investigated on the IDRID (Indian Diabetic Retinopathy Image Dataset) dataset considering accuracy, specificity and sensitivity evaluation metrics. The simulation results showed that the proposed Ar-HGSO-based deep learning approach achieved better results in detecting DR as well as severity level classification.

In [81], the Competitive Swarm Optimizer (CSO) has been incorporated into HGSO to train the DMN to detect the intruders within IoT-based platform. The presented CSHGSO-DMN was examined on the BoT-IoT dataset based on energy, precision, F-measure, as well as recall evaluation metrics. The simulation outcomes proved the robustness of the CSHGSO-DMN for intruder detection.

The authors in [82] addressed the problem of medical data classification through a deep learning-driven hybrid-optimization algorithm. Firstly, the data normalization approach was utilized to preprocess the input data. Afterwards, the feature selection is accomplished by the hybridized algorithm (i.e. HSLnO) which blends the HGSO with the sea lion optimization (SLnO) algorithm. Ultimately, the hybridized algorithm (i.e. SSWOA) which incorporates the shuffled shepherd optimization algorithm (SSOA) with WOA is employed to train the deep Q network to classify the medical data. The simulation results affirmed that the proposed HSLnO algorithm is effective for medical data classification based on the accuracy, specificity and sensitivity evaluation metrics.

The authors in [83] presented a Lion HGSO-based deep fuzzy clustering (LHGSO-DFC) technique for feature selection in image retrieval. The LHGSO was employed to optimize the DFC and thereby enhancing the image retrieval performance considering recall, precision and F-measure

metrics. The simulation results affirmed that the LHGSO-DFC is effective for image retrieval feature selection.

In [84], a double classifier model RF-SVM-HGSO is proposed to forecast the head trauma of neurosurgical patients. The proposed model combines the features of RF, support vector machine (SVM), Aquila optimizer (AQO) as well as HGSO. The proposed model performance was ascertained on the data collected from the Neurosurgical department of Mansoura International Hospital in Egypt by employing recall, F-measure, accuracy, precision and sensitivity evaluation metrics. The simulation results confirmed the effectiveness of the RF-SVM-HGSO model.

To optimally enhance the performance of the hydropower reservoirs, the authors in [85] presented a MVQIHGSO-SVM technique, which blended the multi-verse optimizer (MVO), quadratic interpolation (QI) and SVM with the HGSO. Firstly, the MVO and QI were utilized to improve the exploration phase and exploitation phase, respectively and thereby harmonize the exploration and exploitation phases. Secondly, the MVQIHGSO was employed to optimally determine the hyperparametres of the SVM. Finally, the MVQIHGSO-SVM was used to derive the operation rules of the hydropower reservoirs. The performance of the MVQIHGSO was examined on 23 classical benchmark functions and compared with HGSO, DE, PSO, MVO, GWO, IGWO, OBSCA and SCA. The simulation results affirmed the supremacy of the MVQIHGSO over other compared algorithms considering accuracy and convergence rate. Furthermore, the effectiveness of the MVQIHGSO-SVM technique was ascertained on the data collected from Xiluodu and Xiangjiaba hydropower reservoirs located in the upper Yangtze River (China) in comparison with HGSO-SVM, Grid-SVM, SCA-SVM and PSO-SVM techniques. The simulation results further revealed that the MVQIHGSO-SVM technique outperformed other techniques in optimally deriving the operation rules of the hydropower reservoirs.

The authors in [86] proposed the Inv3-MHL21-RELM algorithm to address the fabric defect detection problem. In this study, the feature extraction was performed through Inception v3. Afterwards, the hybridized MVO-HGSO algorithm was employed to optimize the L2,1-norm regularization extreme learning machine (RELM). The performance of the Inv3-MHL21-RELM algorithm was tested on various fabric detect datasets. The experimental outcomes approved that the Inv3-MHL21-RELM was effective for solving the fabric defect detection.

In [87], a technique called HFGSO-DBN has been proposed to handle the problem of prostate cancer segmentation and detection. Firstly, the image from Prostate MRI dataset has been inputted to ROI extraction. Then, the preprocessing is performed on the ROI extracted image through the T2FCS filter to ameliorate the image quality. Afterwards the hybridized algorithm HFGSO (made by the firefly algorithm (FA) with the HGSO) was employed to train the multi-objective SegNet for image segmentation. At last, the deep belief network (DBN) trained by the HGSO was utilized to detect the cancer. The effectiveness of the HFGSO-DBN technique was compared with other techniques such DCNN, Focal-Net, ResNet and Panoptic models. The simulation outcomes affirmed the supremacy of the HFGSO-DBN over other compared techniques regards to accuracy, specificity and sensitivity evaluation metrics.

To cope with the problem of incremental text classification, the authors in [88] proposed a hybridized algorithm named as HFCO-DMN (Henry Fuzzy Competitive Multi-verse Optimizer-based Deep Maxout Network) which blended the Competitive Multi-verse Optimizer (CMVO), fuzzy concept and DMN with the HGSO. In this study, the selection of the optimal features is performed by the hybridized IWTSO that combines the IWO (Invasive Weed Optimization) and TSA (Tunicate Swarm Algorithm). Then, the HFCO algorithm is used to train the DMN classifier so as to achieve the incremental text classification. The feasibility of the HFCO-DMN has been investigated on different datasets such as 20-Newsgroup, Reuter and Real-time datasets. The simulation results affirmed the effectiveness of the HFCO-DMN for incremental text classification.

In the context of Kannada character script recognition, the work in [89] proposed a novel method named as HHBGGSO-HFE-EDH. Firstly, the HBA algorithm was blended with HGSO to ameliorate the convergence speed of the HGSO. Subsequently, the developed HHBGGSO is integrated with Hybrid Feature Extraction with Ensemble Deep Learning (HFE-EDH) to optimally adjust the parameters of HFE-EDH. The experiment study involved the Kannada handwritten character dataset and employed various evaluation metrics, namely accuracy, precision, sensitivity, specificity, negative predictive value (NPV), F1-Score, Mathews correlation coefficient (MCC), false positive rate (FPR), false negative rate (FNR), false discovery rate (FDR) to assess the effectiveness of the HHBGGSO-HFE-EDH method. The proposed method was compared with other methods including CNN, 1DCNN, ENSEMBLE, XGBOOST, COA-HFE-EDH, AOA-HFE-EDH, HBA-HFE-EDH and HGSO-HFE-EDH. The simulation results proved the outperformance of the HHBGGSO-HFE-EDH method over other compared methods.

To address the autism spectrum disorder (ASD) problem, the work in [90] presented a hybridized algorithm by integrating the artificial feedback tree (FAT) algorithm into the HGSO to train the DNFN classifier. The effectiveness of the FHGSO-DNFN model was ascertained on the ABIDE dataset and compared with other approaches, namely CNN, DBN, deep neural network (DNN), modified grasshopper optimization algorithm (MGOA), two-stream DL network and auto-ASD-network. The assessment metrics considered in this work are accuracy, sensitivity and specificity. The experimental outcomes confirmed the superiority of the FHGSO-DNFN model over other approaches considering the afore-mentioned performance metrics.

To address electronic waste (E-waste) management problem in the IoT-enabled platform, the study in [91] presented the hybrid HGSO algorithm by blending FC concept and Horse Herd Optimization Algorithm (HOA) algorithm with HGSO. The presented algorithm is named as FrHHGSO is employed to perform optimal routing process. Finally, the proposed FrHHGSO-shCNN model performed the E-waste classification task. The FrHHGSO-shCNN performance model was evaluated on Gofile dataset that contains 807 E-waste images and compared with other models. The evaluation metrics considered in this works are specificity, accuracy, sensitivity, energy, delay and ROC. The simulation results proved that the FrHHGSO-shCNN model excelled other compared models.

In [92], the bird swarm algorithm (BSA) is blended with HGSO to constitute the HGBSO algorithm that is employed to train the DCNN for classifying brain tumors. In this model, the noise from the input pre-processing of the MRI (magnetic resonance imaging) input images is removed through Gaussian filter and ROI extraction during the pre-processing stage. Subsequently, the brain tumor regions undergo segmentation via a deep fuzzy clustering method. The segmented images provide the key characteristics to accomplish the classification task. In addition, the data augmentation is accomplished so as to boost the classification accuracy. At last, the augmented data as well as total features are conveyed as the input to the HGBSO-DCNN classifier in order to achieve the brain tumor classification. The datasets considered in this work are the Figshare dataset and BRATS 2018 database. The experimental outcomes demonstrate that the HGBSO-DCNN classifier outperformed other compared classifiers in terms of accuracy, specificity and sensitivity.

To address the problem of securing data publishing, the work in [93] proposed a novel algorithm known as CSHGSO algorithm, which hybridizes cat swarm optimization (CSO) algorithm and HGSO. The prime aim of the CSHGSO algorithm is to attain global optimal solutions and diminish the computational complexity. To assess the performance of the CSHGSO algorithm, the Heart disease dataset comprising various databases has been utilized. In addition, the CSHGSO algorithm performance was assessed by comparing it with other methods considering three evaluation metrics such as NMI (Normalized Mutual Information), accuracy and conditional privacy. The simulation results revealed the outperformance of the CSHGSO algorithm.

A new method for classifying fruit ripening is proposed in [94] taking into account an optimization-driven deep model. The proposed method consists of five phases, namely preprocessing, feature extraction, fruit classification, training algorithm and ripening classification. Initially, the Gaussian filtering is utilized for preprocessing the input images of fruits (i.e. mango, apple, banana) with the aim of de-noising images as well as enhancing their quality. Then, the feature extraction is performed to extract various features including statistical features, color histogram, histogram of gradients (HoG), CNN, significant local binary pattern (SLBP), local Gabor binary pattern (LGBP). The fruit classification is performed through DCNN. The hybridization of TSA with HGSO results in THGSO algorithm which is used for training the DRN. Finally, the THGSO-DRN performs the ripening classification. The THGSO-DRN method performance has been evaluated on fruits 360 along with banana-ripeness classification datasets. The simulation results reveal that the THGSO-DRN method gives better accuracy, sensitivity and specificity values than other methods available in the literature.

To address the problem of quality of service (QoS) routing improvement in MANETs, a technique known as IIWGSO-DResNet was proposed in [95]. In the proposed technique, the deep residual neural network (DResNet) model has been trained by the hybridized IIWGSO algorithm made by the improved invasive weed optimization (IIWO) with HGSO. The proposed technique has been

ascertained on the MANET model and compared with HGSO, DE, FF, CSO-AODV, DE-FF-AODV and IIWO. The simulation outcomes affirmed the supremacy of the IIWGSO-DResNet technique over the compared techniques in terms of the evaluation indicators like packet delivery, jitter, delay, throughput and overhead.

In [96], a novel image classification approach integrating the Flower Pollination Algorithm (FPA), HGSO along with Deep CNN is proposed. The proposed FHGSO-Deep CNN approach comprises 3 stages such as preprocessing, segmentation as well as classification. At first, the median filter is employed to preprocess the input image. Subsequently, an improved invasive weed flower pollination optimization (IIWFPO)-based SegNet carries out the segmentation. At last, FHGSO-Deep CNN accomplishes the image classification. The efficacy of the proposed approach was tested on the Stanford background dataset considering sensitivity, accuracy and specificity evaluation metrics. The experimental results confirmed the superiority of the proposed FHGSO-Deep CNN approach in comparison with other approaches.

In [97], a hybrid HGSO (HHGSO) was developed based on the hybridization of the HGSO with other algorithms and techniques, namely JA, BOA, STOA, OSA, penalized and reward adaptive probability. Furthermore, an enhanced HHGSO (EHHGSO) was developed by incorporating the backtracking technique into the HHGSO. The two algorithms were tested on the six benchmark functions such as sphere, Ackley, Rosenbrock, Quartic with noise, and Rastrigin. The simulation results showed that the EHHGSO achieved better results than HHGSO.

In [98], the RHGSO algorithm has been developed by merging the conventional HGSO algorithm with the ROA algorithm. The proposed RHGSO has been employed to build up two models, namely RHGSO-DNFN and RHGSO-DRN in order to detect and classifier the rice leaf diseases. First and foremost, the ROI was used to preprocess the input images from rice plant and rice disease datasets. Afterwards, the deep fuzzy clustering was utilized for the segmentation. Then the feature extraction was achieved to get the features namely local optimal-oriented pattern (LOOP), CNN features, local Gabor XOR pattern (LGXP), statistical features, and entropy. The volume of the extracted images was increased through data augmentation. Finally, the first level along with second level classifications were achieved by RHGSO-DNFN and RHGSO-DRN, respectively. The performance metrics considered in this work were F1-Score, sensitivity, specificity and accuracy. The experimental outcomes on two datasets revealed that the proposed models surpassed other models including SVM, SVM-CNN, simple CNN and deep CNN regards to both first level as well as second level classifications.

In [99], the squirrel search algorithm (SSA) has been incorporated into the HGSO in order to develop a hybrid algorithm known as SHGSO. The proposed algorithm has been employed to train the DMN classifier for image forgery identification and classification. Initially, the input images

from the multiple image splicing dataset (MISD) were preprocessed then the steerable pyramid transform (SPT) decomposition was performed in order to obtain the multi-oriented and multi-scale sub bands. In addition, the feature extraction was carried out to get the features such as local gradient pattern (LGP), local directional pattern (LDP), local directional texture pattern (LDTP), local ternary pattern (LTP) and pyramid of histogram of oriented gradients (PHOG). Then, the feature selection was achieved through L_0-norm along with local learning based (LLB) model. Finally, the image forgery detection was accomplished by the SHGSO-DMN model. The experimental outcomes demonstrated that the proposed model outperformed other forgery detection models including CNN, DCNN, and semantic segmentation and multi-texture based technique.

In [100], an enhanced HGSO was blended with the sine-cosine mutualism phase from the symbiotic organism search (SOS) algorithm. The proposed EHGSO algorithm was employed to identify the unknown parameters of single-diode along with double-diode PV models. In this study, a new objective function was designed based on the first-order numerical technique known as Berndt-Hall-Hall-Hausman with adaptive damping parameter (AdBHHH). The proposed algorithm was investigated on the RTC France PV module and compared with other algorithms. The experimental results show that the presented EHGSO achieved better results than other compared algorithms in terms of RMSE (root mean square error) , R^2, AE (absolute error), MBE (mean bias error), TS (test statistical), CPU-execution time, and STD(standard test deviation).

A novel wrapper technique comprising the hybridization of HGSO along with EO has been presented in [101] for feature selection. The proposed technique has been validated on the social honeyspot dataset considering various metrics such as precision, accuracy, AUC (area under curve) and recall. The experimental outcomes showed the outperformance of the proposed technique over the filter-based techniques and other feature selection techniques based on PSO, WOA and GA.

In [102], the FHGSO cited in [87] has been merged with the jelly fish (JF) algorithm to develop the FHJO algorithm. Furthermore, the FHJO has been employed to train the classifier based on the CNN with transfer learning (TL) for ASD classification and detection. Primarily, the Kalman filter along with the ROI selection are utilized to preprocess the input autism images from ABIDE I and ABIDE II datasets. Subsequently, the pivotal extraction driven by the functional connectivity is accomplished by the FHJO. Later on, the feature extraction was performed to obtain the features such as speeded up robust features (SURF), local binary pattern (LBP), and statistical features. At the end, the ASD classification and detection are achieved through the proposed FHJO-CNN-TL model. The performance of the proposed model was investigated on the 2 datasets based on the performance metrics including specificity, sensitivity and accuracy. The experimental outcomes

affirmed that the proposed FHJO-CNN-TL model surpassed the FHGSO-DNFN, CNN, two-stream DL network, DBN and DNN models.

3.4. Chaotic HGSO

The chaotic HGSO variants along with quantum HGSO variants are illustrated in Table 5.
The authors in [52] developed a new metaheuristic algorithm incorporating various chaotic maps into HGSO algorithm. The newly proposed CHGSO is applied to different engineering design problems including cantilever beam design, welded beam design optimization, grinding optimization and diaphragm spring optimization problems. The simulation outcomes reveal that the CGHSO yields better results thanks to circular map which harmonizes the exploration and exploitation phases of the HGSO algorithm.

To address the crude oil price prediction problem, the study in [103] presented a novel model integrating the LSTM and logic chaotic map into the HGSO algorithm. The main goal of the logistic chaotic map is to make an equilibrium among exploration and exploitation phases of the HGSO and also to avert local optima. The effectiveness of the CHGSO-LSTM model was examined on two datasets, namely Brent COTS (crude oil time series) and WTI (West Texas Intermediate). Furthermore, different kinds of performance metrics such as momentum, volatility and trend metrics have been used in this study. The momentum metrics comprise commodity channel index (CCI), rate of change (ROC) and relative strength index (RSI). The volatility metrics consist of volatility ratio (VR), highest high lowest low (HHLL) and average true range (ATR). The trend metrics contain Kaufman's adaptive moving average (KAMA), exponential moving average (EMA) and simple moving average (SMA). The simulation outcomes approved the superiority of the CHGSO-LSTM model over PSO-LSTM model in predicting the price of the crude oil.

In [104], the HGSO is integrated with OBL strategy along with chaotic logic map (HOC) to tackle the optimal reactive power dispatch (ORPD) problem. The feasibility of the HGSO for this problem has been examined on the IEEE 14-, 30-, 57-, 118- and 300-bus test systems. The objective functions studied in this work are the voltage deviation (VD), power losses and voltage stability index (VSI) minimization. The simulation results revealed that the HOC is effective in solving the OPRD problem.

In order to address the problem of securing vehicle networks, the work in [105] presented a method known as MDML-CHGSO which incorporates modified deep metric learning (MDML) and the chaotic maps into the HGSO algorithm. The convergence speed of this method is ameliorated by these chaotic maps. The presented MDML-CHGSO method guarantees a security design with trustworthiness. The performance of the presented method was validated on Open Street Map database (India) and compared with other methods including LCPPA (lightweight conditional privacy-preserving authentication), MPDC (multi-party delegated computation), MFSPV (multi-factor secured and lightweight privacy-preserving authentication technique for VANETs) and EBCPA (efficient blockchain-based conditional privacy-preserving authentication). The

simulation results approved that the MDML-CHGSO method accomplished the best values for throughput, average latency as well as packet delivery ratio.

In the context of the liquid level control, the study in [106] proposed an algorithm known as CHGSO-FAT which hybridizes FAT algorithm with the chaotic HGSO algorithm to achieve the optimal gains of the Fractional Order Proportional Integral Derivative (FOPID) controller in two tanks spherical interacting system (TTSIS). The experimental results revealed that the proposed controller provide better outcomes than PSO and PSO algorithms.

To effectively make a design of a hybrid energy system with Diesel-PV-Battery resources, a novel approach named as cHGSO has been developed in [107]. The developed approach integrates both self-adaptive weighting strategy and chaotic logistic map into the conventional HGSO. The objective functions investigated are the load loss probability, system's annual cost as well as CO2 emission. The effectiveness of the cHGSO has been ascertained on the hybrid energy system located in Yarkant, Xinjiang Uyghur Autonomous Region (China). The simulation results confirmed the superiority of the cHGSO over PSO and HOMER in minimizing the considered objective functions.

The authors in [108] have merged the CHGSO proposed in [52] with two methods, namely ResNet101 and Bi-GRU (Bidirectional Gated recurrent unit) in order to accurately detect the ASD. Firstly, the preprocessing of the input data from the EEC microstates dataset has been accomplished through NetStation Waveform Tools in order to get rid of the undesirable features. Afterwards, the CHGSO was employed to optimize the hybrid ensemble model based on Bi-GRU along with ResNet101 so as to obtain precise detection and classification outcomes. The classification effectiveness of the proposed model has been evaluated on the EEC microstates dataset by considering various evaluation metrics such as precision, accuracy, specificity, sensitivity, F1-Score, MCC, mode and median. The simulation results illustrated that the proposed model outperformed other models including MGOA-RF, SVM, DNN and KNN in achieving the best values of the evaluation metrics for ASD detection and classification.

In [109], a chaotic map has been incorporated into the classical HGSO to enhance the resource allocation along with mining decisions for wireless blockchain networks operated by the mobile edge computing (MEC). The presented CHSGSO has been experimented on a blockchain network (BN) where the blockchain users (BUs) were randomly distributed in a square having a side of 1000 m and its center was occupied by the MEC server. The effectiveness of CHSGSO has been investigated using various number of the BUs. The results show that the proposed CHSGSO outperformed DE, ACO, BOToP and DEMiDRA.

The chaotic logistic map has been integrated into the HGSO in [110] to develop the CHGSO. The presented algorithm has been combined with the bag of features (BOF) to accurately classify the soil images. The proposed CHGSO-BOF technique has been evaluated on the soil image dataset comprising seven classes of soil images including clay, sandy clay, clayey sand, humus clay, peat,

clayed peat and silty sand. The effectiveness metrics employed to evaluate the CHGSO-BOF technique are F1-Score, accuracy, precision and recall. The simulation results illustrated the outperformance of the CHGSO-BOF over HGSO-BOF, BOF, GWO-BOF, BA-BOF, GOA-BOF, WOASA-BOF and DE-BOF techniques for soil image classification.

In [111], the chaotic system has been incorporated into the conventional HGSO to assess 47 benchmark functions. The proposed CHGSO has been compared with the conventional HGSO. The simulation results showed that the CHGSO accomplishes better results than the conventional HGSO in terms of std and mean.

In [112], the recalling-enhanced recurrent neural network (RENNN) model has been associated with the chaotic HGSO to tackle the problem of small stability analysis in microgrids considering various uncertainties. The proposed CHGSO-RENNN has been employed to fine-tune the PI (proportional integral) controller gains and achieved better performance.

In [113], the Duffing-Van Der Pol chaotic systems have been embedded into the classical HGSO to develop the chaotic HGSO (CHGSO) algorithm. The NIST (National Institute of Standards and Technology)-800-22 tests were employed to investigate the randomness of the data accomplished from chaotic systems. In addition, the presented CHGSO has been ascertained on the 47 benchmark functions along with DC motor speed control (i.e for achieving the optimal parameters of PID controller). The experimental results show that the CHGSO obtained the best results than SA, EA, PSO, HGSO, GWO and WOA for the considered benchmark functions.

Table 5
HGSO variants (chaotic HGSO and quantum HGSO)

Name	Incorporated method	Application	Datasets/Benchmark functions	Evaluation metrics	Improvement	References
CHGSO	Chaotic Chebyshev map, chaotic iterative map, chaotic Gauss/mouse map, chaotic circle map, chaotic piecewise map, chaotic logistic map, chaotic singer, chaotic sine map, chaotic sinusoidal map, chaotic tent map	Engineering design problems	Cantilever beam design optimization problem, Welded beam design optimization problem, Grinding optimization problem, Diaphragm spring optimization problem	Best, Number of function evaluations (NFE), Workpiece removal parameter (WRP), NFE, Mass, Stress,	Convergence rate ameliorated Exploration and exploitation phases harmonized	[52]
CHGSO	Chaotic logistic map	Crude oil price prediction	WTI and Brent COTS datasets Theil's U and MAPE objective functions	EMA, SMA, KAMA, CCI, ROC, RSI, ATR, VR, HHLL, Phillips-Perron test	Exploration and exploitation phases enhanced, Local optima prevented	[103]
HOC	OBL strategy, Chaotic logic map	ORPD problem	Three objective functions: VD, Power loss, VSI IEEE 14 bus, IEEE 30 bus, IEEE 57 bus, IEEE 118 bus and IEEE 300 bus systems	Best	Initial population quality improved, convergence speed enhanced, exploration phase improved	[104]

HGSO-WIB-ReLU	Chaotic Chebyshev map, chaotic Gauss/mouse map, chaotic circle map, chaotic piecewise map, chaotic iterative map, chaotic tent map, chaotic singer, chaotic sinusoidal map, chaotic sine map	DDoS attack detection	CIC Dos Attacks, Buet-DDoS2020 and Low Rate DDoS datasets	Accuracy, α-error, F-measure	The worst positions of HGSO algorithm enhanced	[123]
CHGSO	Chaotic Chebyshev map, chaotic circle map, chaotic Gauss, chaotic iterative map, chaotic sine map, chaotic tent map	Transportation	Open Street Map database (India)	Packet delivery ratio, Average latency, Throughput	Global optimal solutions obtained	[105]
CHGSO-FAT	Chaotic maps, FAT	Liquid level control	TTSIS	Mean, Median, std, Settling time, Peak time, Rise time, Peak overshoot	Global optimal achieved	[106]
cHGSO	Self-adaptive weighting strategy, Chaotic logistic map	Hybrid PV/Diesel/ Battery energy system optimization problem	10 benchmark functions, Hybrid PV/Diesel/Battery energy system in Yarkant, Xinjiang Uyghur Autonomous Region (China) Three objective functions: load loss probability, system's annual cost, CO_2 emission	Avg, std	Exploration and exploitation phases harmonized, local optima prevented	[107]
CHGSO	Chaotic Chebyshev map, chaotic Gauss/mouse map,	Medical	EEG microstates dataset	Precision, Accuracy,	Convergence rate boosted	[108]

	chaotic iterative map chaotic circle map, chaotic logistic map, chaotic piecewise map, chaotic singer, chaotic sinusoidal map, chaotic sine map, chaotic tent map			Specificity, Sensitivity, F1-Score, MCC, Mode, Median, Mean	Exploration and exploitation phases harmonized	
CHSGSO	Chaotic sine map	Mobile edge computing, Blockchain networks	Blockchain networks having various blockchain users located on a square having a side of 1000 m and its center is occupied by the MEC server	Mean, std, Friedman's test Wilcoxon's rank-sum test	Exploration and exploitation phases balanced, convergence rate speeded up	[109]
CHGSO	Chaotic logistic map	Global optimization, Soil image classification	23 benchmark functions from CEC2005, Soil image dataset	Mean, Std, Recall, Accuracy, F1-Score, Precision	Exploration and exploitation phases improved	[110]
CHGSO	Chaotic system	Global optimization	47 benchmark functions	Mean, Std	Initialization enhanced, Exploration and exploitation phases improved	[111]
CHGSO	Chaotic map	Power system	Microgrid system		Initialization enhanced, Exploration and exploitation phases improved	[112]
CHGSO	Duffing-Van Der Pol chaotic system	DC motor speed control	NIST-800 22 tests, 47 benchmark functions, error-based ITSE objective function	Overshoot, Rise time, Settling time	Initialization enhanced, Exploration and exploitation phases improved	[113]

QHGSO	Chaotic efficient-based quantum behavior mechanism	Global optimization, Engineering design problems	47 benchmark functions from CEC'05 test suite, 3 engineering design problems: pressure vessel design, welded beam design, tension/compression spring design	Mean, std, Friedman's test Wilcoxon's rank-sum test	Exploration and exploitation phases balanced	[114]

Table 6
MHGSO variants (multi-objective HGSO).

Name	Incorporated method	Application	Datasets/Benchmark functions	Evaluation metrics	Improvement	References
MOO-HGSO	Weighted sum approach	CHP	Griewank, Rastrigin and Bohachevisky benchmark functions, CHP system in Thailand	Mean, std	Algorithm performance enhanced	[115]
MHGSO-AHP-VIKOR	Hybrid MCDM approaches, AHP, VIKOR approaches	Energy management,	Energy consumption dataset	Pricing rates: time of use (ToU) and adaptive consumption level pricing scheme (ACLPS)	Optimal solution quality enhanced	[116]
MOHGSO	Effective archiving strategy, effective leader selection strategy, crowding distance computation	Benchmark functions, engineering design problems	Multi-objective benchmark functions: ZDT1, ZDT2, ZDT3, ZDT4, ZDT6, DTLZ1-DTLZ7 Engineering design problems: four-bar truss design problem, welded beam design problem, disk brake design problem, speed reducer design problem	IGD, SP, Wilcoxon signed-rank test	Convergence speed improved, local optima avoided, diversity of solutions ameliorated, exploration and exploitation phases harmonized	[117]

3.5. Quantum HGSO

In [114], the authors introduced the chaotic efficient-based quantum behavior mechanism into the HGSO to handle global optimization as well as engineering design problems. The QHGSO has been investigated on 47 benchmark functions from CEC'05 and three engineering design problems like pressure vessel design, welded beam design and tension/compression spring design problems. The outcomes from the simulation proved that the QHGSO yielded better results than HGSO, GOA, SSA, WOA, SCA, DA, MFO, GWO and ALO. Table 5 provides a brief description of the QHGSO.

3.6. Multi-objective HGSO

Table 6 portrays the multi-objective HGSO variants.

A multi-objective HGSO (MOO-HGSO) has been proposed in [115] to address the problem of combined heat power (CHP) plant system considering three factors, namely economy, exergy and energy (3E). Moreover, the conservation of the energy for the CHP system via heat energy exchanger (HEN) design was investigated. In the MOO-HGSO, the weighted sum approach has been employed to enhance the performance of the method. The proposed algorithm was validated on Griewank, Rastrigin and Bohachevisky benchmark functions and also on the CHP system in Thailand. The simulation results demonstrated that the MOO-HGSO was effective in enhancing the economy, energy and exergy efficiencies for the CHP system.

To tackle the problem of residential load management, the work in [116] proposed a technique known as MHGSO-AHP-VIKOR, which integrates the multi-objective HGSO, analytic hierarchy process (AHP) as well as VIKOR multi-criteria decision making (MCDM) approaches. The performance of the proposed technique has been examined on energy consumption dataset considering time of use (ToU) and adaptive consumption level pricing scheme (ACLPS). The simulation results demonstrated that the proposed MHGSO-AHP-VIKOR technique was effective and robust in saving energy cost and also in diminishing the peak load of customer household.

In [117], a multi-objective HGSO (MOHGSO) is employed to handle the multi-objective optimization problems along with engineering design problems. The developed MOHGSO algorithm introduces the effective archiving strategy and effective leader selection strategy based on crowding distance computation to boost the convergence speed and further ameliorate the diversity of solutions, respectively. The feasibility of the MOHGSO algorithm was ascertained on the multi-objective benchmark functions, namely ZDT1, ZDT2, ZDT3, ZDT4, ZDT6, DTLZ1-DTLZ7; and engineering design problems such as four-bar truss design, welded beam design, disk brake design and speed reducer design problems. The evaluation metrics utilized to attest the ability of the MOHGSO algorithm to accomplish the appropriate solutions are inverted generational distance (IGD), spacing (SP) and Wilcoxon signed-rank test. The experimental outcomes approved the superiority of the MOHGSO algorithm over MOGWO, MOEA/D and MSSA.

4. Henry Gas Solubility Optimization Applications

The conventional HGSO and its variants find their applications to a wide range of areas comprising computer science, electrical engineering, medical applications, engineering design problems, etc. The distribution of HGSO-related publications based on their application areas is illustrated in Fig. 3.

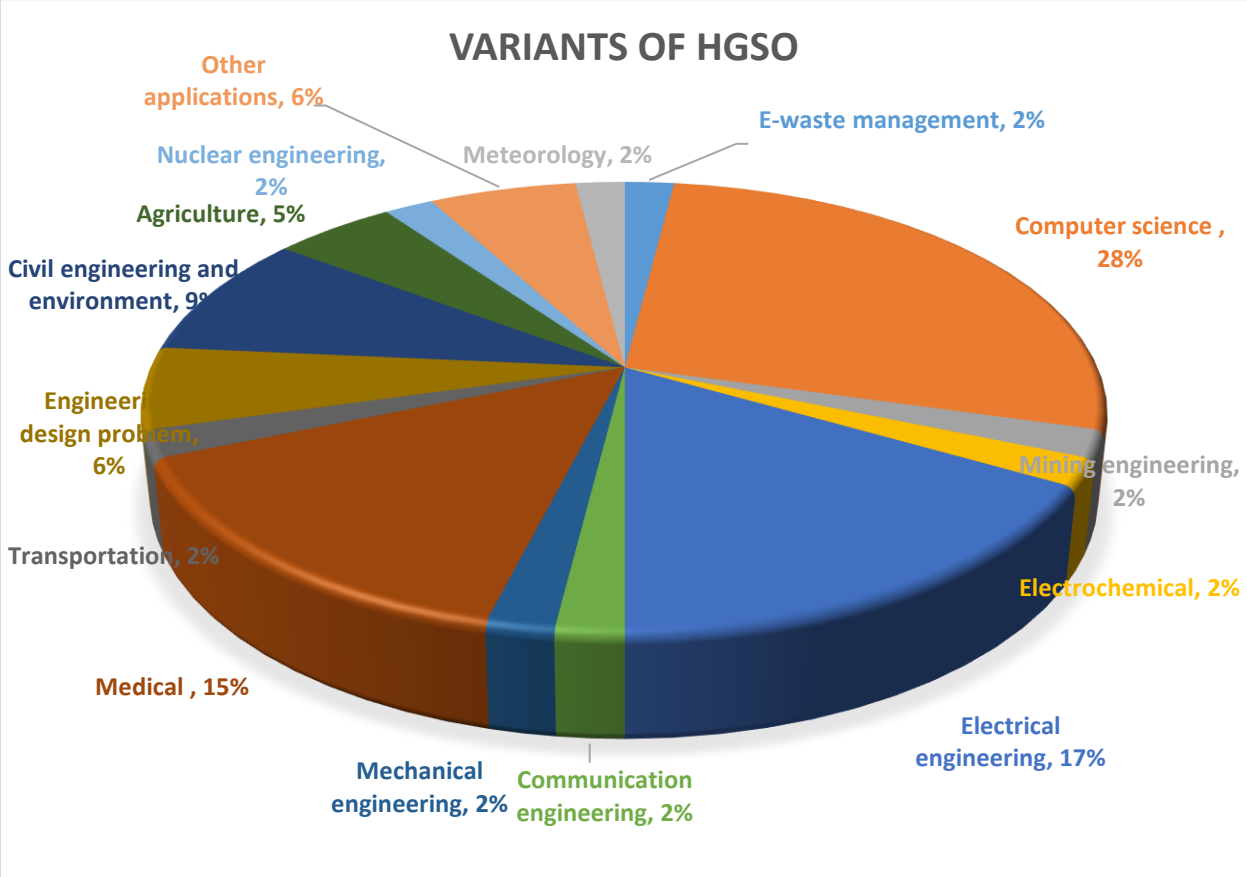


Fig. 3. Proportional distribution of HGSO-based publications in accordance with their areas of applications.

According to Fig. 3, the highest percentage (28%) belongs to computer science applications, followed by electrical engineering applications (17%), medical applications (15%). A summary of various areas of applications for HGSO variants along with their references is given in Table 7. Their details are presented in the next sections.

Table 7
HGSO Applications

Applications		Variant	References
Computer Science	Feature Selection	HGSO-KNN	[118]
		DHGHHD	[75]
		HGSOFS	[119]
		HGSO	[120]
		SFS-HGSO	[66]
		bEHGSO	[53]
		βHC-HGSO	[67]
		HGSOEO	[101]
	Feature Extraction	LHGSO-DFC	[83]
		HHBGGSO-HFE-EDH	[89]
	Classification	HGSO-OLSTM-JTCC	[121]
		HFCVO-DNM	[88]
		THGSO-DRN	[94]
		IIWFPO-SegNet	[96]
		HGSO-ADBN	[122]
	Image Processing	RHGSO-FC	[56]
		FHGSO-Deep CNN	[96]
	IoT	CSHGSO	[81]
	Blockchain Networks	CHSGSO	[109]
	DDoS Attack Detection	HGSO-WIB-RELU	[123]
		EHGSO-DNFN	[65]
	Data Mining	ANFIS-HGSO	[124]
		CSHGSO	[93]
	Cloud Computing	HGSWC	[74]
	Software Engineering	HHGSO	[72]
	Facial Emotion Recognition	HGSO-DLFER	[125]
	Machine Learning	SVR-HGSO	[126]
	Image Forgery Detection	SHGSO-DMN	[99]
	Global Optimization	bEGHSO	[53]
		BL-HGSO	[58]
		HHO-HGSO	[49]
		DOLHGSO	[76]
		EHHGSO	[97]
		QHGSO	[114]
		CHGSO	[111]
Electrical engineering	ORPD	HGSO	[128]
		HOC	[104]
	PMU	HGSO	[129]
	CHP	MOO-HGSO	[115]
	ELD	LR-HGSO	[69]
	Power system stability	HGSO-PID	[130]
		HGSO-PSS	[131]
		CHGSO-RENNN-PID	[112]
	Distribution systems	HGSO	[132]
	DC motor speed control	OBL-HGSO-PID	[62]
		HGSO-FPID	[133]
		CHGSO-PID	[113]

	Automatic voltage regulator		HGSO-FOPID	[134]
	Power LED driver		HHGSO-DL	[64]
	Hydropower reservoir		MVQIHGSO-SVM	[85]
	Energy management		MHGSO-AHP-VIKOR	[116]
	PRO		EHO	[73]
	Solar Photovoltaic		MHGSO	[70]
			HGSO	[135]
			EHGSO	[100]
			cHGSO	[107]
Electrochemical	PEMFC		HGSO	[136]
	SOFC		SAHGSO	[68]
Medical	Lung Cancer Detection		DHGSO	[77]
			MFABC-ACV-HGSO	[79]
	C-Section Prediction		HGSORF	[137]
	COVID-19 Detection		HGWWO-Deep GAN	[78]
			HGSO	[138]
	Diabetic Retinopathy Detection		Ar-HGSO-DCNN Ar-HGSO-shCNN	[80]
	Automatic Alcoholism Detection		HGSO-FFNN	[139]
	Epileptic Seizure Detection		Taylor HGSO	[57]
	Skin Cancer Detection		HGSO	[140]
	Brain Tumor Detection		HGBSO-DCNN	[92]
	Head Trauma Prediction		RF-SVM-AQO-HGSO	[84]
	Pediatric Sepsis Forecasting		SVM-RBF-HGSO	[141]
	Autism Spectrum Disorder Detection		FHGSO-DNFN	[90]
			CHGSO-ResNet101-Bi-GRU	[108]
			FHJO-CNN	[102]
	Prostate Cancer Detection		HFGSO-DBN	[87]
	Chronic Kidney Disease Detection		CKDD-HGSODL	[142]
			HSLnO	[82]
Engineering design problem			HGSO	[43]
			HHO-HGSO	[49]
			CHGSO	[52]
			QHGSO	[114]
			MOHGSO	[117]
			BL-HGSO DOLHGSO	[76]
Mechanical Engineering	FSW		HGSO-RVFL	[143]
	Fault Diagnosis		HGSO-ADBN	[145]
			HGSO-RBF	[146]
Civil engineering and environment			HGSO-ANFIS	[147]
			HGSO	[148]
			GMDH-HGSO	[149]
			GMDH-HGSO	[150]
			HGSO-SVR	[151]
			HGSO	[152]
			SVR-HGSO	[153]
			HGSO-SVR	[154]
			HGSO-SVR	[155]
			HGSO-RBFNN	[156]
			HGSO-RBFNN	[157]

Mining engineering		ANFIS-HGSO, MLP-HGSO	[158]
		ANFIS-HGSO	[159]
Communication Engineering		MKELMRF-OHGSA	[63]
		IIWGSO-DResNet	[95]
		EHGSO	[127]
Nuclear Engineering		HGSO-PID	[160]
		HGSO-PID	[161]
Transportation		CNN-OHGSO	[61]
		HHGSO	[55]
		HGSODL-TFF	[162]
Agriculture	Plant Leaf Disease Detection	ExpRHGSO-DNFN	[71]
		RHGSO-DNFN RHGSO-DRN	[98]
		MHGSO	[59]
	Soil Image Classification	HGSO-BOF	[163]
		CHGSO-BOF	[110]
E-waste management		FrHHGSO-ShCNN	[91]
		FHGSO-DCNN	[60]
Meteorology		HGSO	[164]
		HGSO	[165]
Other applications	Automotive industry	HGSO-RBF	[51]
	Bioinformatics	MHGSO	[54]
	Multi-object tracking	HGSO-UKF	[166]
	Crude oil price prediction	CHGSO	[103]
	Robotics	PI-HGSO	[50]
	Fabric defect detection	Inv3-MHL21-RELM	[86]
	Liquid level control	CHGSO-FAT	[106]

4.1. Computer Science

Different articles have been published employing the conventional HGSO and its variants to handle various optimization problems in the area of computer science applications as below:

4.1.1. Feature selection

As far as feature selection problems are concerned, the authors in [66, 75, 118, 119, 120] presented various HGSO-based methods to handle them.

In [118], the HGSO has been used to tackle the feature selection problems. The effectiveness of the conventional HGSO has been ascertained on 18 datasets from UCI based on various metrics, namely average accuracy, average fitness, average number of selected features, average CPU time and overall selection ratio. In addition, the Wilcoxon's rank sum test has been performed to examine the significance of the accuracy results of the proposed approach in comparison with DA, GOA, WOA, SSA and GWO. The simulation results approved the supremacy of the HGSO in dealing with the feature selection problems.

In [119], the HGSO and Equilibrium Optimizer (EO) algorithms have been employed with three classifiers, namely RF, Naive Bayes (NB) and k-Nearest Neighbor (KNN), respectively to solve the feature selection (FS) problem. The proposed HGSFC and EOFS techniques have been ascertained on 10 datasets (Banknote, Iris, Authentication, Wine, Glass, Segment, Spambase, Lung Cancer, Libras Movement, Musk and Hill-Valley). The results obtained by the simulation revealed that the HGSOFC outperformed EOFS, FAFS and PSOFS in providing the best accuracy and the least number of features.

The authors in [120] proposed a model known as MFSFL-IDS (metaheuristics feature selection with fuzzy logic enabled intrusion detection system) for intrusion detection in IoT platform. Initially, the data preprocessing was performed for obtaining the adequate data format. Afterwards, the HGSO was employed for feature selection. Finally, the binary bat algorithm (BBA) has been utilized to optimally tune the parameters of the ANFIS (adaptive network-based fuzzy inference system) and thereby to recognize and classify the network intrusion detection. The efficacy of the MFSFL-IDS model was examined on the Kaggle dataset considering different evaluation metrics like specificity, accuracy, recall, MCC, F-Score, Kappa score and threat score. The experimental results attest the supreme outperformance of the MFSFL-IDS models over RF-RF, RF-Feature Selection with Recursive Feature Elimination (RFECV), RF-recursive feature elimination (RFE), XGB-RF, RF-weighted feature selection (WFS) and RF-Select K models.

4.1.2. Feature extraction

The HGSO variants have been presented in [83, 89] to cope with the feature extraction problems.

4.1.3. Classification

Classification problems are solved by employing the HGSO and its variants in [88, 94, 96, 121, 122].

In order to classify the emotions for Japanese tweets, the HGSO has been employed in [121] to optimally find the hyperparameters of the OLSTM-JTCC (optimal long short-term memory-based Japanese tweet emotion classification) model in wireless networks. The performance metrics considered in this work are accuracy, recall, precision and F-Score. The simulation results proved that the HGSO-OLSTM-JTCC method was effective to classify the Japanese tweet emotion.

The authors in [122], presented a novel technique to Group Recommender System (GRS). In the proposed technique, a Text Convolutional Neural Network (TCNN) is used for feature extraction and an adaptive deep belief network (ADBN) is utilized to yield efficient recommendations which are finally optimized by HGSO algorithm. The presented technique was investigated on four datasets and benchmarked with other approaches like Neural Networks (NN), SVM, DBN as well as DNN. The simulation results indicated that the HGSO-ADBN technique gives better results than other methods based on MAP (Mean Average Precision) indicator.

4.1.4. Image Processing

To address the image processing problems, the HGSO variants have been employed in [56, 96].

4.1.5. IoT

IoT applications employing the HGSO variant are illustrated in [81].

4.1.6. DDoS Attack Detection

The problems related to DDoS attack detection are handled by the authors in [65, 123] by utilizing the HGSO along with its variants.

In [123], the HGSO is employed to optimize the WIB-RELU model so as to classify various DDoS attacks including DNS flood attacks, HTTP flood attacks as well ICMP flood attacks. The datasets utilized in this work are CIC DoS, Low Rate DDoS, and BUET-DDoS2020. The HGSO-WIB-RELU approach has been benchmarked with DASC, ARIMA, and SADBSCAN approaches. The evaluation metrics considered are α error, accuracy, F1 measure, memory utilization and detection rate. The simulation outcomes demonstrated the superiority of the HGSO-WIB-RELU approach in comparison with other approaches.

4.1.7. Data Mining

In the context of data mining, the authors in [93, 124] coped with data mining problems through HGSO as well as its variants.

In [124], the ANFIS-HGSO model has been implemented to tackle the problem related to the student performance prediction (SPP). In this work, the optimal parameters of ANFIS are achieved via HGSO. The ANFIS-HGSO performance was examined on the Kalboard 360 dataset based on four measurement indicators, namely F-measure, recall, accuracy and precision. The experimental results illustrated that the ANFIS-HGSO achieved better results than ANFIS-PSO, ANFIS-CS, ANFIS-BA and ANFIS-ACO in solving the SPP problem

4.1.8. Cloud Computing

The authors in [74] used the HGSO variant to address cloud computing optimization problems.

4.1.9. Software Engineering

In [72], the software engineering optimization problems have been handled via the HGSO variant.

4.1.10. Facial Emotion Recognition

To address the problem of facial emotion recognition (FER), the authors in [125] proposed a HGSO-DLFER technique. In this study, the HGSO has been utilized to optimize the DLFER (data learning based FER) model. The effectiveness of the HGSO-DLFER has been evaluated on the CK database based on various evaluation metrics like accuracy, specificity, sensitivity, MCC and F-score. The simulation results confirmed that the HGSO-DLFER was effective for identifying and recognizing different kinds of facial emotions.

4.1.11. Machine Learning

In [126], the HGSO has been used to optimally adjust the parameters of SVRs so as to achieve the convergence stability along with high predictive accuracy. The effectiveness of the presented SVR-HGSO has been evaluated on the ten datasets containing both low and high-dimensional data. The evaluation metrics considered in this study are computation complexity, prediction accuracy as well as convergence performance. The experimental results approved the supremacy of the HGSO-SVR over SVR, SVR-ALO, SVR-SSA, SVR-PSO, SVR-DA and SVR-FA methods.

4.1.12. Image Forgery Detection

The SHGSO-DMN model has been employed in [99] to detect and classify the image forgery.

4.1.13. Global Optimization

The global optimization problems have been addressed in bEGHSO [53], BL-HGSO [58], HHO-HGSO [49], DOLHGSO [76], EHHGSO [97], QHGSO [114], [110], [111].

4.2. Electrical Engineering

The applications of the HGSO and its variants in various areas of electrical engineering are explained in the following sections:

4.2.1. ORPD

The author in [104, 128] presented the solutions of the ORPD problem by employing the HGSO-based algorithm.

In [128], the HGSO is employed to deal with the ORPD problem. Its feasibility has been investigated on the IEEE 14-, 30-, 57-, 118- and 300-bus systems. The objective functions considered in this study are the minimization of the VD, power losses and voltage stability index (VSI). The experimental results affirmed the robustness of the HGSO for solving the ORPD problem.

4.2.2. Phasor measurement unit

In [129], the HGSO has been employed to optimally allocate the phasor measurement units (PMUs) with and without taking into consideration Zero Injection Buses (ZIBs). The effectiveness of the HGSO has been examined on IEEE 14-bus and 30-bus systems. The simulation results illustrated that the HGSO is effective for optimal PMU placement.

4.2.3. Combined heat and power (CHP)

The HGSO variant named as MOO-HGSO has been utilized in [115] to address the CHP problem.

4.2.4. Economic load dispatch (ELD)

The authors in [69] handled the ELD problem through the HGSO variant known as LR-HGSO.

4.2.5. Power system stability

In [130], the HGSO algorithm is utilized to find the optimal parameters of the static VAR compensator (SVC) to ameliorate the voltage stability as well as rotor angle stability. The effectiveness of the HGSO-based PID controller was examined on the single machine infinite bus system taking into account three-phase short circuit fault and input mechanical power disturbance. The simulation results confirmed the supremacy of the HGSO-based PID controller over the conventional PI-controller in providing better solutions.

The optimal parameters of a power system stabilizer (PSS) controller has been identified in [131] by using the HGSO. In this study, the objective function considered was the ITAE and the single-machine infinite-bus (SMIB) system was used to assess the effectiveness of the HGSO. The simulation results illustrated that the HGSO-based PSS controller accomplished better results than ASO-based PSS.

In [112], a linear model has been proposed to tackle the small-stability problem in microgrids under diverse uncertainties. The optimal gain values of the PI controller have been obtained by the proposed CHGSO-RENNN model.

4.2.6. Distribution systems

In [132], the HGSO has been used to determine the optimal parameters of the PI controller along with optimal coefficients of the droop control for an islanded microgrid. The objective function considered in this study is the ITAE. The effectiveness of the HGSO has been evaluated on an islanded MG with a 70 kW (0.7 p.u.) considering both fixed cyclic load and continuous cyclic load scenarios. The simulation results affirmed the supremacy of the HGSO over ALO and PSO for the studied problem.

4.2.7. DC Motor Speed Control

The authors in [62, 113, 133] tackled the problem related to the regulation of the DC motor speed via the HGSO-based algorithms.

The optimal parameters of the PID controller have been identified in [113] for the DC speed control by using the CHGSO. The objective function minimized was the ITSE (integral of the time-weighted square error). The DC motor system was employed to assess the performance of the CHGSO-PID model in comparison with HGSO-PID, PSO-PID, WOA-PID, GWO-PID, EA (evolutionary algorithm)-PI and SA-PID. The experimental results revealed that the proposed CHGSO-PID model achieved the least values of settling time, rise time and overshooting in comparison with its counterparts.

In [133], the HGSO has been employed to determine the optimal parameters of the fractionalized PID (FPID) controller so as to regulate the speed of a DC motor. The proposed HGSO-FPID controller and Matsuda approximation approach were used to minimize the objective function known as the ITAE. The effectiveness of the proposed model was investigated on the DC motor system and compared with PSO-PID, GWO-PID, IWO-PID, ASOA-PID, SCA-PID and SFS-PID. The simulation results based on frequency-domain, time-domain and disturbance rejection analysis demonstrated the superiority of the HGSO-FPID model over other models to provide strong output disturbance rejection and the least values of overshoot.

4.2.8. Automatic Voltage Regulator

The authors in [134] employed the HGSO to optimally determine the gain parameters of a FOPID controller for automatic voltage regulator (AVR) considering the minimization of the effective time domain objective function. The simulation results attested the supremacy the HGSO-FOPID controller over SSA-FOPID, IKA-PID and SFS-PID controllers.

4.2.9. Power LED driver

The LED power driver system has been modelled in [64] through deep learning method optimized by the hybridized HGSO variant with deep-learning.

4.2.10. Hydropower reservoir

The optimal operation model of a hydropower model has been established in [85] by employing the hybridized HGSO variant combined with SVM.

4.2.11. Energy management

The problem related to the energy management for smart homes has been dealt with the multi-objective HGSO in [116].

4.2.12. Pressure Retarded Osmosis (PRO)

The applications of the HGSO-based algorithm on PRO are presented in [73].

4.2.13. Solar photovoltaic

Some works in [70, 107, 135] proposed the HGSO-related algorithms to identify the optimal parameters of a variety of PV models.

Table 8
Merits and demerits of HGSO

Merits [43, 160, 161]	Demerits [58, 62, 70, 75]
Facility in implementation	Slow convergence speed
Less control parameters (i.e., $S_{i,j}$, γ, F)	Trend to be stuck in local optima
Better adjustability	Having a single position updating mechanism
Ability to harmonize exploration and exploitation phases	Poor exploitation ability
Easiness in making hybridized algorithms with other metaheuristics	

Table 9
Comparison results for the HGSO against its variants on the unimodal test functions

Function	Dimension	Metrics	HGSO [43]	OHGSO [61]	QHGSO [114]	HHO-HGSO [49]	SAHGSO [68]	SHGSO [99]	CHSGSO [109]	MVQIHGSO [85]	HFGSO [87]	HHBGGSO [89]	ACVHGSO [79]	Ar-HGSO [80]
F_1	10	Avg	9.31E+08	8.57E+08	1.05E+09	6.50E+03	1.00E+09	5.63E+08	6.52E+09	7.47E+05	4.36E+09	7.28E+07	4.28E+09	8.81E+09
		Min	3.10E+08	3.13E+08	2.97E+08	**1.29E+02**	3.72E+08	2.10E+08	3.35E+09	2.92E+05	1.66E+09	1.36E+07	1.80E+09	5.17E+09
		Std	3.61E+08	3.54E+08	8.82E+08	1.52E+04	3.95E+08	2.52E+08	1.73E+09	3.87E+05	1.24E+09	6.20E+07	1.34E+09	1.70E+09
		Rank	6	7	5	**1**	8	4	11	2	9	3	10	12
	30	Avg	2.00E+10	2.02E+10	1.54E+10	4.35E+06	1.95E+10	3.89E+10	4.75E+10	6.00E+08	4.02E+10	4.98E+09	3.57E+10	5.17E+10
		Min	1.24E+10	1.32E+10	1.03E+10	**1.41E+06**	1.36E+10	2.37E+10	3.97E+10	2.30E+08	3.10E+10	2.50E+09	3.00E+10	4.56E+10
		Std	4.48E+09	3.40E+09	3.21E+09	3.43E+06	3.33E+09	6.96E+09	3.66E+09	2.03E+08	4.76E+09	1.51E+09	2.09E+09	2.23E+09
		Rank	5	6	4	**1**	7	8	11	2	10	3	9	12
	50	Avg	5.97E+10	6.06E+10	5.06E+10	1.21E+08	5.81E+10	1.12E+11	1.08E+11	7.67E+09	9.57E+10	2.15E+10	8.85E+10	1.17E+11
		Min	3.70E+10	4.98E+10	3.74E+10	**4.04E+07**	3.85E+10	8.00E+10	9.92E+10	5.26E+09	7.96E+10	1.06E+10	8.23E+10	1.01E+11
		Std	9.99E+09	8.05E+09	7.20E+09	7.18E+07	8.37E+09	1.00E+10	4.73E+09	1.72E+09	7.22E+09	6.18E+09	3.25E+09	4.46E+09
		Rank	4	7	5	**1**	6	9	11	2	8	3	10	12
	100	Avg	1.99E+11	1.88E+11	1.73E+11	7.13E+09	1.91E+11	2.59E+11	2.74E+11	6.72E+10	2.57E+11	1.01E+11	2.34E+11	2.71E+11
		Min	1.56E+11	1.63E+11	1.51E+11	**1.41E+09**	1.50E+11	2.35E+11	2.67E+11	4.93E+10	2.38E+11	7.35E+10	2.18E+11	2.63E+11
		Std	1.81E+10	1.62E+10	1.08E+10	7.14E+09	1.58E+10	6.86E+09	3.45E+09	7.88E+09	7.93E+09	1.23E+10	6.25E+09	4.06E+09
		Rank	6	7	5	**1**	4	9	12	2	10	3	8	11
F_3	10	Avg	2.01E+03	1.97E+03	3.28E+03	3.02E+02	2.17E+03	5.88E+03	7.98E+03	9.70E+02	5.71E+03	1.57E+03	5.76E+03	1.06E+04
		Min	5.70E+02	8.08E+02	7.18E+02	**3.00E+02**	8.95E+02	1.08E+03	5.15E+03	5.14E+02	2.85E+03	5.38E+02	3.48E+03	5.21E+03
		Std	1.12E+03	8.21E+02	2.64E+03	1.10E+01	1.07E+03	2.14E+03	1.70E+03	3.44E+02	1.55E+03	7.68E+02	8.36E+02	3.04E+03
		Rank	4	6	5	**1**	7	8	11	2	9	3	10	12
	30	Avg	6.18E+04	6.17E+04	5.81E+04	2.75E+04	5.84E+04	8.69E+04	8.02E+04	5.89E+04	8.50E+04	5.60E+04	7.28E+04	8.77E+04
		Min	4.50E+04	4.48E+04	4.25E+04	**1.18E+04**	4.16E+04	7.14E+04	6.11E+04	3.85E+04	6.73E+04	3.38E+04	6.59E+04	7.33E+04
		Std	6.40E+03	7.28E+03	8.78E+03	8.18E+03	8.18E+03	9.61E+03	5.80E+03	7.39E+03	6.24E+03	9.84E+03	2.91E+03	4.70E+03
		Rank	7	6	5	**1**	4	11	8	3	10	2	9	12

Table 9
(Continued)

Function	Dimension	Metrics	HGSO [43]	OHGSO [61]	QHGSO [114]	HHO-HGSO [49]	SAHGSO [68]	SHGSO [99]	CHSGSO [109]	MVQIHGSO [85]	HFGSO [87]	HHBGGSO [89]	ACVHGSO [79]	Ar-HGSO [80]
	50	Avg	1.67E+05	1.66E+05	1.81E+05	1.08E+05	1.68E+05	1.84E+05	1.75E+05	1.60E+05	2.31E+05	1.89E+05	1.69E+05	3.63E+07
		Min	1.44E+05	1.48E+05	1.27E+05	**7.61E+04**	1.39E+05	1.61E+05	1.49E+05	1.34E+05	1.53E+05	1.19E+05	1.48E+05	2.11E+05
		Std	1.12E+04	1.10E+04	3.67E+04	1.68E+04	1.16E+04	1.64E+04	1.19E+04	1.13E+04	6.56E+04	3.14E+04	1.02E+04	1.32E+08
		Rank	6	8	3	**1**	5	11	9	4	10	2	7	12
	100	Avg	1.99E+11	1.88E+11	1.73E+11	7.13E+09	1.91E+11	2.59E+11	2.74E+11	6.72E+10	2.57E+11	1.01E+11	2.34E+11	2.71E+11
		Min	3.20E+05	3.17E+05	5.75E+05	**2.76E+05**	3.06E+05	3.29E+05	3.09E+05	2.99E+05	4.18E+05	3.10E+05	3.25E+05	3.34E+05
		Std	8.98E+03	1.01E+04	1.88E+09	1.68E+04	9.74E+03	2.63E+04	8.52E+03	1.21E+04	7.76E+05	1.79E+04	3.51E+09	2.46E+06
		Rank	7	6	12	**1**	3	9	4	2	11	5	8	10
Friedman Test	10	Average Rank	5	6.5	5	1	7.5	6	11	2	9	3	10	12
		Overall Rank	4	7	4	**1**	8	6	11	2	9	3	10	12
	30	Average Rank	6	6	4.5	1	5.5	9.5	9.5	2.5	10	2.5	9	12
		Overall Rank	6	6	4	**1**	5	9	9	2	11	2	8	12
	50	Average Rank	5	6	4.5	1	5.5	9.5	9.5	2.5	10	2.5	9	12
		Overall Rank	5	7	4	**1**	6	9	9	2	11	2	8	12
	100	Average Rank	6.5	6.5	8.5	1	3.5	9	8	2	10.5	4	8	10.5
		Overall Rank	5	5	9	**1**	3	10	7	2	11	4	7	11
Effectiveness	10	W/T/L	0/0/2	0/0/2	0/0/2	**2/0/0**	0/0/2	0/0/2	0/0/2	0/0/2	0/0/2	0/0/2	0/0/2	0/0/2
	30	W/T/L	0/0/2	0/0/2	0/0/2	**2/0/0**	0/0/2	0/0/2	0/0/2	0/0/2	0/0/2	0/0/2	0/0/2	0/0/2
	50	W/T/L	0/0/2	0/0/2	0/0/2	**2/0/0**	0/0/2	0/0/2	0/0/2	0/0/2	0/0/2	0/0/2	0/0/2	0/0/2
	100	W/T/L	0/0/2	0/0/2	0/0/2	**2/0/0**	0/0/2	0/0/2	0/0/2	0/0/2	0/0/2	0/0/2	0/0/2	0/0/2

Table 10
Comparison results for the HGSO against its variants on the multimodal test functions

Function	Dimension	Metrics	HGSO [43]	OHGSO [61]	QHGSO [114]	HHO-HGSO [49]	SAHGSO [68]	SHGSO [99]	CHSGSO [109]	MVQIHGSO [85]	HFGSO [87]	HHBGGSO [89]	ACVHGSO [79]	Ar-HGSO [80]
F_4	10	Avg	4.722E+02	4.666E+02	4.536E+02	4.134E+02	4.575E+02	4.420E+02	7.862E+02	4.032E+02	5.806E+02	4.600E+02	5.906E+02	1.337E+03
		Min	4.399E+02	4.266E+02	4.225E+02	**4.001E+02**	4.207E+02	4.148E+02	5.304E+02	4.003E+02	4.668E+02	4.094E+02	4.987E+02	9.528E+02
		Std	1.780E+01	1.909E+01	3.019E+01	2.354E+01	2.048E+01	1.503E+01	1.289E+02	1.500E+00	7.381E+01	4.888E+01	5.257E+01	2.949E+02
		Rank	8	7	6	**1**	5	4	11	2	9	3	10	12
	30	Avg	3.965E+03	3.860E+03	2.888E+03	5.328E+02	4.044E+03	6.127E+03	1.313E+04	5.808E+02	9.596E+03	1.837E+03	9.098E+03	1.698E+04
		Min	1.423E+03	1.528E+03	1.679E+03	**4.849E+02**	1.699E+03	3.075E+03	1.027E+04	5.227E+02	6.068E+03	7.730E+02	6.433E+03	1.395E+04
		Std	1.327E+03	1.053E+03	1.304E+03	2.663E+01	1.032E+03	1.346E+03	1.637E+03	3.292E+01	1.454E+03	8.878E+02	1.373E+03	1.181E+03
		Rank	4	5	6	**1**	7	8	11	2	9	3	10	12
	50	Avg	1.238E+04	1.162E+04	8.382E+03	7.232E+02	1.159E+04	2.394E+04	3.246E+04	1.477E+03	2.545E+04	4.998E+03	1.914E+04	4.293E+04
		Min	6.293E+03	7.731E+03	5.696E+03	**5.457E+02**	7.272E+03	1.548E+04	2.492E+04	1.063E+03	1.819E+04	2.356E+03	1.611E+04	3.440E+04
		Std	2.552E+03	2.378E+03	1.596E+03	6.614E+01	2.330E+03	4.236E+03	3.346E+03	2.065E+02	3.375E+03	1.755E+03	1.586E+03	3.262E+03
		Rank	5	7	4	**1**	6	8	11	2	10	3	9	12
	100	Avg	4.436E+04	4.630E+04	3.623E+04	1.879E+03	4.162E+04	8.572E+04	1.008E+05	8.844E+03	8.989E+04	2.327E+04	7.168E+04	1.137E+05
		Min	2.954E+04	2.674E+04	2.681E+04	**1.283E+03**	2.831E+04	6.847E+04	8.502E+04	5.273E+03	7.141E+04	1.265E+04	6.180E+04	9.040E+04
		Std	8.371E+03	7.519E+03	6.038E+03	5.925E+02	6.993E+03	1.111E+04	8.531E+03	1.827E+03	8.519E+03	4.966E+03	5.201E+03	7.566E+03
		Rank	7	4	5	**1**	6	9	11	2	10	3	8	12
F_5	10	Avg	5.542E+02	5.561E+02	5.503E+02	5.393E+02	5.543E+02	5.513E+02	5.809E+02	5.179E+02	5.846E+02	5.643E+02	5.733E+02	6.332E+02
		Min	5.462E+02	5.395E+02	5.325E+02	5.160E+02	5.317E+02	5.321E+02	5.420E+02	**5.091E+02**	5.727E+02	5.277E+02	5.631E+02	6.004E+02
		Std	5.441E+00	6.856E+00	8.686E+00	1.379E+01	8.568E+00	8.086E+00	1.073E+01	5.143E+00	8.295E+00	1.514E+01	6.447E+00	1.538E+01
		Rank	9	7	6	2	4	5	8	**1**	11	3	10	12
	30	Avg	8.420E+02	8.428E+02	8.004E+02	7.134E+02	8.419E+02	8.693E+02	9.110E+02	7.108E+02	9.159E+02	8.601E+02	9.130E+02	9.585E+02
		Min	7.841E+02	8.053E+02	7.582E+02	**6.278E+02**	8.001E+02	8.003E+02	8.505E+02	6.773E+02	8.715E+02	7.879E+02	8.909E+02	9.174E+02
		Std	2.712E+01	1.839E+01	1.941E+01	3.851E+01	1.818E+01	2.620E+01	1.777E+01	1.700E+01	1.849E+01	3.008E+01	1.261E+01	1.907E+01
		Rank	4	8	3	**1**	6	7	9	2	10	5	11	12
	50	Avg	1.111E+03	1.115E+03	1.066E+03	8.601E+02	1.102E+03	1.202E+03	1.209E+03	9.585E+02	1.208E+03	1.094E+03	1.164E+03	1.248E+03
		Min	1.029E+03	1.032E+03	1.018E+03	**7.853E+02**	1.037E+03	1.088E+03	1.149E+03	8.739E+02	1.157E+03	1.025E+03	1.137E+03	1.189E+03
		Std	3.138E+01	3.305E+01	3.270E+01	4.027E+01	2.446E+01	3.487E+01	2.322E+01	2.611E+01	2.203E+01	3.563E+01	1.639E+01	2.629E+01
		Rank	5	6	3	**1**	7	8	10	2	11	4	9	12
	100	Avg	1.943E+03	1.948E+03	1.899E+03	1.476E+03	1.955E+03	2.098E+03	2.137E+03	1.767E+03	2.135E+03	1.940E+03	2.039E+03	2.149E+03
		Min	1.818E+03	1.847E+03	1.795E+03	**1.395E+03**	1.869E+03	2.016E+03	2.076E+03	1.663E+03	2.061E+03	1.833E+03	1.968E+03	2.097E+03
		Std	4.819E+01	4.386E+01	5.836E+01	4.647E+01	4.105E+01	3.332E+01	3.005E+01	3.830E+01	3.433E+01	6.520E+01	2.512E+01	2.655E+01
		Rank	4	6	3	**1**	7	9	11	2	10	5	8	12
F_6	10	Avg	6.292E+02	6.289E+02	6.188E+02	6.217E+02	6.254E+02	6.254E+02	6.451E+02	6.095E+02	6.463E+02	6.361E+02	6.500E+02	6.555E+02
		Min	6.194E+02	6.202E+02	6.102E+02	6.064E+02	6.119E+02	6.127E+02	6.308E+02	**6.021E+02**	6.347E+02	6.124E+02	6.380E+02	6.386E+02
		Std	5.189E+00	5.444E+00	5.006E+00	1.030E+01	6.490E+00	6.240E+00	4.840E+00	3.579E+00	5.735E+00	1.056E+01	5.192E+00	6.316E+00
		Rank	7	8	3	2	4	6	9	**1**	10	5	11	12

Table 10
(Continued)

Function	Dimension	Metrics	HGSO [43]	OHGSO [61]	QHGSO [114]	HHO-HGSO [49]	SAHGSO [68]	SHGSO [99]	CHSGSO [109]	MVQIHGSO [85]	HFGSO [87]	HHBGGSO [89]	ACVHGSO [79]	Ar-HGSO [80]
F_4	10	Avg	4.722E+02	4.666E+02	4.536E+02	4.134E+02	4.575E+02	4.420E+02	7.862E+02	4.032E+02	5.806E+02	4.600E+02	5.906E+02	1.337E+03
		Min	4.399E+02	4.266E+02	4.225E+02	**4.001E+02**	4.207E+02	4.148E+02	5.304E+02	4.003E+02	4.668E+02	4.094E+02	4.987E+02	9.528E+02
		Std	1.780E+01	1.909E+01	3.019E+01	2.354E+01	2.048E+01	1.503E+01	1.289E+02	1.500E+00	7.381E+01	4.888E+01	5.257E+01	2.949E+02
		Rank	8	7	6	**1**	5	4	11	2	9	3	10	12
	30	Avg	3.965E+03	3.860E+03	2.888E+03	5.328E+02	4.044E+03	6.127E+03	1.313E+04	5.808E+02	9.596E+03	1.837E+03	9.098E+03	1.698E+04
		Min	1.423E+03	1.528E+03	1.679E+03	**4.849E+02**	1.699E+03	3.075E+03	1.027E+04	5.227E+02	6.068E+03	7.730E+02	6.433E+03	1.395E+04
		Std	1.327E+03	1.053E+03	1.304E+03	2.663E+01	1.032E+03	1.346E+03	1.637E+03	3.292E+01	1.454E+03	8.878E+02	1.373E+03	1.181E+03
		Rank	4	5	6	**1**	7	8	11	2	9	3	10	12
	50	Avg	1.238E+04	1.162E+04	8.382E+03	7.232E+02	1.159E+04	2.394E+04	3.246E+04	1.477E+03	2.545E+04	4.998E+03	1.914E+04	4.293E+04
		Min	6.293E+03	7.731E+03	5.696E+03	**5.457E+02**	7.272E+03	1.548E+04	2.492E+04	1.063E+03	1.819E+04	2.356E+03	1.611E+04	3.440E+04
		Std	2.552E+03	2.378E+03	1.596E+03	6.614E+01	2.330E+03	4.236E+03	3.346E+03	2.065E+02	3.375E+03	1.755E+03	1.586E+03	3.262E+03
		Rank	5	7	4	**1**	6	8	11	2	10	3	9	12
	100	Avg	4.436E+04	4.630E+04	3.623E+04	1.879E+03	4.162E+04	8.572E+04	1.008E+05	8.844E+03	8.989E+04	2.327E+04	7.168E+04	1.137E+05
		Min	2.954E+04	2.674E+04	2.681E+04	**1.283E+03**	2.831E+04	6.847E+04	8.502E+04	5.273E+03	7.141E+04	1.265E+04	6.180E+04	9.040E+04
		Std	8.371E+03	7.519E+03	6.038E+03	5.925E+02	6.993E+03	1.111E+04	8.531E+03	1.827E+03	8.519E+03	4.966E+03	5.201E+03	7.566E+03
		Rank	7	4	5	**1**	6	9	11	2	10	3	8	12
F_5	10	Avg	5.542E+02	5.561E+02	5.503E+02	5.393E+02	5.543E+02	5.513E+02	5.809E+02	5.179E+02	5.846E+02	5.643E+02	5.733E+02	6.332E+02
		Min	5.462E+02	5.395E+02	5.325E+02	5.160E+02	5.317E+02	5.321E+02	5.420E+02	**5.091E+02**	5.727E+02	5.277E+02	5.631E+02	6.004E+02
		Std	5.441E+00	6.856E+00	8.686E+00	1.379E+01	8.568E+00	8.086E+00	1.073E+01	5.143E+00	8.295E+00	1.514E+01	6.447E+00	1.538E+01
		Rank	9	7	6	2	4	5	8	**1**	11	3	10	12
	30	Avg	8.420E+02	8.428E+02	8.004E+02	7.134E+02	8.419E+02	8.693E+02	9.110E+02	7.108E+02	9.159E+02	8.601E+02	9.130E+02	9.585E+02
		Min	7.841E+02	8.053E+02	7.582E+02	**6.278E+02**	8.001E+02	8.003E+02	8.505E+02	6.773E+02	8.715E+02	7.879E+02	8.909E+02	9.174E+02
		Std	2.712E+01	1.839E+01	1.941E+01	3.851E+01	1.818E+01	2.620E+01	1.777E+01	1.700E+01	1.849E+01	3.008E+01	1.261E+01	1.907E+01
		Rank	4	8	3	**1**	6	7	9	2	10	5	11	12
	50	Avg	1.111E+03	1.115E+03	1.066E+03	8.601E+02	1.102E+03	1.202E+03	1.209E+03	9.585E+02	1.208E+03	1.094E+03	1.164E+03	1.248E+03
		Min	1.029E+03	1.032E+03	1.018E+03	**7.853E+02**	1.037E+03	1.088E+03	1.149E+03	8.739E+02	1.157E+03	1.025E+03	1.137E+03	1.189E+03
		Std	3.138E+01	3.305E+01	3.270E+01	4.027E+01	2.446E+01	3.487E+01	2.322E+01	2.611E+01	2.203E+01	3.563E+01	1.639E+01	2.629E+01
		Rank	5	6	3	**1**	7	8	10	2	11	4	9	12
	100	Avg	1.943E+03	1.948E+03	1.899E+03	1.476E+03	1.955E+03	2.098E+03	2.137E+03	1.767E+03	2.135E+03	1.940E+03	2.039E+03	2.149E+03
		Min	1.818E+03	1.847E+03	1.795E+03	**1.395E+03**	1.869E+03	2.016E+03	2.076E+03	1.663E+03	2.061E+03	1.833E+03	1.968E+03	2.097E+03
		Std	4.819E+01	4.386E+01	5.836E+01	4.647E+01	4.105E+01	3.332E+01	3.005E+01	3.830E+01	3.433E+01	6.520E+01	2.512E+01	2.655E+01
		Rank	4	6	3	**1**	7	9	11	2	10	5	8	12

Table 10
(Continued)

Function	Dimension	Metrics	HGSO [43]	OHGSO [61]	QHGSO [114]	HHO-HGSO [49]	SAHGSO [68]	SHGSO [99]	CHSGSO [109]	MVQIHGSO [85]	HFGSO [87]	HHBGGSO [89]	ACVHGSO [79]	Ar-HGSO [80]
F_6	10	Avg	6.292E+02	6.289E+02	6.188E+02	6.217E+02	6.254E+02	6.254E+02	6.451E+02	6.095E+02	6.463E+02	6.361E+02	6.500E+02	6.555E+02
		Min	6.194E+02	6.202E+02	6.102E+02	6.064E+02	6.119E+02	6.127E+02	6.308E+02	**6.021E+02**	6.347E+02	6.124E+02	6.380E+02	6.386E+02
		Std	5.189E+00	5.444E+00	5.006E+00	1.030E+01	6.490E+00	6.240E+00	4.840E+00	3.579E+00	5.735E+00	1.056E+01	5.192E+00	6.316E+00
		Rank	7	8	3	2	4	6	9	**1**	10	5	11	12
	30	Avg	6.776E+02	6.755E+02	6.573E+02	6.592E+02	6.754E+02	6.750E+02	6.886E+02	6.518E+02	6.934E+02	6.819E+02	6.912E+02	7.030E+02
		Min	6.628E+02	6.577E+02	6.475E+02	6.417E+02	6.657E+02	6.679E+02	6.778E+02	**6.363E+02**	6.834E+02	6.729E+02	6.814E+02	6.923E+02
		Std	5.765E+00	6.286E+00	5.496E+00	7.566E+00	5.294E+00	4.929E+00	5.031E+00	6.977E+00	4.717E+00	6.047E+00	4.591E+00	4.113E+00
		Rank	5	4	3	2	6	7	9	**1**	11	8	10	12
	50	Avg	6.934E+02	6.939E+02	6.790E+02	6.700E+02	6.913E+02	6.961E+02	7.053E+02	6.699E+02	7.085E+02	6.950E+02	7.051E+02	7.169E+02
		Min	6.851E+02	6.858E+02	6.698E+02	6.611E+02	6.814E+02	6.862E+02	6.901E+02	**6.575E+02**	7.021E+02	6.773E+02	6.984E+02	7.083E+02
		Std	4.107E+00	3.675E+00	5.290E+00	5.489E+00	3.669E+00	4.859E+00	4.499E+00	6.513E+00	3.393E+00	6.072E+00	2.867E+00	3.730E+00
		Rank	6	7	3	2	5	8	9	**1**	11	4	10	12
	100	Avg	7.029E+02	7.033E+02	6.947E+02	6.772E+02	7.039E+02	7.116E+02	7.140E+02	6.903E+02	7.173E+02	7.049E+02	7.120E+02	7.223E+02
		Min	6.955E+02	6.988E+02	6.843E+02	**6.700E+02**	6.965E+02	7.039E+02	7.085E+02	6.829E+02	7.121E+02	6.963E+02	7.069E+02	7.142E+02
		Std	3.201E+00	2.191E+00	4.273E+00	3.698E+00	2.978E+00	3.801E+00	2.631E+00	3.463E+00	2.444E+00	3.829E+00	2.371E+00	2.643E+00
		Rank	4	7	3	**1**	6	8	10	2	11	5	9	12
F_7	10	Avg	7.768E+02	7.783E+02	7.606E+02	7.725E+02	7.708E+02	7.960E+02	8.119E+02	7.413E+02	8.123E+02	7.768E+02	8.004E+02	8.237E+02
		Min	7.602E+02	7.629E+02	7.411E+02	7.305E+02	7.543E+02	7.600E+02	7.931E+02	**7.299E+02**	7.906E+02	7.466E+02	7.838E+02	7.908E+02
		Std	8.464E+00	7.083E+00	1.034E+01	2.422E+01	6.971E+00	1.764E+01	9.566E+00	6.485E+00	1.015E+01	1.694E+01	7.605E+00	1.080E+01
		Rank	7	8	3	2	5	6	12	**1**	10	4	9	11
	30	Avg	1.204E+03	1.206E+03	1.117E+03	1.166E+03	1.175E+03	1.493E+03	1.426E+03	1.022E+03	1.360E+03	1.258E+03	1.284E+03	1.495E+03
		Min	1.072E+03	1.098E+03	1.051E+03	**9.488E+02**	1.074E+03	1.374E+03	1.323E+03	9.632E+02	1.271E+03	1.128E+03	1.244E+03	1.399E+03
		Std	5.733E+01	6.152E+01	4.106E+01	9.024E+01	5.673E+01	4.398E+01	3.294E+01	2.901E+01	4.462E+01	9.090E+01	2.668E+01	3.265E+01
		Rank	4	6	3	**1**	5	11	10	2	9	7	8	12
	50	Avg	1.768E+03	1.762E+03	1.573E+03	1.703E+03	1.721E+03	2.182E+03	2.030E+03	1.436E+03	1.998E+03	1.876E+03	1.831E+03	2.102E+03
		Min	1.622E+03	1.606E+03	1.470E+03	1.401E+03	1.583E+03	2.071E+03	1.980E+03	**1.276E+03**	1.878E+03	1.665E+03	1.741E+03	2.013E+03
		Std	8.290E+01	8.826E+01	6.672E+01	9.236E+01	7.515E+01	4.825E+01	1.910E+01	6.286E+01	5.181E+01	9.172E+01	4.449E+01	3.545E+01
		Rank	6	5	3	2	4	12	10	**1**	9	7	8	11
	100	Avg	3.640E+03	3.635E+03	3.236E+03	3.331E+03	3.593E+03	4.193E+03	4.020E+03	3.034E+03	4.002E+03	3.780E+03	3.785E+03	4.124E+03
		Min	3.240E+03	3.318E+03	2.957E+03	3.088E+03	3.362E+03	3.914E+03	3.969E+03	**2.752E+03**	3.863E+03	3.446E+03	3.704E+03	4.063E+03
		Std	1.630E+02	1.600E+02	1.308E+02	1.231E+02	1.234E+02	7.898E+01	2.295E+01	1.456E+02	6.786E+01	1.464E+02	5.296E+01	2.901E+01
		Rank	4	5	2	3	6	10	11	**1**	9	7	8	12

Table 10
(Continued)

Function	Dimension	Metrics	HGSO [43]	OHGSO [61]	QHGSO [114]	HHO-HGSO [49]	SAHGSO [68]	SHGSO [99]	CHSGSO [109]	MVQIHGSO [85]	HFGSO [87]	HHBGGSO [89]	ACVHGSO [79]	Ar-HGSO [80]
F_8	10	Avg	8.359E+02	8.364E+02	8.306E+02	8.278E+02	8.353E+02	8.478E+02	8.515E+02	8.178E+02	8.558E+02	8.336E+02	8.471E+02	8.555E+02
		Min	8.283E+02	8.285E+02	8.180E+02	**8.090E+02**	8.267E+02	8.351E+02	8.390E+02	8.112E+02	8.416E+02	8.206E+02	8.379E+02	8.450E+02
		Std	3.962E+00	4.350E+00	5.866E+00	1.052E+01	4.301E+00	5.739E+00	6.359E+00	3.697E+00	5.479E+00	6.417E+00	5.338E+00	6.628E+00
		Rank	6	7	3	**1**	5	8	10	2	11	4	9	12
	30	Avg	1.085E+03	1.079E+03	1.047E+03	9.629E+02	1.077E+03	1.129E+03	1.137E+03	9.752E+02	1.145E+03	1.066E+03	1.125E+03	1.180E+03
		Min	1.017E+03	1.041E+03	1.015E+03	**9.087E+02**	1.015E+03	1.071E+03	1.107E+03	9.476E+02	1.078E+03	1.019E+03	1.091E+03	1.135E+03
		Std	2.146E+01	1.452E+01	1.802E+01	2.818E+01	1.945E+01	2.550E+01	1.451E+01	1.571E+01	1.771E+01	2.594E+01	1.283E+01	1.810E+01
		Rank	5	7	4	**1**	3	8	11	2	9	6	10	12
	50	Avg	1.434E+03	1.437E+03	1.386E+03	1.154E+03	1.429E+03	1.566E+03	1.535E+03	1.260E+03	1.508E+03	1.412E+03	1.500E+03	1.569E+03
		Min	1.379E+03	1.383E+03	1.327E+03	**1.073E+03**	1.381E+03	1.486E+03	1.476E+03	1.189E+03	1.440E+03	1.331E+03	1.460E+03	1.529E+03
		Std	2.204E+01	2.441E+01	2.954E+01	3.182E+01	2.786E+01	3.372E+01	2.319E+01	3.140E+01	2.790E+01	3.558E+01	1.868E+01	2.197E+01
		Rank	5	7	3	**1**	6	11	10	2	8	4	9	12
	100	Avg	2.392E+03	2.393E+03	2.290E+03	1.900E+03	2.391E+03	2.637E+03	2.625E+03	2.162E+03	2.606E+03	2.413E+03	2.498E+03	2.657E+03
		Min	2.224E+03	2.274E+03	2.207E+03	**1.738E+03**	2.243E+03	2.556E+03	2.566E+03	2.039E+03	2.511E+03	2.210E+03	2.437E+03	2.593E+03
		Std	7.151E+01	4.598E+01	6.090E+01	7.803E+01	6.261E+01	4.276E+01	3.370E+01	6.971E+01	5.349E+00	7.336E+01	3.456E+01	3.059E+01
		Rank	5	7	3	**1**	6	10	11	2	9	4	8	12
F_9	10	Avg	1.024E+03	1.048E+03	9.805E+02	1.118E+03	1.023E+03	1.169E+03	1.370E+03	9.083E+02	1.252E+03	1.186E+03	1.221E+03	1.821E+03
		Min	9.516E+02	9.622E+02	9.210E+02	9.066E+02	9.509E+02	9.767E+02	1.224E+03	**9.011E+02**	1.083E+03	9.180E+02	1.076E+03	1.379E+03
		Std	3.880E+01	4.054E+01	4.354E+01	1.523E+02	4.320E+01	1.031E+02	9.184E+01	5.581E+00	9.259E+01	2.053E+02	8.799E+01	2.381E+02
		Rank	6	7	4	2	5	8	11	**1**	10	3	9	12
	30	Avg	8.192E+03	8.251E+03	6.141E+03	5.339E+03	8.094E+03	1.010E+04	1.105E+04	5.516E+03	1.162E+04	9.426E+03	1.042E+04	1.328E+04
		Min	5.491E+03	5.532E+03	4.007E+03	**3.362E+03**	5.823E+03	7.419E+03	9.090E+03	3.686E+03	9.448E+03	6.637E+03	7.505E+03	1.103E+04
		Std	1.023E+03	1.163E+03	1.285E+03	9.680E+02	1.088E+03	1.486E+03	9.412E+02	1.189E+03	1.044E+03	1.544E+03	9.896E+02	1.065E+03
		Rank	4	5	3	**1**	6	8	10	2	11	7	9	12
	50	Avg	3.277E+04	3.354E+04	2.786E+04	1.607E+04	3.334E+04	3.709E+04	3.980E+04	2.456E+04	4.213E+04	3.336E+04	3.748E+04	4.485E+04
		Min	2.647E+04	2.814E+04	1.963E+04	**1.005E+04**	2.586E+04	2.827E+04	3.488E+04	1.909E+04	3.647E+04	2.564E+04	3.211E+04	4.131E+04
		Std	2.814E+03	2.277E+03	4.095E+03	2.633E+03	2.288E+03	3.552E+03	2.263E+03	3.248E+03	2.714E+03	4.115E+03	1.881E+03	2.145E+03
		Rank	6	7	3	**1**	5	8	10	2	11	4	9	12
	100	Avg	7.364E+04	7.397E+04	7.230E+04	3.726E+04	7.475E+04	8.019E+04	7.722E+04	6.592E+04	8.724E+04	7.522E+04	8.011E+04	8.856E+04
		Min	6.464E+04	6.626E+04	5.793E+04	**2.819E+04**	6.624E+04	7.300E+04	6.891E+04	6.069E+04	7.570E+04	6.376E+04	7.418E+04	7.995E+04
		Std	3.770E+03	4.053E+03	6.109E+03	4.265E+03	3.295E+03	3.120E+03	2.619E+03	2.804E+03	4.729E+03	5.753E+03	2.512E+03	3.810E+03
		Rank	5	7	2	**1**	6	9	8	3	11	4	10	12

Table 10
(Continued)

Function	Dimension	Metrics	HGSO [43]	OHGSO [61]	QHGSO [114]	HHO-HGSO [49]	SAHGSO [68]	SHGSO [99]	CHSGSO [109]	MVQIHGSO [85]	HFGSO [87]	HHBGGSO [89]	ACVHGSO [79]	Ar-HGSO [80]
F10	10	Avg	2.588E+03	2.550E+03	2.400E+03	1.934E+03	2.547E+03	2.369E+03	2.765E+03	1.564E+03	2.700E+03	2.452E+03	2.869E+03	2.975E+03
		Min	2.354E+03	2.141E+03	1.949E+03	1.363E+03	2.132E+03	1.891E+03	2.318E+03	1.273E+03	2.281E+03	1.816E+03	2.572E+03	2.568E+03
		Std	1.303E+02	1.601E+02	2.388E+02	2.925E+02	1.919E+02	1.813E+02	1.729E+02	1.541E+02	1.749E+02	3.121E+02	1.745E+02	2.199E+02
		Rank	10	7	5	2	6	4	9	1	8	3	12	11
	30	Avg	7.273E+03	7.232E+03	8.596E+03	5.401E+03	7.559E+03	8.619E+03	8.509E+03	5.741E+03	8.969E+03	7.916E+03	7.901E+03	8.753E+03
		Min	6.570E+03	6.220E+03	7.585E+03	3.641E+03	6.355E+03	7.608E+03	7.824E+03	4.921E+03	8.364E+03	6.766E+03	7.620E+03	8.241E+03
		Std	3.872E+02	4.442E+02	4.436E+02	7.151E+02	5.499E+02	3.086E+02	2.868E+02	3.345E+02	3.626E+02	6.727E+02	1.532E+02	3.764E+02
		Rank	5	3	7	**1**	4	8	10	2	12	6	9	11
	50	Avg	1.384E+04	1.389E+04	1.502E+04	8.921E+03	1.397E+04	1.528E+04	1.508E+04	1.079E+04	1.584E+04	1.413E+04	1.514E+04	1.623E+04
		Min	1.216E+04	1.201E+04	1.361E+04	6.022E+03	1.231E+04	1.452E+04	1.451E+04	9.857E+03	1.493E+04	1.224E+04	1.419E+04	1.482E+04
		Std	6.413E+02	6.616E+02	6.269E+02	1.131E+03	6.055E+02	3.673E+02	3.135E+02	4.501E+02	4.411E+02	8.758E+02	4.780E+02	5.272E+02
		Rank	4	3	7	**1**	6	10	9	2	12	5	8	11
	100	Avg	2.903E+04	2.908E+04	3.350E+04	2.140E+04	2.943E+04	3.248E+04	3.210E+04	2.530E+04	3.413E+04	3.081E+04	3.086E+04	3.397E+04
		Min	2.735E+04	2.700E+04	3.094E+04	1.800E+04	2.764E+04	3.162E+04	3.111E+04	2.384E+04	3.236E+04	2.852E+04	2.989E+04	3.266E+04
		Std	9.189E+02	1.072E+03	9.149E+02	2.324E+03	9.474E+02	4.835E+02	5.395E+02	6.959E+02	7.367E+02	1.172E+03	6.150E+02	6.313E+02
		Rank	4	3	8	**1**	5	10	9	2	11	6	7	12
Friedman Test	10	Average Rank	7.57142857	7.285714286	4.285714286	1.714285714	4.857142857	5.85714286	10	1.285714286	9.85714286	3.571428571	10	11.71428571
		Overall Rank	8	7	4	2	5	6	10	1	9	3	10	12
	30	Average Rank	4.42857143	5.428571429	4.142857143	1.142857143	5.285714286	8.14285714	10	1.857142857	10.1428571	6	9.571428571	11.85714286
		Overall Rank	4	6	3	**1**	5	8	10	2	11	7	9	12
	50	Average Rank	5.28571429	6	3.714285714	1.285714286	5.571428571	9.28571429	9.857142857	1.714285714	10.2857143	4.428571429	8.857142857	11.71428571
		Overall Rank	5	7	3	**1**	6	9	10	2	11	4	8	12
	100	Average Rank	4.71428571	5.571428571	3.714285714	1.285714286	6	9.28571429	10.14285714	2	10.1428571	4.857142857	8.285714286	12
		Overall Rank	4	6	3	**1**	7	9	10	2	10	5	8	12
Effectiveness	10	W/T/L	0/0/7	0/0/7	0/0/7	2/0/5	0/0/7	0/0/7	0/0/7	**5/0/2**	0/0/7	0/0/7	0/0/7	0/0/7
	30	W/T/L	0/0/7	0/0/7	0/0/7	**6/0/1**	0/0/7	0/0/7	0/0/7	1/0/6	0/0/7	0/0/7	0/0/7	0/0/7
	50	W/T/L	0/0/7	0/0/7	0/0/7	**5/0/2**	0/0/7	0/0/7	0/0/7	2/0/5	0/0/7	0/0/7	0/0/7	0/0/7
	100	W/T/L	0/0/7	0/0/7	0/0/7	**6/0/1**	0/0/7	0/0/7	0/0/7	1/0/6	0/0/7	0/0/7	0/0/7	0/0/7

Table 11
Comparison results for the HGSO against its variants on the hybrid test functions

Function	Dimension	Metrics	HGSO [43]	OHGSO [61]	QHGSO [114]	HHO-HGSO [49]	SAHGSO [68]	SHGSO [99]	CHSGSO [109]	MVQIHGSO [85]	HFGSO [87]	HHBGGSO [89]	ACVHGSO [79]	Ar-HGSO [80]
F_{11}	10	Avg	1.31E+03	1.30E+03	1.35E+03	1.16E+03	1.32E+03	1.41E+03	1.61E+03	1.13E+03	1.38E+03	1.24E+03	1.37E+03	5.12E+03
		Min	1.15E+03	1.16E+03	1.14E+03	1.111E+03	1.23E+03	1.24E+03	1.24E+03	**1.110E+03**	1.23E+03	1.14E+03	1.24E+03	2.02E+03
		Std	7.41E+01	8.66E+01	8.05E+02	6.85E+01	6.21E+01	1.83E+02	3.40E+02	8.59E+00	1.18E+02	7.92E+01	8.80E+01	2.51E+03
		Rank	5	6	3	2	7	9	11	**1**	8	4	10	12
	30	Avg	4.99E+03	5.06E+03	3.22E+03	1.27E+03	5.00E+03	8.45E+03	6.95E+03	1.94E+03	6.42E+03	3.06E+03	4.98E+03	1.34E+04
		Min	2.72E+03	3.61E+03	1.92E+03	**1.20E+03**	2.31E+03	5.88E+03	4.36E+03	1.64E+03	4.04E+03	2.04E+03	3.26E+03	9.60E+03
		Std	8.90E+02	1.00E+03	1.17E+03	4.43E+01	1.09E+03	1.60E+03	9.28E+02	2.16E+02	1.07E+03	6.77E+02	9.21E+02	3.54E+03
		Rank	6	8	3	**1**	5	11	10	2	9	4	7	12
	50	Avg	1.03E+04	1.06E+04	2.17E+05	1.60E+03	1.05E+04	2.01E+04	2.16E+04	6.80E+03	2.06E+04	8.95E+03	1.66E+04	2.33E+04
		Min	7.31E+03	6.38E+03	6.20E+03	**1.44E+03**	5.93E+03	1.40E+04	1.77E+04	4.23E+03	1.54E+04	5.60E+03	1.43E+04	1.98E+04
		Std	1.74E+03	2.22E+03	7.86E+05	1.54E+02	2.28E+03	3.19E+03	1.98E+03	1.44E+03	2.05E+03	1.96E+03	1.14E+03	1.40E+03
		Rank	7	6	5	**1**	4	8	11	2	10	3	9	12
	100	Avg	1.73E+05	1.69E+05	2.66E+05	5.01E+04	1.79E+05	2.45E+05	1.95E+05	1.42E+05	2.99E+05	1.91E+05	1.20E+06	3.74E+06
		Min	1.45E+05	1.36E+05	1.29E+05	**2.16E+04**	1.42E+05	1.53E+05	1.56E+05	1.16E+05	1.81E+05	1.29E+05	1.72E+05	1.88E+05
		Std	1.93E+04	1.66E+04	1.45E+05	2.12E+04	2.03E+04	4.46E+04	2.15E+04	1.41E+04	1.16E+05	2.56E+04	4.60E+06	1.71E+07
		Rank	7	5	3	**1**	6	8	9	2	11	4	10	12
F_{12}	10	Avg	1.03E+07	1.04E+07	7.20E+06	1.41E+06	1.28E+07	9.97E+06	9.02E+07	6.19E+04	2.88E+07	5.05E+06	3.48E+07	1.19E+08
		Min	3.16E+06	7.09E+05	8.51E+05	2.39E+04	2.15E+06	1.47E+06	7.93E+06	**1.10E+04**	8.41E+06	1.86E+05	6.52E+06	2.21E+07
		Std	6.22E+06	6.03E+06	4.33E+06	1.64E+06	9.62E+06	6.98E+06	5.50E+07	4.82E+04	1.22E+07	4.56E+06	2.41E+07	1.13E+08
		Rank	8	4	5	2	7	6	10	**1**	11	3	9	12
	30	Avg	3.02E+09	2.73E+09	2.10E+09	1.34E+07	2.41E+09	2.97E+09	1.18E+10	2.19E+07	9.40E+09	1.10E+09	9.70E+09	1.79E+10
		Min	1.67E+09	5.66E+08	5.39E+08	**2.61E+06**	1.20E+09	7.66E+08	9.30E+09	1.01E+07	4.49E+09	1.20E+08	6.45E+09	1.29E+10
		Std	8.46E+08	9.72E+08	1.13E+09	1.03E+07	6.67E+08	1.45E+09	1.33E+09	9.04E+06	2.05E+09	6.75E+08	1.80E+09	2.08E+09
		Rank	8	5	4	**1**	7	6	11	2	9	3	10	12
	50	Avg	2.68E+10	2.51E+10	2.27E+10	1.06E+08	2.67E+10	4.18E+10	7.30E+10	4.28E+08	6.90E+10	1.08E+10	6.10E+10	1.01E+11
		Min	1.61E+10	1.13E+10	1.01E+10	**2.16E+07**	1.13E+10	3.09E+10	5.77E+10	2.26E+08	5.19E+10	4.55E+09	4.78E+10	6.51E+10
		Std	6.67E+09	7.89E+09	7.71E+09	5.18E+07	6.34E+09	7.74E+09	7.43E+09	1.17E+08	9.14E+09	7.13E+09	6.13E+09	1.15E+10
		Rank	7	5	4	**1**	6	8	11	2	10	3	9	12
	100	Avg	1.03E+11	9.51E+10	8.76E+10	9.35E+08	9.55E+10	1.59E+11	1.96E+11	1.10E+10	1.87E+11	5.16E+10	1.65E+11	2.28E+11
		Min	6.49E+10	6.90E+10	5.90E+10	**4.18E+08**	5.47E+10	1.26E+11	1.47E+11	7.22E+09	1.63E+11	2.27E+10	1.47E+11	1.78E+11
		Std	2.12E+10	1.57E+10	1.24E+10	4.32E+08	2.08E+10	1.36E+10	1.41E+10	2.49E+09	1.20E+10	2.23E+10	1.07E+10	1.20E+10
		Rank	6	7	5	**1**	4	8	9	2	11	3	10	12

Table 11
(Continued)

Function	Dimension	Metrics	HGSO [43]	OHGSO [61]	QHGSO [114]	HHO-HGSO [49]	SAHGSO [68]	SHGSO [99]	CHSGSO [109]	MVQIHGSO [85]	HFGSO [87]	HHBGGSO [89]	ACVHGSO [79]	Ar-HGSO [80]
F_{13}	10	Avg	2.01E+03	1.97E+03	3.28E+03	3.02E+02	2.17E+03	5.88E+03	7.98E+03	9.70E+02	5.71E+03	1.57E+03	5.76E+03	1.06E+04
		Min	5.70E+02	8.08E+02	7.18E+02	**3.00E+02**	8.95E+02	1.08E+03	5.15E+03	5.14E+02	2.85E+03	5.38E+02	3.48E+03	5.21E+03
		Std	1.12E+03	8.21E+02	2.64E+03	1.10E+01	1.07E+03	2.14E+03	1.70E+03	3.44E+02	1.55E+03	7.68E+02	8.36E+02	3.04E+03
		Rank	4	6	5	**1**	7	8	11	2	9	3	10	12
	30	Avg	1.10E+09	1.19E+09	1.22E+09	1.21E+05	1.12E+09	7.63E+08	9.80E+09	5.92E+05	6.51E+09	3.25E+08	7.16E+09	1.74E+10
		Min	2.15E+08	4.65E+08	2.54E+08	**1.87E+04**	4.01E+08	7.98E+07	5.33E+09	2.36E+05	2.18E+09	2.31E+07	4.47E+09	8.48E+09
		Std	5.57E+08	5.32E+08	1.05E+09	8.50E+04	4.89E+08	3.74E+08	2.07E+09	2.10E+05	2.20E+09	8.18E+08	1.76E+09	5.37E+09
		Rank	5	8	6	**1**	7	4	11	2	9	3	10	12
	50	Avg	7.61E+09	6.53E+09	7.87E+09	2.03E+05	9.16E+09	1.61E+10	3.97E+10	1.25E+07	3.49E+10	4.31E+09	3.14E+10	6.59E+10
		Min	1.56E+09	2.08E+09	2.36E+09	**6.10E+04**	2.23E+09	6.16E+09	2.94E+10	5.57E+06	2.03E+10	6.42E+08	1.92E+10	4.05E+10
		Std	3.35E+09	2.51E+09	5.68E+09	1.34E+05	4.22E+09	4.89E+09	5.11E+09	4.98E+06	8.11E+09	3.90E+09	5.04E+09	1.15E+10
		Rank	4	5	7	**1**	6	8	11	2	10	3	9	12
	100	Avg	1.98E+10	1.87E+10	1.91E+10	1.49E+06	2.02E+10	3.42E+10	4.66E+10	3.18E+08	4.38E+10	8.81E+09	3.73E+10	5.67E+10
		Min	1.28E+10	9.80E+09	1.26E+10	**2.66E+05**	7.10E+09	2.42E+10	3.67E+10	1.06E+08	3.51E+10	2.67E+09	3.08E+10	4.93E+10
		Std	3.85E+09	5.93E+09	3.87E+09	2.01E+06	5.23E+09	4.90E+09	3.70E+09	1.30E+08	3.56E+09	4.72E+09	2.79E+09	2.49E+09
		Rank	7	5	6	**1**	4	8	11	2	10	3	9	12
F_{14}	10	Avg	2.68E+03	2.59E+03	2.53E+03	1.78E+03	3.16E+03	2.17E+03	3.78E+03	1.58E+03	2.44E+03	3.48E+03	4.39E+03	8.41E+04
		Min	1.49E+03	1.48E+03	1.49E+03	**1.45E+03**	1.47E+03	1.52E+03	1.59E+03	1.47E+03	1.52E+03	1.49E+03	1.67E+03	2.91E+03
		Std	1.17E+03	1.14E+03	1.40E+03	3.89E+02	1.26E+03	1.63E+03	1.09E+03	1.06E+02	6.86E+02	3.20E+03	1.14E+03	1.74E+05
		Rank	6	4	7	**1**	3	8	10	2	9	5	11	12
	30	Avg	9.74E+05	9.02E+05	7.43E+05	1.76E+05	1.02E+06	1.45E+06	2.03E+06	1.09E+05	1.55E+06	9.40E+05	1.67E+06	2.60E+07
		Min	4.09E+05	2.27E+05	8.74E+04	1.88E+04	2.98E+05	3.15E+05	7.97E+05	**6.04E+03**	5.07E+05	6.74E+04	7.15E+05	5.67E+06
		Std	4.34E+05	4.00E+05	4.92E+05	1.68E+05	4.13E+05	6.37E+05	9.93E+05	9.76E+04	7.00E+05	8.40E+05	7.14E+05	2.07E+07
		Rank	8	5	4	2	6	7	11	**1**	9	3	10	12
	50	Avg	1.20E+07	1.07E+07	9.22E+06	1.07E+06	1.13E+07	1.50E+07	5.46E+07	4.53E+05	2.35E+07	2.24E+07	2.45E+07	2.14E+08
		Min	3.51E+06	4.13E+06	1.81E+06	**7.91E+04**	1.26E+06	2.51E+06	1.23E+07	1.20E+05	7.48E+06	5.30E+05	8.65E+06	9.05E+07
		Std	6.88E+06	3.75E+06	9.93E+06	8.09E+05	4.44E+06	8.54E+06	2.06E+07	2.82E+05	9.77E+06	2.35E+07	9.37E+06	8.98E+07
		Rank	7	8	5	**1**	4	6	11	2	9	3	10	12
	100	Avg	2.75E+07	2.96E+07	2.95E+07	4.42E+06	3.11E+07	4.11E+07	8.17E+07	6.13E+06	5.29E+07	2.48E+07	4.20E+07	1.70E+08
		Min	1.92E+07	1.78E+07	8.74E+06	**2.02E+06**	1.56E+07	2.03E+07	3.95E+07	3.21E+06	3.25E+07	5.14E+06	2.46E+07	5.97E+07
		Std	5.86E+06	5.35E+06	1.60E+07	1.64E+06	7.76E+06	1.30E+07	2.73E+07	1.35E+06	1.30E+07	9.31E+06	6.72E+06	7.31E+07
		Rank	7	6	4	**1**	5	8	11	2	10	3	9	12

Table 11
(Continued)

Function	Dimension	Metrics	HGSO [43]	OHGSO [61]	QHGSO [114]	HHO-HGSO [49]	SAHGSO [68]	SHGSO [99]	CHSGSO [109]	MVQIHGSO [85]	HFGSO [87]	HHBGGSO [89]	ACVHGSO [79]	Ar-HGSO [80]
F_{15}	10	Avg	6.12E+03	6.35E+03	4.31E+03	3.24E+03	6.98E+03	4.67E+03	1.02E+04	3.49E+03	6.69E+03	6.98E+03	1.10E+04	2.35E+04
		Min	2.88E+03	2.70E+03	1.84E+03	**1.58E+03**	2.47E+03	2.72E+03	3.20E+03	1.81E+03	2.56E+03	2.25E+03	2.58E+03	3.02E+03
		Std	2.11E+03	2.09E+03	2.31E+03	1.73E+03	2.78E+03	1.50E+03	3.87E+03	1.14E+03	2.14E+03	3.14E+03	5.44E+03	1.92E+04
		Rank	10	8	3	**1**	5	9	12	2	6	4	7	11
	30	Avg	9.41E+06	7.92E+06	1.19E+07	5.54E+04	9.99E+06	8.97E+07	1.43E+08	6.14E+04	7.68E+07	2.42E+06	2.23E+07	1.01E+09
		Min	1.77E+06	1.41E+06	1.19E+06	**1.13E+04**	1.70E+06	8.95E+06	1.09E+07	2.15E+04	2.66E+07	3.17E+05	1.16E+07	6.53E+07
		Std	3.55E+06	4.52E+06	2.08E+07	4.90E+04	5.56E+06	7.56E+07	1.09E+08	3.14E+04	2.85E+07	2.36E+06	7.33E+06	6.94E+08
		Rank	7	5	4	**1**	6	8	9	2	11	3	10	12
	50	Avg	5.33E+08	4.95E+08	5.90E+08	6.75E+04	4.86E+08	8.78E+08	4.23E+09	1.24E+06	1.58E+09	1.96E+08	1.13E+09	1.42E+10
		Min	2.94E+08	1.73E+08	1.03E+08	**1.23E+04**	2.98E+08	3.93E+08	2.01E+09	5.05E+05	8.88E+08	3.41E+07	7.09E+08	4.24E+09
		Std	2.15E+08	1.67E+08	6.11E+08	4.71E+04	1.28E+08	3.13E+08	9.85E+08	6.77E+05	4.91E+08	2.59E+08	2.26E+08	4.83E+09
		Rank	6	5	4	**1**	7	8	11	2	10	3	9	12
	100	Avg	6.27E+09	6.11E+09	7.99E+09	1.27E+05	6.51E+09	1.76E+10	2.37E+10	2.31E+07	2.18E+10	2.20E+09	1.85E+10	2.92E+10
		Min	3.00E+09	2.27E+09	3.21E+09	**4.60E+04**	3.19E+09	1.01E+10	1.78E+10	1.09E+07	1.60E+10	3.89E+08	1.50E+10	2.06E+10
		Std	1.68E+09	1.98E+09	2.53E+09	6.89E+04	1.88E+09	3.61E+09	2.74E+09	6.82E+06	2.75E+09	2.35E+09	1.77E+09	4.52E+09
		Rank	5	4	7	**1**	6	8	11	2	10	3	9	12
F_{16}	10	Avg	1.92E+03	8.67E+01	1.81E+03	1.85E+03	1.83E+03	1.80E+03	2.00E+03	1.72E+03	1.98E+03	1.98E+03	2.01E+03	2.22E+03
		Min	1.71E+03	1.72E+03	1.66E+03	**1.60E+03**	1.67E+03	1.65E+03	1.80E+03	1.62E+03	1.72E+03	1.64E+03	1.78E+03	1.94E+03
		Std	7.79E+01	8.20E+01	1.33E+02	1.39E+02	7.01E+01	6.28E+01	9.68E+01	5.96E+01	9.82E+01	1.41E+02	1.01E+02	1.13E+02
		Rank	7	8	5	**1**	6	4	11	2	9	3	10	12
	30	Avg	4.01E+03	4.06E+03	3.83E+03	3.05E+03	4.07E+03	4.07E+03	5.36E+03	2.79E+03	5.04E+03	4.58E+03	4.75E+03	7.53E+03
		Min	3.32E+03	3.56E+03	3.24E+03	**2.39E+03**	3.67E+03	3.75E+03	4.52E+03	2.47E+03	4.33E+03	3.01E+03	3.96E+03	5.80E+03
		Std	2.85E+02	2.32E+02	2.65E+02	3.12E+02	1.90E+02	1.85E+02	4.01E+02	1.63E+02	3.52E+02	6.87E+02	2.88E+02	1.03E+03
		Rank	5	6	4	**1**	7	8	11	2	10	3	9	12
	50	Avg	5.61E+03	5.86E+03	5.53E+03	4.09E+03	5.71E+03	6.67E+03	8.57E+03	3.66E+03	8.21E+03	7.01E+03	7.47E+03	1.25E+04
		Min	4.73E+03	4.84E+03	4.30E+03	**3.10E+03**	4.39E+03	5.75E+03	7.38E+03	3.19E+03	7.20E+03	5.34E+03	6.54E+03	9.43E+03
		Std	5.00E+02	4.96E+02	6.00E+02	4.31E+02	5.43E+02	4.02E+02	6.01E+02	2.38E+02	6.22E+02	9.22E+02	5.67E+02	1.63E+03
		Rank	5	6	3	**1**	4	8	11	2	10	7	9	12
	100	Avg	1.44E+04	1.41E+04	1.45E+04	8.03E+03	1.44E+04	1.82E+04	2.21E+04	9.01E+03	2.08E+04	1.67E+04	1.86E+04	2.95E+04
		Min	1.20E+04	1.20E+04	1.29E+04	**6.53E+03**	1.27E+04	1.45E+04	1.85E+04	7.69E+03	1.81E+04	1.22E+04	1.67E+04	2.64E+04
		Std	1.29E+03	1.11E+03	1.14E+03	7.09E+02	7.30E+02	1.38E+03	1.50E+03	5.40E+02	1.74E+03	1.95E+03	9.49E+02	1.59E+03
		Rank	3	4	7	**1**	6	8	11	2	10	5	9	12

Table 11
(Continued)

Function	Dimension	Metrics	HGSO [43]	OHGSO [61]	QHGSO [114]	HHO-HGSO [49]	SAHGSO [68]	SHGSO [99]	CHSGSO [109]	MVQIHGSO [85]	HFGSO [87]	HHBGGSO [89]	ACVHGSO [79]	Ar-HGSO [80]
F_{17}	10	Avg	1.79E+03	1.78E+03	1.78E+03	1.76E+03	1.78E+03	1.80E+03	1.80E+03	1.76E+03	1.82E+03	1.79E+03	1.81E+03	1.84E+03
		Min	1.77E+03	1.76E+03	1.74E+03	**1.72E+03**	1.76E+03	1.77E+03	1.77E+03	1.74E+03	1.77E+03	1.74E+03	1.79E+03	1.79E+03
		Std	1.02E+01	9.26E+00	1.81E+01	2.53E+01	8.95E+00	1.53E+01	1.58E+01	5.76E+00	2.18E+01	2.65E+01	1.23E+01	3.58E+01
		Rank	9	6	2	**1**	5	7	8	3	10	4	11	12
	30	Avg	2.77E+03	2.81E+03	2.57E+03	2.47E+03	2.70E+03	2.74E+03	3.69E+03	2.06E+03	3.63E+03	2.91E+03	3.55E+03	9.05E+03
		Min	2.41E+03	2.39E+03	2.03E+03	2.04E+03	2.34E+03	2.41E+03	2.97E+03	**1.97E+03**	3.20E+03	2.45E+03	3.01E+03	3.17E+03
		Std	1.81E+02	1.79E+02	1.96E+02	2.35E+02	1.65E+02	1.62E+02	4.11E+02	7.83E+01	2.65E+02	2.97E+02	2.20E+02	6.60E+03
		Rank	7	5	2	3	4	6	9	**1**	12	8	10	11
	50	Avg	4.58E+03	4.47E+03	4.49E+03	3.67E+03	4.61E+03	5.26E+03	7.47E+03	3.04E+03	6.84E+03	4.45E+03	6.36E+03	1.35E+04
		Min	3.97E+03	4.05E+03	3.54E+03	2.89E+03	3.88E+03	4.56E+03	5.77E+03	**2.64E+03**	5.32E+03	3.34E+03	5.05E+03	8.80E+03
		Std	3.15E+02	3.03E+02	6.73E+02	3.93E+02	3.25E+02	4.21E+02	1.23E+03	2.04E+02	9.01E+02	5.21E+02	6.57E+02	3.60E+03
		Rank	6	7	4	2	5	8	11	**1**	10	3	9	12
	100	Avg	1.73E+05	1.64E+05	2.78E+05	6.55E+03	2.58E+05	2.85E+06	5.29E+06	6.22E+03	2.63E+06	4.43E+04	1.74E+06	1.79E+07
		Min	1.53E+04	1.54E+04	1.50E+04	**4.97E+03**	3.58E+04	7.02E+05	9.73E+05	5.48E+03	4.41E+05	9.44E+03	7.81E+05	5.80E+06
		Std	1.16E+05	1.39E+05	2.47E+05	6.64E+02	1.84E+05	1.65E+06	2.48E+06	3.67E+02	1.82E+06	4.84E+04	9.52E+05	8.79E+06
		Rank	5	6	4	**1**	7	9	11	2	8	3	10	12
F_{18}	10	Avg	4.93E+05	5.20E+05	1.94E+05	1.58E+04	7.32E+05	1.13E+06	2.90E+06	4.46E+03	1.10E+06	4.60E+05	9.31E+05	4.49E+07
		Min	8.91E+03	1.20E+04	2.15E+04	2.69E+03	2.68E+04	5.65E+04	6.90E+04	**2.53E+03**	1.80E+04	2.85E+03	3.03E+04	1.85E+05
		Std	4.11E+05	4.77E+05	2.06E+05	1.20E+04	6.89E+05	1.13E+06	3.53E+06	1.68E+03	1.10E+06	2.41E+06	1.19E+06	4.19E+07
		Rank	4	5	7	2	8	10	11	**1**	6	3	9	12
	30	Avg	6.71E+06	8.23E+06	4.59E+06	1.54E+06	8.49E+06	6.21E+06	1.90E+07	4.80E+05	1.95E+07	8.60E+06	7.96E+06	1.10E+08
		Min	9.80E+05	1.44E+06	1.02E+06	**6.36E+04**	1.27E+06	1.25E+06	7.23E+06	1.15E+05	7.51E+06	3.50E+05	1.44E+06	1.33E+07
		Std	3.57E+06	3.46E+06	3.13E+06	2.31E+06	5.26E+06	3.41E+06	1.12E+07	2.54E+05	6.86E+06	1.03E+07	2.86E+06	5.22E+07
		Rank	4	8	5	**1**	7	6	10	2	11	3	9	12
	50	Avg	3.47E+07	3.30E+07	4.29E+07	3.20E+06	3.11E+07	3.76E+07	1.06E+08	6.04E+06	8.26E+07	4.00E+07	6.78E+07	3.79E+08
		Min	1.07E+07	1.38E+07	7.05E+06	**3.57E+05**	1.40E+07	1.25E+07	4.50E+07	1.30E+06	1.45E+07	3.49E+06	3.21E+07	1.02E+08
		Std	1.58E+07	1.03E+07	3.21E+07	2.75E+06	1.02E+07	1.80E+07	3.25E+07	3.37E+06	3.12E+07	2.29E+07	1.81E+07	1.49E+08
		Rank	5	7	4	**1**	8	6	11	2	9	3	10	12
	100	Avg	4.41E+07	4.54E+07	6.53E+07	3.58E+06	4.75E+07	6.26E+07	1.67E+08	5.98E+06	1.15E+08	3.41E+07	7.32E+07	4.71E+08
		Min	2.58E+07	1.78E+07	1.34E+07	**1.26E+06**	2.97E+07	3.02E+07	7.73E+07	2.60E+06	6.18E+07	1.04E+07	3.44E+07	2.55E+08
		Std	1.12E+07	1.31E+07	9.91E+07	1.72E+06	1.11E+07	2.31E+07	6.28E+07	1.73E+06	3.53E+07	1.32E+07	2.34E+07	1.15E+08
		Rank	6	5	4	**1**	7	8	11	2	10	3	9	12

Table 11 (Continued)

Function	Dimension	Metrics	HGSO [43]	OHGSO [61]	QHGSO [114]	HHO-HGSO [49]	SAHGSO [68]	SHGSO [99]	CHS GSO [109]	MVQIHGSO [85]	HFGSO [87]	HHBG GSO [89]	ACVHGSO [79]	Ar-HGSO [80]
F_{19}	10	Avg	1.07E+04	1.26E+04	4.62E+04	5.90E+03	2.18E+04	1.51E+04	5.48E+04	2.80E+03	1.61E+04	1.45E+04	1.95E+04	7.00E+05
		Min	2.46E+03	2.74E+03	1.95E+03	**1.92E+03**	5.34E+03	3.07E+03	2.90E+03	2.01E+03	3.35E+03	2.12E+03	3.43E+03	4.56E+04
		Std	7.32E+03	7.90E+03	1.05E+05	5.32E+03	1.79E+04	1.31E+04	4.57E+04	7.83E+02	8.10E+03	2.06E+04	2.05E+04	9.57E+05
		Rank	5	6	2	**1**	11	8	7	3	9	4	10	12
	30	Avg	3.14E+07	2.64E+07	3.64E+07	4.21E+05	2.95E+07	3.58E+07	4.34E+08	2.97E+05	1.82E+08	2.05E+07	1.63E+08	1.19E+09
		Min	1.06E+07	9.77E+06	7.76E+06	**1.59E+04**	4.66E+06	1.39E+07	1.12E+08	8.82E+04	5.74E+07	1.10E+06	3.15E+07	5.44E+08
		Std	1.40E+07	9.67E+06	3.27E+07	2.20E+05	1.88E+07	1.50E+07	1.80E+08	1.56E+05	6.69E+07	1.94E+07	5.13E+07	4.19E+08
		Rank	7	6	5	**1**	4	8	11	2	10	3	9	12
	50	Avg	3.71E+08	3.88E+08	4.76E+08	8.50E+05	4.45E+08	5.60E+08	3.53E+09	9.34E+05	3.27E+09	8.51E+07	2.62E+09	5.38E+09
		Min	1.58E+08	1.18E+08	1.83E+08	**1.33E+05**	1.58E+08	1.36E+08	1.10E+09	3.57E+05	1.60E+09	1.07E+07	7.20E+08	1.57E+09
		Std	1.73E+08	1.63E+08	3.54E+08	7.23E+05	2.16E+08	2.62E+08	7.74E+08	3.71E+05	7.58E+08	1.83E+08	7.21E+08	1.62E+09
		Rank	7	4	8	**1**	6	5	10	2	12	3	9	11
	100	Avg	5.87E+09	6.33E+09	6.79E+09	6.89E+06	6.56E+09	1.74E+10	2.38E+10	3.61E+07	2.11E+10	2.42E+09	1.60E+10	3.17E+10
		Min	2.93E+09	3.47E+09	2.11E+09	**1.19E+06**	4.01E+09	1.29E+10	1.71E+10	1.90E+07	1.37E+10	6.13E+08	1.23E+10	2.15E+10
		Std	1.58E+09	1.52E+09	3.06E+09	4.40E+06	1.89E+09	3.15E+09	2.24E+09	1.23E+07	2.74E+09	2.32E+09	1.82E+09	3.74E+09
		Rank	5	6	4	**1**	7	9	11	2	10	3	8	12
F_{20}	10	Avg	2.14E+03	2.15E+03	2.10E+03	2.08E+03	2.14E+03	2.12E+03	2.20E+03	2.06E+03	2.21E+03	2.21E+03	2.23E+03	2.32E+03
		Min	2.08E+03	2.09E+03	2.06E+03	**2.03E+03**	2.09E+03	2.06E+03	2.12E+03	2.04E+03	2.13E+03	2.09E+03	2.12E+03	2.22E+03
		Std	3.49E+01	3.99E+01	4.00E+01	3.78E+01	3.24E+01	2.18E+01	3.34E+01	1.68E+01	3.19E+01	5.76E+01	3.76E+01	5.92E+01
		Rank	5	7	3	**1**	8	4	10	2	11	6	9	12
	30	Avg	2.79E+03	2.78E+03	2.74E+03	2.74E+03	2.72E+03	2.90E+03	2.93E+03	2.40E+03	3.05E+03	2.86E+03	2.89E+03	3.38E+03
		Min	2.47E+03	2.60E+03	2.47E+03	2.35E+03	2.52E+03	2.65E+03	2.76E+03	**2.32E+03**	2.72E+03	2.52E+03	2.73E+03	3.10E+03
		Std	1.22E+02	9.05E+01	1.69E+02	1.80E+02	1.14E+02	1.05E+02	1.10E+02	4.30E+01	1.63E+02	1.94E+02	8.52E+01	1.34E+02
		Rank	4	7	3	2	5	8	11	**1**	9	6	10	12
	50	Avg	3.79E+03	3.80E+03	4.01E+03	3.26E+03	3.77E+03	4.17E+03	4.13E+03	3.02E+03	4.27E+03	3.95E+03	4.10E+03	4.63E+03
		Min	3.49E+03	3.46E+03	3.33E+03	**2.64E+03**	3.06E+03	3.53E+03	3.86E+03	2.77E+03	3.96E+03	3.24E+03	3.76E+03	4.28E+03
		Std	1.68E+02	1.59E+02	3.31E+02	2.81E+02	2.43E+02	1.97E+02	1.50E+02	1.24E+02	1.53E+02	3.01E+02	1.68E+02	2.04E+02
		Rank	7	6	5	**1**	3	8	10	2	11	4	9	12
	100	Avg	7.42E+03	7.47E+03	8.17E+03	5.89E+03	7.46E+03	7.79E+03	7.68E+03	5.57E+03	8.27E+03	7.19E+03	7.65E+03	8.34E+03
		Min	6.92E+03	6.58E+03	7.41E+03	**5.14E+03**	7.11E+03	7.05E+03	6.88E+03	5.18E+03	7.56E+03	6.08E+03	6.92E+03	7.61E+03
		Std	2.52E+02	3.47E+02	6.16E+02	4.47E+02	1.96E+02	2.87E+02	2.90E+02	1.80E+02	3.08E+02	5.18E+02	2.72E+02	2.90E+02
		Rank	7	4	10	**1**	9	8	5	2	11	3	6	12
Friedman Test	10	Average Rank	6.3	6	4.2	1.3	6.7	7.3	10.1	1.9	8.8	3.9	9.6	11.9
		Overall Rank	6	5	4	**1**	7	8	11	2	9	3	10	12
	30	Average Rank	6.1	6.3	4	1.4	5.8	7.2	10.4	1.7	9.9	3.9	9.4	11.9
		Overall Rank	6	7	4	**1**	5	8	11	2	10	3	9	12
	50	Average Rank	6.1	5.9	4.9	1.1	5.3	7.3	10.8	1.9	10.1	3.5	9.2	11.9
		Overall Rank	7	6	4	**1**	5	8	11	2	10	3	9	12
	100	Average Rank	5.8	5.2	5.4	1	6.1	8.2	10	2	10.1	3.3	8.9	12

		Overall Rank	6	4	5	**1**	7	8	10	2	11	3	9	12	
Effectiveness	10	W/T/L	0/0/10	0/0/10	0/0/10	**7/0/3**	0/0/10	0/0/10	0/0/10	3/0/7	0/0/10	0/0/10	0/0/10	0/0/10	
	30	W/T/L	0/0/10	0/0/10	0/0/10	**7/0/3**	0/0/10	0/0/10	0/0/10	3/0/7	0/0/10	0/0/10	0/0/10	0/0/10	
	50	W/T/L	0/0/10	0/0/10	0/0/10	**9/0/1**	0/0/10	0/0/10	0/0/10	1/0/9	0/0/10	0/0/10	0/0/10	0/0/10	
	100	W/T/L	0/0/10	0/0/10	0/0/10	**10/0/1**	0/0/10	0/0/10	0/0/10	0/0/10	0/0/10	0/0/10	0/0/10	0/0/10	

Table 12
Comparison results for the HGSO against its variants on the composition test functions

Function	Dimension	Metrics	HGSO [43]	OHGSO [61]	QHGSO [114]	HHO-HGSO [49]	SAHGSO [68]	SHGSO [99]	CHSGSO [109]	MVQIHGSO [85]	HFGSO [87]	HHBGGSO [89]	ACVHGSO [79]	Ar-HGSO [80]
F_{21}	10	Avg	2.297E+03	2.286E+03	2.310E+03	2.216E+03	2.278E+03	2.236E+03	2.279E+03	2.208E+03	2.256E+03	2.295E+03	2.351E+03	2.343E+03
		Min	2.216E+03	2.222E+03	2.207E+03	**2.200E+03**	2.218E+03	2.206E+03	2.253E+03	2.203E+03	2.217E+03	2.207E+03	2.243E+03	2.263E+03
		Std	4.977E+01	5.012E+01	5.715E+01	3.736E+01	4.918E+01	1.364E+01	1.868E+01	4.446E+00	1.891E+01	6.833E+01	5.035E+01	3.705E+01
		Rank	6	9	4	**1**	8	3	11	2	7	5	10	12
	30	Avg	2.615E+03	2.608E+03	2.579E+03	2.506E+03	2.609E+03	2.632E+03	2.728E+03	2.465E+03	2.712E+03	2.667E+03	2.700E+03	2.845E+03
		Min	2.565E+03	2.559E+03	2.537E+03	2.436E+03	2.561E+03	2.454E+03	2.672E+03	**2.432E+03**	2.636E+03	2.578E+03	2.631E+03	2.759E+03
		Std	2.324E+01	2.216E+01	2.720E+01	3.583E+01	2.521E+01	4.645E+01	2.237E+01	2.118E+01	2.919E+01	3.799E+01	2.241E+01	4.380E+01
		Rank	7	5	4	2	6	3	11	**1**	10	8	9	12
	50	Avg	2.973E+03	2.978E+03	2.923E+03	2.761E+03	2.969E+03	3.062E+03	3.189E+03	2.722E+03	3.176E+03	3.051E+03	3.124E+03	3.415E+03
		Min	2.870E+03	2.869E+03	2.842E+03	**2.590E+03**	2.874E+03	2.947E+03	3.095E+03	2.661E+03	3.093E+03	2.903E+03	3.007E+03	3.287E+03
		Std	4.410E+01	4.926E+01	4.115E+01	7.981E+01	5.369E+01	4.916E+01	3.483E+01	3.238E+01	3.836E+01	8.488E+01	3.995E+01	7.167E+01
		Rank	5	4	3	**1**	6	8	11	2	10	7	9	12
	100	Avg	4.488E+03	4.406E+03	4.228E+03	3.759E+03	4.371E+03	4.727E+03	5.106E+03	3.784E+03	4.868E+03	4.709E+03	4.702E+03	5.521E+03
		Min	4.011E+03	4.099E+03	4.028E+03	**3.391E+03**	4.070E+03	4.441E+03	4.859E+03	3.487E+03	4.591E+03	4.266E+03	4.546E+03	5.121E+03
		Std	1.891E+02	1.917E+02	2.086E+02	1.657E+02	1.662E+02	1.300E+02	1.209E+02	1.307E+02	1.537E+02	2.392E+02	6.658E+01	2.417E+02
		Rank	3	6	4	**1**	5	8	11	2	10	7	9	12
F_{22}	10	Avg	2.404E+03	2.421E+03	2.364E+03	2.308E+03	2.399E+03	2.324E+03	2.725E+03	2.297E+03	2.611E+03	2.335E+03	2.688E+03	3.177E+03
		Min	2.348E+03	2.359E+03	2.331E+03	**2.240E+03**	2.334E+03	2.272E+03	2.486E+03	2.241E+03	2.440E+03	2.313E+03	2.523E+03	2.671E+03
		Std	3.404E+01	3.872E+01	3.268E+01	1.695E+01	2.953E+01	3.140E+01	1.003E+02	2.339E+01	8.047E+01	2.575E+01	7.632E+01	2.307E+02
		Rank	7	8	5	**1**	6	3	10	2	9	4	11	12
	30	Avg	4.898E+03	4.776E+03	7.155E+03	4.358E+03	4.647E+03	6.456E+03	8.428E+03	2.458E+03	8.110E+03	4.967E+03	7.566E+03	1.019E+04
		Min	3.962E+03	3.939E+03	3.581E+03	**2.309E+03**	3.393E+03	4.833E+03	6.867E+03	2.406E+03	6.665E+03	2.980E+03	6.070E+03	9.311E+03
		Std	5.788E+02	5.485E+02	2.894E+03	2.419E+03	5.744E+02	9.007E+02	5.704E+02	3.822E+01	8.741E+02	2.019E+03	4.825E+02	3.824E+02
		Rank	7	6	5	**1**	4	8	11	2	10	3	9	12
	50	Avg	1.608E+04	1.622E+04	1.681E+04	1.104E+04	1.573E+04	1.662E+04	1.724E+04	9.923E+03	1.767E+04	1.603E+04	1.748E+04	1.825E+04
		Min	1.386E+04	1.339E+04	1.546E+04	9.047E+03	1.143E+04	1.480E+04	1.629E+04	**3.479E+03**	1.632E+04	1.493E+04	1.653E+04	1.651E+04
		Std	7.340E+02	7.616E+02	6.214E+02	1.004E+03	1.236E+03	6.647E+02	3.566E+02	3.182E+03	4.605E+02	8.529E+02	3.311E+02	4.947E+02
		Rank	5	4	8	2	3	6	9	**1**	10	7	12	11
	100	Avg	3.281E+04	3.265E+04	3.584E+04	2.386E+04	3.263E+04	3.517E+04	3.491E+04	2.871E+04	3.609E+04	3.282E+04	3.469E+04	3.641E+04
		Min	3.053E+04	3.130E+04	3.344E+04	**2.121E+04**	3.130E+04	3.310E+04	3.308E+04	2.725E+04	3.427E+04	2.876E+04	3.405E+04	3.480E+04
		Std	8.401E+02	7.757E+02	1.388E+03	1.397E+03	7.718E+02	8.242E+02	6.049E+02	7.206E+02	8.978E+02	1.668E+03	3.923E+02	7.935E+02
		Rank	4	6	9	**1**	5	8	7	2	11	3	10	12

Table 12
(Continued)

Function	Dimension	Metrics	HGSO [43]	OHGSO [61]	QHGSO [114]	HHO-HGSO [49]	SAHGSO [68]	SHGSO [99]	CHSGSO [109]	MVQIHGSO [85]	HFGSO [87]	HHBGGSO [89]	ACVHGSO [79]	Ar-HGSO [80]
F_{23}	10	Avg	2.681E+03	2.678E+03	2.666E+03	2.645E+03	2.670E+03	2.659E+03	2.748E+03	2.626E+03	2.709E+03	2.705E+03	2.731E+03	2.778E+03
		Min	2.651E+03	2.655E+03	2.646E+03	**2.611E+03**	2.650E+03	2.636E+03	2.701E+03	2.616E+03	2.692E+03	2.642E+03	2.701E+03	2.687E+03
		Std	1.130E+01	1.193E+01	1.076E+01	1.589E+01	9.307E+00	1.040E+01	2.082E+01	6.015E+00	1.060E+01	3.866E+01	1.180E+01	3.042E+01
		Rank	7	8	5	**1**	6	3	11	2	10	4	12	9
	30	Avg	3.199E+03	3.186E+03	3.081E+03	3.003E+03	3.158E+03	3.220E+03	3.612E+03	2.936E+03	3.288E+03	3.460E+03	3.312E+03	3.826E+03
		Min	3.036E+03	3.036E+03	2.989E+03	**2.834E+03**	2.961E+03	3.114E+03	3.361E+03	2.868E+03	3.179E+03	3.171E+03	3.243E+03	3.413E+03
		Std	6.812E+01	6.510E+01	4.239E+01	9.136E+01	6.654E+01	6.127E+01	1.059E+02	3.253E+01	4.870E+01	1.751E+02	4.977E+01	1.715E+02
		Rank	5	6	4	**1**	3	7	11	2	9	8	10	12
	50	Avg	3.833E+03	3.816E+03	3.652E+03	3.533E+03	3.836E+03	4.044E+03	4.569E+03	3.436E+03	3.561E+03	4.480E+03	3.499E+03	4.796E+03
		Min	3.386E+03	3.489E+03	3.316E+03	3.273E+03	3.448E+03	3.683E+03	4.321E+03	**3.255E+03**	3.465E+03	3.862E+03	3.429E+03	4.076E+03
		Std	1.842E+02	1.365E+02	1.356E+02	1.457E+02	1.493E+02	1.506E+02	1.725E+02	9.888E+01	4.071E+01	2.906E+02	2.793E+01	3.454E+02
		Rank	4	8	3	2	6	9	12	**1**	7	10	5	11
	100	Avg	7.846E+03	8.061E+03	6.764E+03	4.652E+03	6.110E+03	7.291E+03	7.656E+03	5.766E+03	6.043E+03	7.062E+03	5.878E+03	8.118E+03
		Min	5.275E+03	5.852E+03	4.899E+03	**4.245E+03**	5.088E+03	6.044E+03	6.103E+03	4.939E+03	5.570E+03	6.042E+03	5.651E+03	6.689E+03
		Std	8.585E+02	6.278E+02	1.691E+03	2.514E+02	4.885E+02	4.526E+02	7.366E+02	3.280E+02	2.393E+02	5.171E+02	1.441E+02	4.274E+02
		Rank	5	8	2	**1**	4	10	11	3	6	9	7	12
F_{24}	10	Avg	2.607E+03	2.599E+03	2.783E+03	2.640E+03	2.671E+03	2.586E+03	2.727E+03	2.519E+03	2.740E+03	2.733E+03	2.862E+03	2.913E+03
		Min	2.521E+03	2.536E+03	2.557E+03	2.500E+03	2.542E+03	2.534E+03	2.598E+03	**2.448E+03**	2.561E+03	2.519E+03	2.690E+03	2.745E+03
		Std	9.101E+01	6.704E+01	6.336E+01	1.406E+02	1.080E+02	5.120E+01	4.796E+01	6.362E+01	8.892E+01	1.417E+02	7.082E+01	6.658E+01
		Rank	4	6	8	2	7	5	10	**1**	9	3	11	12
	30	Avg	3.394E+03	3.398E+03	3.312E+03	3.182E+03	3.358E+03	3.401E+03	3.935E+03	3.067E+03	3.559E+03	3.692E+03	3.592E+03	4.124E+03
		Min	3.264E+03	3.242E+03	3.204E+03	3.013E+03	3.230E+03	3.275E+03	3.792E+03	**2.984E+03**	3.443E+03	3.428E+03	3.504E+03	3.891E+03
		Std	6.234E+01	7.595E+01	5.472E+01	1.062E+02	5.824E+01	6.177E+01	7.883E+01	4.886E+01	6.089E+01	1.810E+02	4.642E+01	1.211E+02
		Rank	6	5	3	2	4	7	11	**1**	9	8	10	12
	50	Avg	4.153E+03	4.110E+03	3.932E+03	3.730E+03	4.116E+03	4.433E+03	5.237E+03	3.565E+03	4.434E+03	4.777E+03	4.420E+03	5.438E+03
		Min	3.877E+03	3.872E+03	3.786E+03	3.485E+03	3.805E+03	4.021E+03	4.923E+03	**3.369E+03**	4.166E+03	4.194E+03	4.245E+03	4.983E+03
		Std	1.363E+02	1.264E+02	9.958E+01	1.588E+02	1.541E+02	1.838E+02	2.365E+02	9.190E+01	9.952E+01	3.226E+02	1.001E+02	2.854E+02
		Rank	6	5	3	2	4	7	11	**1**	8	9	10	12
	100	Avg	7.635E+03	7.465E+03	6.679E+03	6.032E+03	7.662E+03	1.177E+04	1.187E+04	**6.116E+03**	7.942E+03	1.120E+04	7.627E+03	1.226E+04
		Min	7.072E+03	6.687E+03	6.180E+03	5.350E+03	6.816E+03	1.011E+04	8.310E+03	**5.654E+03**	7.293E+03	9.324E+03	7.332E+03	8.719E+03
		Std	3.385E+02	3.630E+02	2.692E+02	4.151E+02	5.424E+02	8.186E+02	1.890E+03	**3.236E+02**	3.343E+02	8.755E+02	1.324E+02	1.571E+03
		Rank	6	4	3	**1**	5	12	9	2	7	11	8	10

Table 12
(Continued)

Function	Dimension	Metrics	HGSO [43]	OHGSO [61]	QHGSO [114]	HHO-HGSO [49]	SAHGSO [68]	SHGSO [99]	CHSGSO [109]	MVQIHGSO [85]	HFGSO [87]	HHBGGSO [89]	ACVHGSO [79]	Ar-HGSO [80]
F_{25}	10	Avg	2.976E+03	2.967E+03	2.989E+03	2.923E+03	2.959E+03	2.981E+03	3.165E+03	2.899E+03	3.162E+03	2.937E+03	3.168E+03	3.386E+03
		Min	2.937E+03	2.929E+03	2.919E+03	2.898E+03	2.934E+03	2.923E+03	3.028E+03	2.898E+03	3.040E+03	**2.794E+03**	3.037E+03	3.095E+03
		Std	2.795E+01	2.560E+01	6.046E+01	2.425E+01	1.875E+01	2.750E+01	8.113E+01	7.315E-01	6.235E+01	3.649E+01	5.092E+01	1.367E+02
		Rank	8	6	4	2	7	5	9	3	11	1	10	12
	30	Avg	3.557E+03	3.493E+03	3.415E+03	2.928E+03	3.509E+03	3.795E+03	5.016E+03	2.995E+03	4.161E+03	3.255E+03	4.028E+03	5.834E+03
		Min	3.254E+03	3.225E+03	3.173E+03	**2.892E+03**	3.299E+03	3.491E+03	4.422E+03	2.957E+03	3.671E+03	3.055E+03	3.635E+03	5.059E+03
		Std	1.734E+02	1.525E+02	1.974E+02	2.349E+01	1.404E+02	1.999E+02	2.949E+02	1.947E+01	2.110E+02	1.202E+02	1.528E+02	4.177E+02
		Rank	6	5	4	**1**	7	8	11	2	10	3	9	12
	50	Avg	8.404E+03	7.938E+03	7.318E+03	3.217E+03	8.428E+03	1.180E+04	1.581E+04	3.889E+03	1.342E+04	5.413E+03	1.129E+04	1.578E+04
		Min	5.992E+03	6.338E+03	5.571E+03	**3.149E+03**	6.640E+03	1.062E+04	1.359E+04	3.601E+03	1.204E+04	4.289E+03	9.832E+03	1.423E+04
		Std	1.056E+03	1.005E+03	9.164E+02	6.092E+01	1.058E+03	5.764E+02	1.016E+03	1.469E+02	7.934E+02	7.796E+02	7.716E+02	6.641E+02
		Rank	5	6	4	**1**	7	9	11	2	10	3	8	12
	100	Avg	1.653E+04	1.739E+04	1.480E+04	4.306E+03	1.756E+04	3.050E+04	2.874E+04	7.796E+03	2.541E+04	1.186E+04	2.158E+04	3.188E+04
		Min	1.319E+04	1.388E+04	1.209E+04	**3.830E+03**	1.333E+04	2.480E+04	2.541E+04	6.519E+03	2.184E+04	8.585E+03	1.987E+04	2.941E+04
		Std	1.669E+03	1.722E+03	1.491E+03	3.421E+02	2.006E+03	1.656E+03	1.297E+03	6.230E+02	1.477E+03	1.038E+03	9.500E+02	1.146E+03
		Rank	5	7	4	**1**	6	10	11	2	9	3	8	12
F_{26}	10	Avg	3.257E+03	3.266E+03	3.228E+03	3.086E+03	3.226E+03	3.127E+03	3.736E+03	2.843E+03	3.724E+03	3.179E+03	3.913E+03	4.128E+03
		Min	3.098E+03	3.073E+03	3.028E+03	2.800E+03	3.082E+03	2.861E+03	3.263E+03	**2.611E+03**	3.224E+03	2.690E+03	3.466E+03	3.697E+03
		Std	1.066E+02	1.019E+02	2.060E+02	1.896E+02	8.983E+01	9.396E+01	1.668E+02	5.432E+01	2.149E+02	2.650E+02	2.166E+02	2.019E+02
		Rank	8	6	5	3	7	4	10	**1**	9	2	11	12
	30	Avg	7.909E+03	8.045E+03	7.307E+03	6.794E+03	7.565E+03	8.719E+03	1.043E+04	3.760E+03	7.771E+03	8.243E+03	8.466E+03	1.066E+04
		Min	5.483E+03	6.908E+03	5.214E+03	**2.836E+03**	6.296E+03	6.449E+03	9.707E+03	3.240E+03	7.140E+03	4.552E+03	7.677E+03	1.027E+04
		Std	6.882E+02	5.336E+02	1.029E+03	1.316E+03	5.954E+02	8.681E+02	3.251E+02	3.074E+02	2.850E+02	1.517E+03	7.027E+02	1.996E+02
		Rank	5	8	4	**1**	6	7	11	2	9	3	10	12
	50	Avg	1.302E+04	1.322E+04	1.222E+04	1.065E+04	1.310E+04	1.863E+04	1.735E+04	6.469E+03	1.243E+04	1.282E+04	1.203E+04	1.761E+04
		Min	1.153E+04	1.122E+04	9.889E+03	6.251E+03	9.888E+03	1.353E+04	1.615E+04	**5.474E+03**	1.119E+04	8.266E+03	1.054E+04	1.682E+04
		Std	7.679E+02	8.932E+02	8.642E+02	1.401E+03	9.300E+02	1.558E+03	5.856E+02	6.696E+02	1.287E+03	2.055E+03	1.256E+03	3.295E+02
		Rank	9	8	5	2	4	10	11	**1**	7	3	6	12
	100	Avg	4.004E+04	4.066E+04	3.832E+04	2.734E+04	3.928E+04	5.883E+04	5.605E+04	2.441E+04	4.918E+04	3.765E+04	4.771E+04	5.299E+04
		Min	3.391E+04	3.504E+04	3.399E+04	1.673E+04	3.196E+04	4.867E+04	5.072E+04	**1.548E+04**	4.320E+04	3.311E+04	4.481E+04	4.996E+04
		Std	2.449E+03	2.703E+03	2.646E+03	3.243E+03	3.006E+03	4.595E+03	2.459E+03	2.688E+03	2.062E+03	2.317E+03	1.601E+03	1.368E+03
		Rank	5	7	6	2	3	10	12	**1**	8	4	9	11

Table 12
(Continued)

Function	Dimension	Metrics	HGSO [43]	OHGSO [61]	QHGSO [114]	HHO-HGSO [49]	SAHGSO [68]	SHGSO [99]	CHSGSO [109]	MVQIHGSO [85]	HFGSO [87]	HHBGGSO [89]	ACVHGSO [79]	Ar-HGSO [80]
F_{27}	10	Avg	3.139E+03	3.138E+03	3.140E+03	3.108E+03	3.133E+03	3.112E+03	3.211E+03	3.097E+03	3.188E+03	3.184E+03	3.198E+03	3.199E+03
		Min	3.115E+03	3.103E+03	3.106E+03	**3.090E+03**	3.109E+03	3.105E+03	3.187E+03	3.092E+03	3.153E+03	3.116E+03	3.172E+03	3.188E+03
		Std	1.568E+01	1.632E+01	2.962E+01	2.078E+01	1.513E+01	5.871E+00	1.498E+01	2.288E+00	1.422E+01	4.277E+01	5.796E+00	2.307E+00
		Rank	7	3	5	1	6	4	11	2	9	8	10	12
	30	Avg	3.200E+03	3.200E+03	3.200E+03	3.360E+03	3.200E+03	3.302E+03	4.040E+03	3.220E+03	3.200E+03	4.174E+03	3.200E+03	3.200E+03
		Min	3.200E+03	3.200E+03	3.200E+03	3.219E+03	3.200E+03	3.200E+03	3.200E+03	**3.176E+03**	3.200E+03	3.200E+03	3.200E+03	3.200E+03
		Std	1.224E-04	1.112E-04	1.650E-04	1.074E+02	1.331E-04	1.566E+02	7.300E+02	3.450E+01	1.133E-04	4.199E+02	1.067E-04	1.599E-04
		Rank	4	4	2	12	2	10	8	**1**	7	11	6	9
	50	Avg	3.235E+03	3.200E+03	3.200E+03	4.136E+03	3.200E+03	5.005E+03	5.919E+03	3.817E+03	3.200E+03	6.833E+03	3.200E+03	3.200E+03
		Min	3.200E+03	3.200E+03	**3.200E+03**	3.650E+03	3.200E+03	3.202E+03	3.200E+03	3.200E+03	3.200E+03	5.234E+03	3.200E+03	3.200E+03
		Std	1.916E+02	1.859E-04	1.361E-04	2.925E+02	1.283E-04	7.528E+02	1.564E+03	2.879E+02	9.003E-05	9.917E+02	1.226E-04	8.072E-03
		Rank	6	2	**1**	11	2	10	8	2	7	12	2	9
	100	Avg	4.289E+03	4.479E+03	3.200E+03	4.552E+03	4.080E+03	1.301E+04	1.221E+04	5.280E+03	3.200E+03	1.193E+04	3.200E+03	3.200E+03
		Min	3.2000235E+03	3.2000236E+03	3.2000235E+03	4.0651744E+03	**3.2000234E+03**	1.0830116E+04	3.2000242E+03	4.6650347E+03	3.2000238E+03	9.2146330E+03	3.2000236E+03	3.2000246E+03
		Std	2.618E+03	2.618E+03	1.605E-04	3.397E+02	2.270E+03	8.712E+02	4.902E+03	3.916E+02	1.966E-04	1.323E+03	1.446E-04	2.644E-01
		Rank	2	4	2	9	**1**	12	7	10	6	11	4	8
F_{28}	10	Avg	3.459E+03	3.398E+03	3.438E+03	3.287E+03	3.406E+03	3.259E+03	3.691E+03	3.153E+03	3.291E+03	3.385E+03	3.299E+03	3.300E+03
		Min	3.212E+03	3.227E+03	3.191E+03	3.100E+03	3.222E+03	3.217E+03	3.437E+03	**2.855E+03**	3.284E+03	3.159E+03	3.294E+03	3.300E+03
		Std	1.604E+02	1.434E+02	1.634E+02	1.110E+02	1.272E+02	3.384E+01	8.615E+01	8.405E+01	5.903E+00	1.512E+02	1.678E+00	2.696E-03
		Rank	5	8	4	2	7	6	12	**1**	9	3	10	11
	30	Avg	4.246E+03	4.253E+03	3.970E+03	3.291E+03	4.171E+03	5.270E+03	6.436E+03	3.363E+03	3.300E+03	3.818E+03	3.300E+03	3.300E+03
		Min	3.300E+03	3.300E+03	3.300E+03	**3.231E+03**	3.300E+03	3.300E+03	3.557E+03	3.300E+03	3.299E+03	3.300E+03	3.300E+03	3.300E+03
		Std	7.644E+02	7.832E+02	5.656E+02	3.152E+01	6.893E+02	5.552E+02	7.144E+02	3.164E+01	1.441E-01	3.141E+02	1.954E-01	1.040E-02
		Rank	9	6	5	**1**	6	11	12	6	2	10	3	4
	50	Avg	7.977E+03	7.649E+03	6.374E+03	3.643E+03	7.542E+03	1.147E+04	1.227E+04	4.450E+03	3.300E+03	5.431E+03	3.300E+03	3.300E+03
		Min	3.3000116E+03	3.3000115E+03	3.3000110E+03	3.3706783E+03	3.3000114E+03	1.0022031E+04	1.0515813E+04	4.0588455E+03	3.2999327E+03	3.3000122E+03	**3.2998805E+03**	3.3000119E+03
		Std	1.084E+03	1.865E+03	1.671E+03	1.663E+02	1.839E+03	8.554E+02	6.389E+02	1.726E+02	2.918E-02	1.183E+03	3.746E-02	1.705E-04
		Rank	6	5	3	9	4	11	12	10	2	8	**1**	7
	100	Avg	2.334E+04	2.295E+04	1.944E+04	4.924E+03	2.296E+04	4.175E+04	3.461E+04	1.055E+04	3.300E+03	1.233E+04	3.300E+03	3.300E+03
		Min	1.921124E+04	1.874566E+04	3.300024E+03	4.062546E+03	1.881338E+04	3.522918E+04	2.992906E+04	9.392558E+03	3.300024E+03	3.300025E+03	**3.300023E+03**	3.300025E+03
		Std	1.745E+03	1.963E+03	4.865E+03	7.085E+02	2.124E+03	3.274E+03	1.418E+03	7.858E+02	2.009E-04	6.208E+03	1.534E-04	1.372E-04
		Rank	10	8	2	6	9	12	11	7	3	4	**1**	4

Table 12 (Continued)

Function	Dimension	Metrics	HGSO [43]	OHGSO [61]	QHGSO [114]	HHO-HGSO [49]	SAHGSO [68]	SHGSO [99]	CHSGSO [109]	MVQIHGSO [85]	HFGSO [87]	HHBGGSO [89]	ACVHGSO [79]	Ar-HGSO [80]
F_{29}	10	Avg	3.280E+03	3.271E+03	3.273E+03	3.248E+03	3.270E+03	3.242E+03	3.388E+03	3.191E+03	3.383E+03	3.322E+03	3.381E+03	3.623E+03
		Min	3.211E+03	3.229E+03	3.190E+03	**3.162E+03**	3.219E+03	3.199E+03	3.322E+03	3.165E+03	3.287E+03	3.195E+03	3.299E+03	3.288E+03
		Std	3.028E+01	2.515E+01	4.785E+01	4.763E+01	2.886E+01	3.326E+01	4.835E+01	1.358E+01	5.024E+01	8.082E+01	4.825E+01	1.155E+02
		Rank	6	8	3	**1**	7	5	12	2	9	4	11	10
	30	Avg	4.958E+03	4.987E+03	4.466E+03	4.369E+03	4.888E+03	5.263E+03	6.686E+03	4.118E+03	5.321E+03	5.696E+03	5.054E+03	8.681E+03
		Min	3.929E+03	3.966E+03	3.800E+03	**3.668E+03**	4.106E+03	4.579E+03	5.965E+03	3.750E+03	4.739E+03	4.515E+03	4.440E+03	6.363E+03
		Std	5.448E+02	6.045E+02	4.466E+02	3.691E+02	3.727E+02	2.988E+02	3.423E+02	1.823E+02	3.346E+02	4.857E+02	3.199E+02	1.545E+03
		Rank	4	5	3	**1**	6	9	11	2	10	8	7	12
	50	Avg	9.764E+03	9.925E+03	7.018E+03	5.746E+03	1.024E+04	1.236E+04	3.375E+04	5.690E+03	1.995E+04	1.121E+04	1.990E+04	1.837E+05
		Min	6.875E+03	8.087E+03	5.123E+03	**4.687E+03**	6.048E+03	8.559E+03	1.797E+04	4.779E+03	9.312E+03	8.005E+03	8.378E+03	2.847E+04
		Std	1.459E+03	1.228E+03	1.356E+03	5.479E+02	1.744E+03	2.180E+03	1.052E+04	2.767E+02	6.891E+03	2.840E+03	7.330E+03	1.363E+05
		Rank	5	7	3	**1**	4	9	11	2	10	6	8	12
	100	Avg	3.653E+04	3.274E+04	3.084E+04	1.043E+04	3.763E+04	1.514E+05	4.515E+05	1.172E+04	3.308E+05	2.538E+04	1.999E+05	8.091E+05
		Min	1.956E+04	1.836E+04	1.333E+04	**8.824E+03**	1.624E+04	4.195E+04	1.869E+05	1.013E+04	1.233E+05	1.620E+04	7.764E+04	3.081E+05
		Std	1.135E+04	9.975E+03	2.037E+04	8.927E+02	1.702E+04	7.275E+04	1.320E+05	7.240E+02	1.323E+05	8.233E+03	7.868E+04	1.851E+05
		Rank	7	6	3	**1**	5	8	11	2	10	4	9	12
F_{30}	10	Avg	1.851E+05	2.490E+05	3.358E+05	6.261E+05	4.998E+05	7.731E+04	1.126E+07	4.375E+04	1.932E+04	5.704E+06	4.643E+04	1.520E+07
		Min	3.660E+03	3.682E+03	3.468E+03	7.447E+03	4.926E+03	3.560E+03	4.467E+05	**3.293E+03**	3.653E+03	3.168E+04	5.012E+03	6.752E+05
		Std	2.697E+05	4.833E+05	4.218E+05	1.242E+06	6.827E+05	9.327E+04	7.180E+06	5.382E+04	1.842E+04	7.429E+06	1.618E+05	1.000E+07
		Rank	5	6	2	9	7	3	11	**1**	4	10	8	12
	30	Avg	1.123E+08	1.564E+08	6.894E+07	2.120E+06	1.488E+08	1.530E+08	1.058E+09	3.613E+06	8.407E+08	9.911E+07	4.045E+08	3.910E+09
		Min	5.899E+07	5.930E+07	1.484E+07	**4.159E+05**	5.223E+07	4.304E+07	2.316E+08	7.640E+05	1.575E+08	1.560E+07	1.074E+08	9.875E+08
		Std	3.998E+07	6.489E+07	4.315E+07	1.066E+06	5.438E+07	6.379E+07	3.962E+08	1.767E+06	4.023E+08	1.187E+08	1.861E+08	1.341E+09
		Rank	7	8	3	**1**	6	5	11	2	10	4	9	12
	50	Avg	1.033E+09	1.047E+09	9.228E+08	4.125E+07	1.048E+09	1.540E+09	5.960E+09	1.437E+08	4.315E+09	5.328E+08	3.015E+09	1.157E+10
		Min	4.381E+08	5.653E+08	2.844E+08	**2.071E+07**	5.835E+08	6.500E+08	3.738E+09	8.675E+07	1.162E+09	2.738E+08	1.750E+09	6.483E+09
		Std	2.868E+08	2.269E+08	9.010E+08	1.298E+07	2.155E+08	5.796E+08	1.021E+09	2.715E+07	1.562E+09	2.305E+08	9.578E+08	2.313E+09
		Rank	5	6	4	**1**	7	8	11	2	9	3	10	12
	100	Avg	1.684E+10	1.724E+10	1.596E+10	9.271E+07	1.546E+10	2.796E+10	4.123E+10	6.009E+08	4.113E+10	7.869E+09	3.504E+10	5.063E+10
		Min	8.590E+09	9.137E+09	9.422E+09	**3.797E+07**	8.336E+09	1.795E+10	3.512E+10	3.596E+08	3.203E+10	3.032E+09	2.945E+10	4.561E+10
		Std	4.793E+09	3.033E+09	3.223E+09	5.367E+07	3.174E+09	4.368E+09	2.870E+09	1.810E+08	3.512E+09	4.993E+09	2.768E+09	2.244E+09
		Rank	5	6	7	**1**	4	8	11	2	10	3	9	12
Friedman Test	10	Average Rank	6.3	6.8	4.5	2.3	6.8	4.1	10.7	1.7	8.6	4.4	10.4	11.4
		Overall Rank	6	7	5	2	7	3	11	**1**	9	4	10	12
	30	Average Rank	6	5.8	3.7	2.3	5	7.5	10.8	2.1	8.6	6.6	8.2	10.9
		Overall Rank	6	5	3	2	4	8	11	**1**	10	7	9	12
	50	Average Rank	5.6	5.5	3.7	3.2	4.7	8.7	10.7	2.4	8	6.8	7.1	11
		Overall Rank	6	5	3	2	4	10	11	**1**	9	7	8	12
	100	Average Rank	5.2	6.2	4.2	2.4	4.7	9.8	10.1	3.3	8	5.9	7.4	10.5
		Overall Rank	5	7	3	**1**	4	10	11	2	9	6	8	12

Effectiveness	10	W/T/L	0/0/10	0/0/10	0/0/10	5/0/5	0/0/10	0/0/10	0/0/10	4/0/6	0/0/10	1/0/9	0/0/10	0/0/10
	30	W/T/L	0/0/10	0/0/10	0/0/10	7/0/3	0/0/10	0/0/10	0/0/10	3/0/7	0/0/10	0/0/10	0/0/10	0/0/10
	50	W/T/L	0/0/10	0/0/10	1/0/9	4/0/6	0/0/10	0/0/10	0/0/10	4/0/6	0/0/10	0/0/10	1/0/9	0/0/10
	100	W/T/L	0/0/10	0/0/10	0/0/10	7/0/3	1/0/9	0/0/10	0/0/10	1/0/9	0/0/10	0/0/10	1/0/9	0/0/10

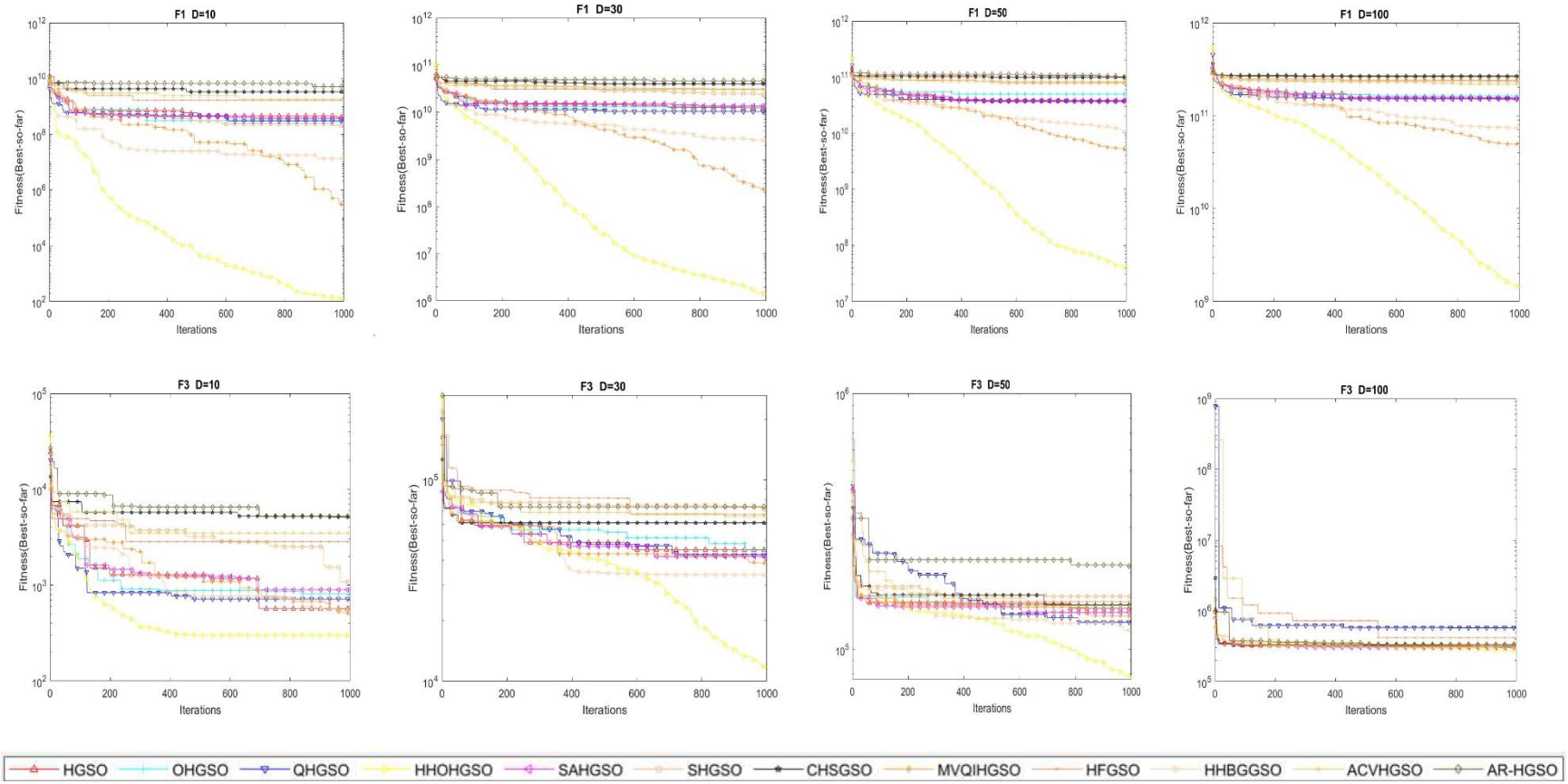


Fig. 4. Comparison of convergence capability of the HGSO along with its variants on the unimodal test functions

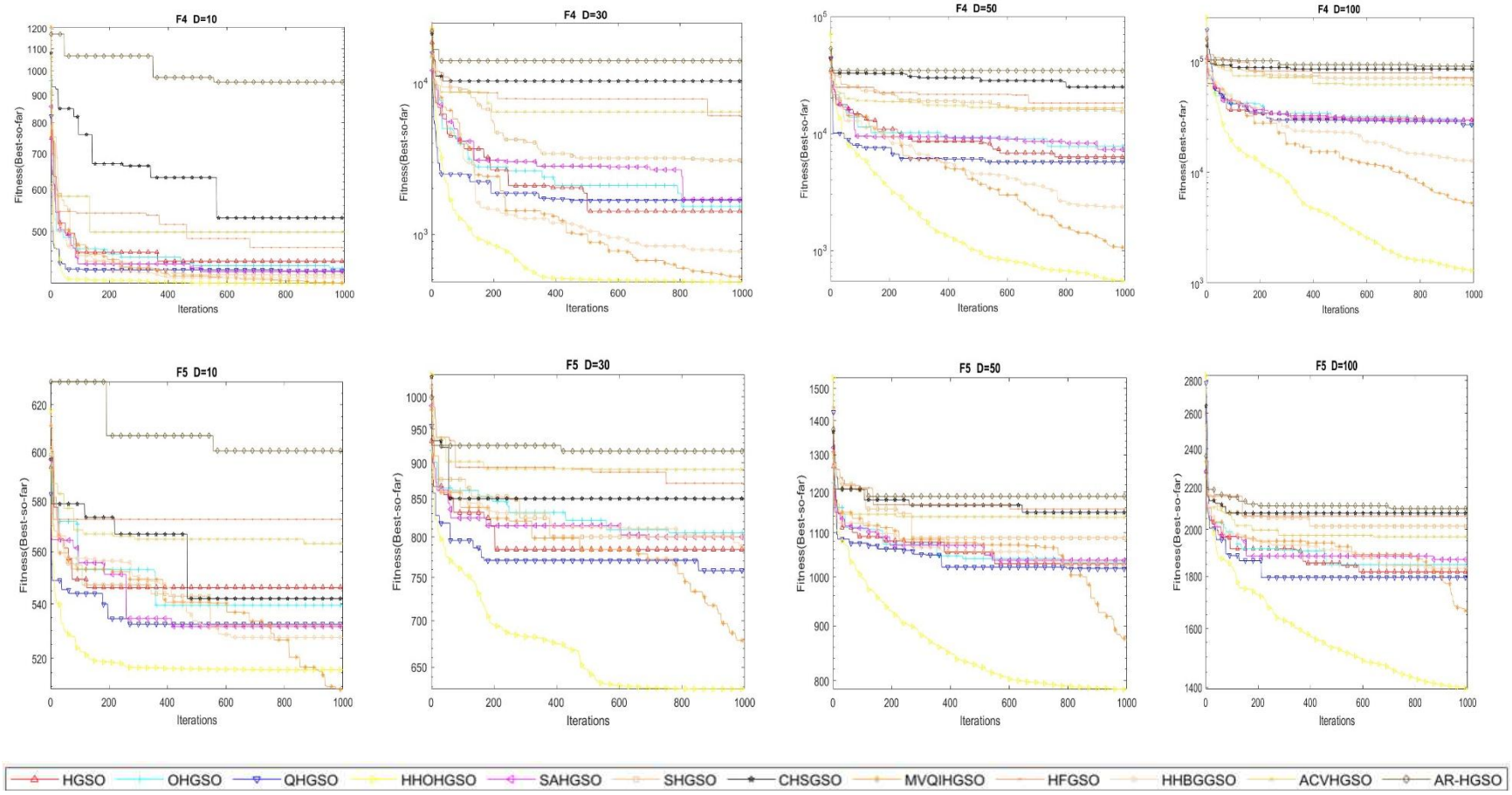


Fig. 5. Comparison of convergence capability of the HGSO along with its variants on the multimodal test functions

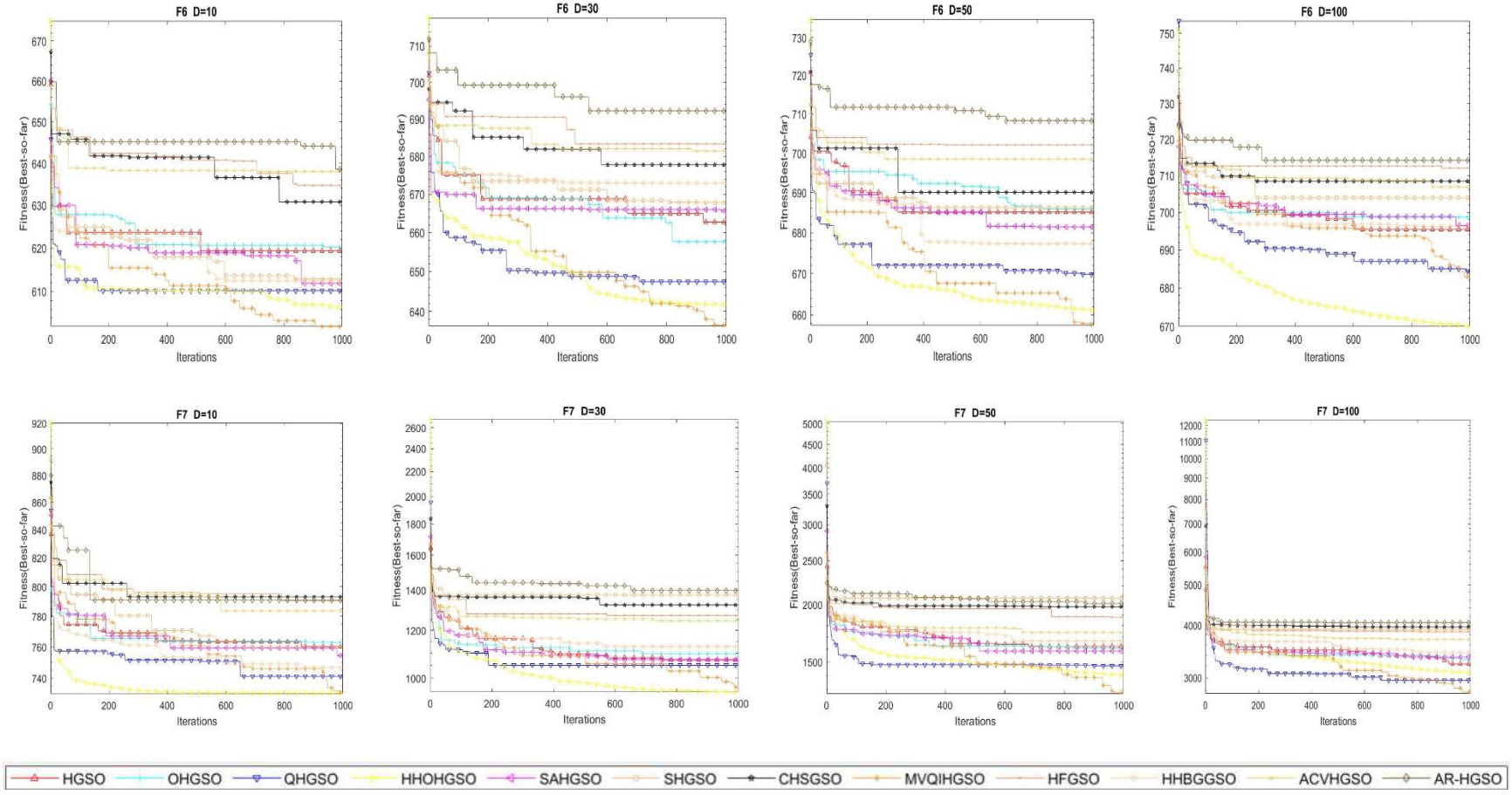


Fig. 5. (Continued)

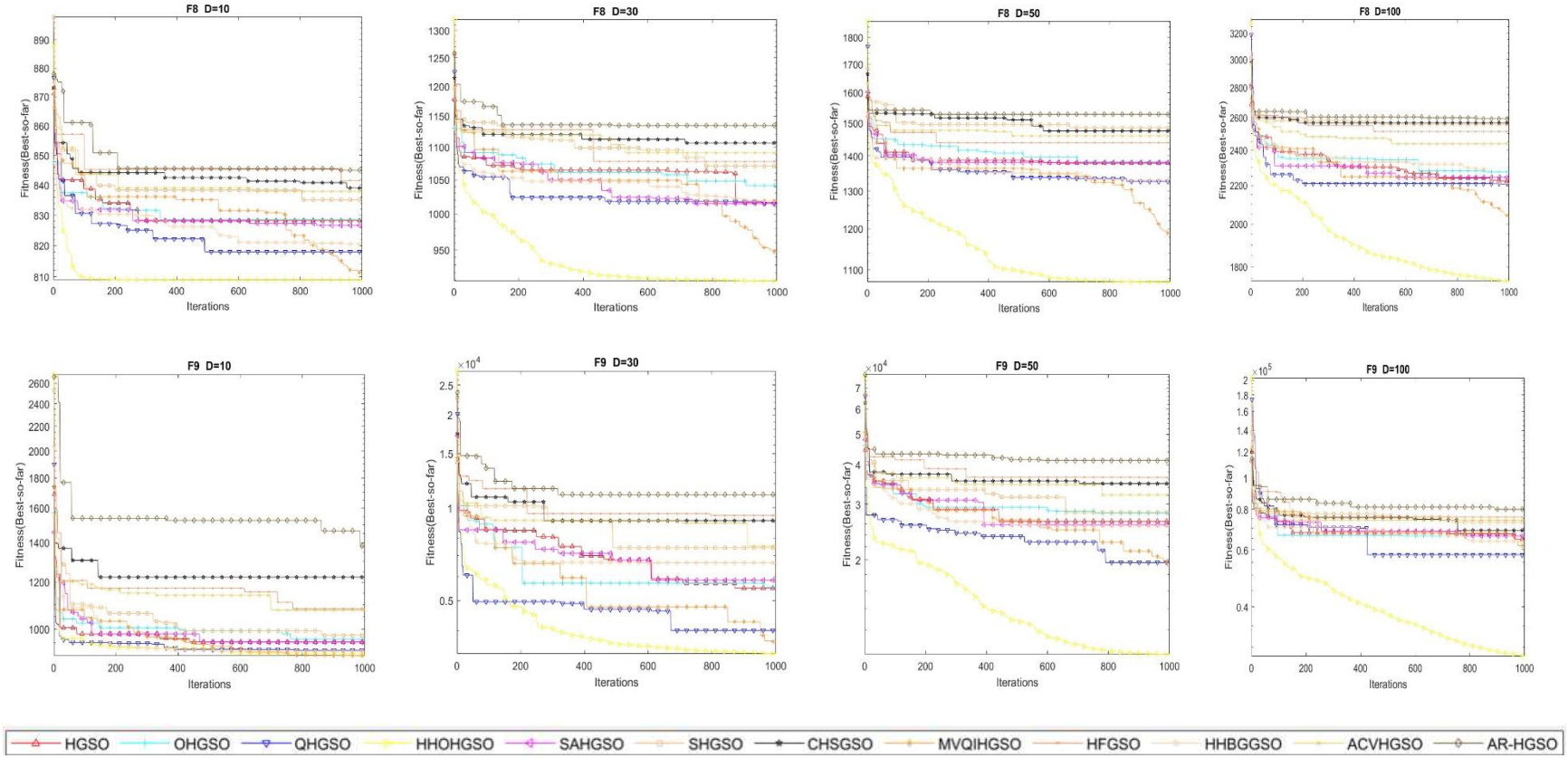


Fig. 5. (Continued)

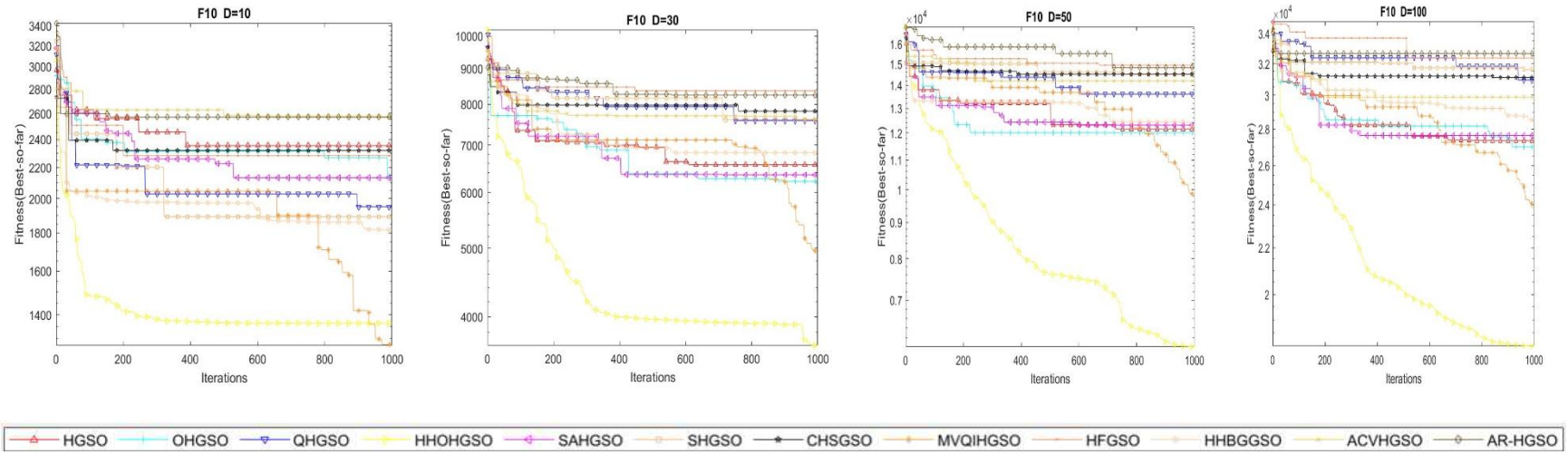
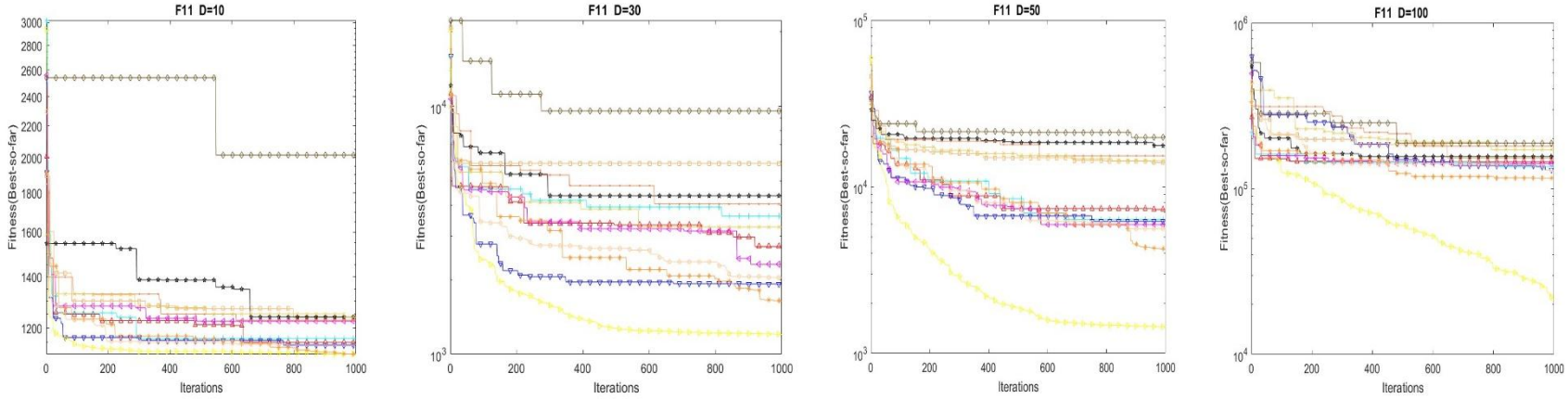


Fig. 5. (Continued)



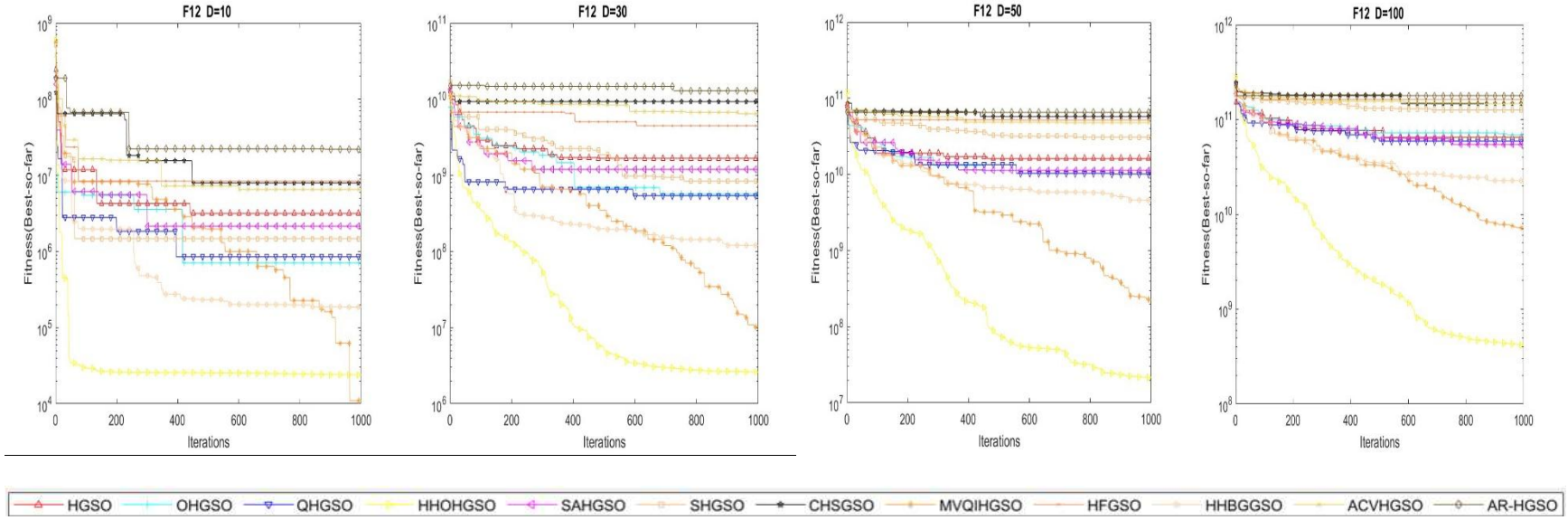
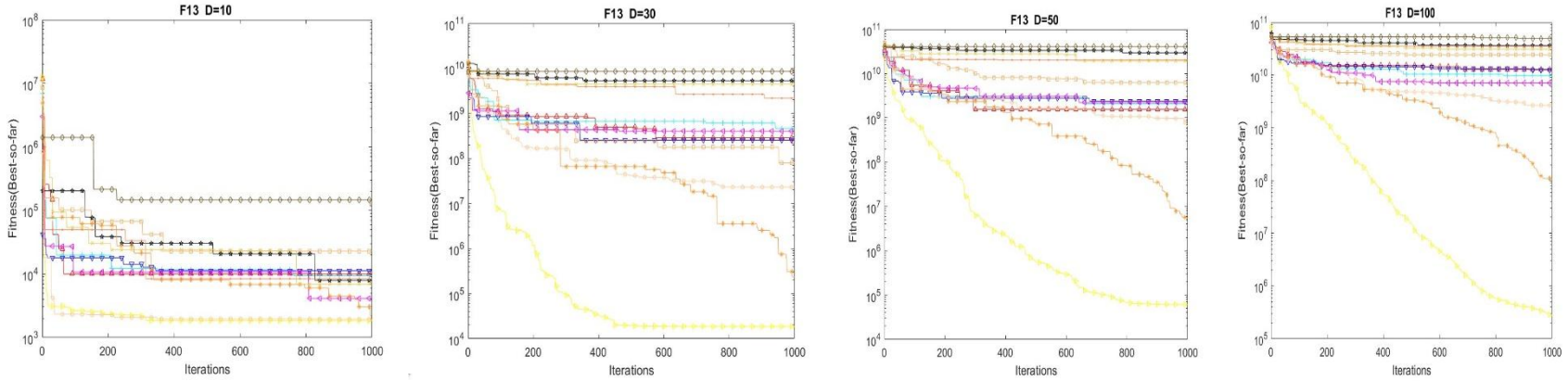


Fig. 6. Comparison of convergence capability of the HGSO along with its variants on the hybrid test functions



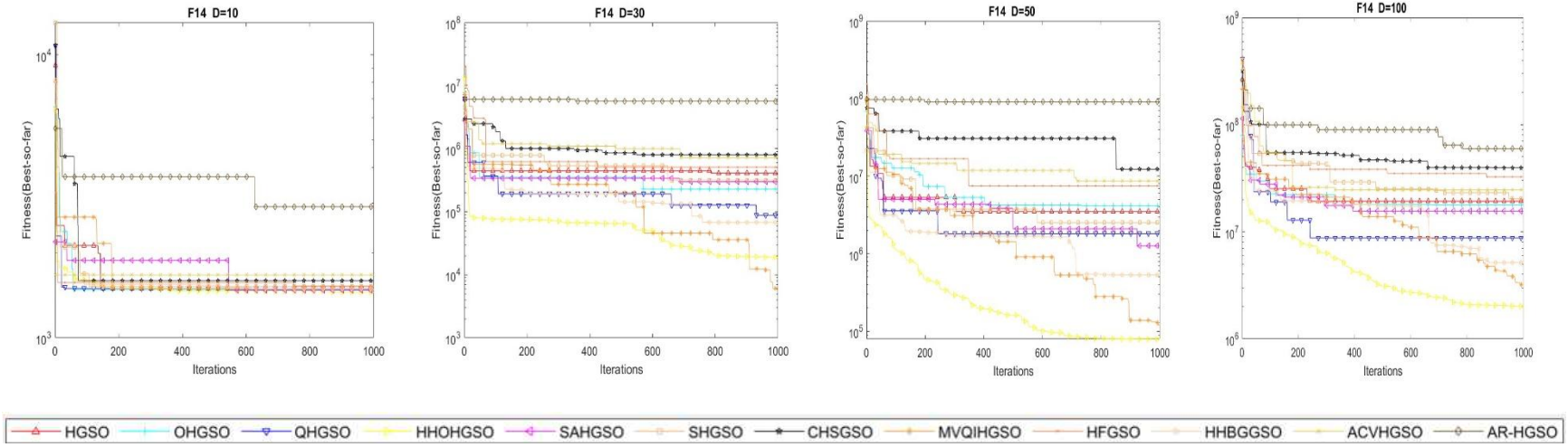
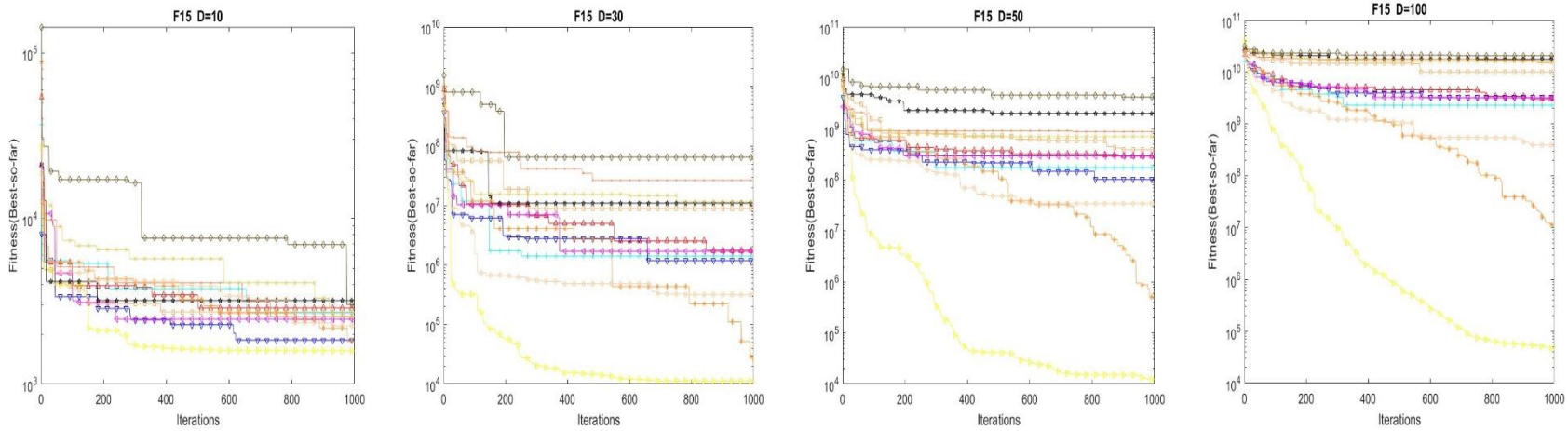


Fig. 6. (Continued)



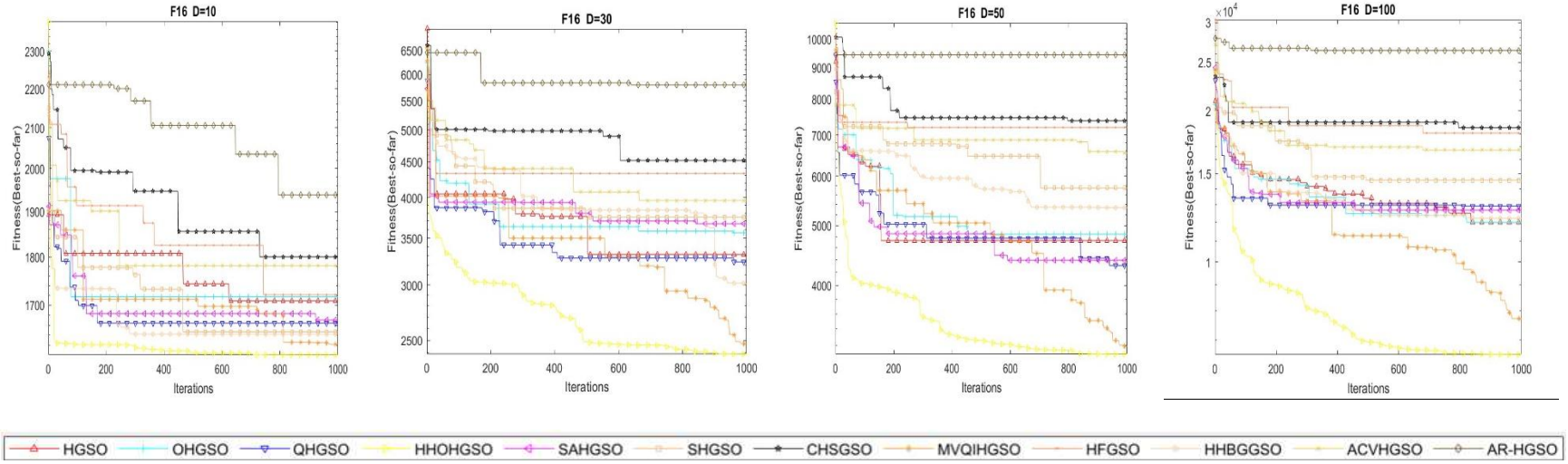
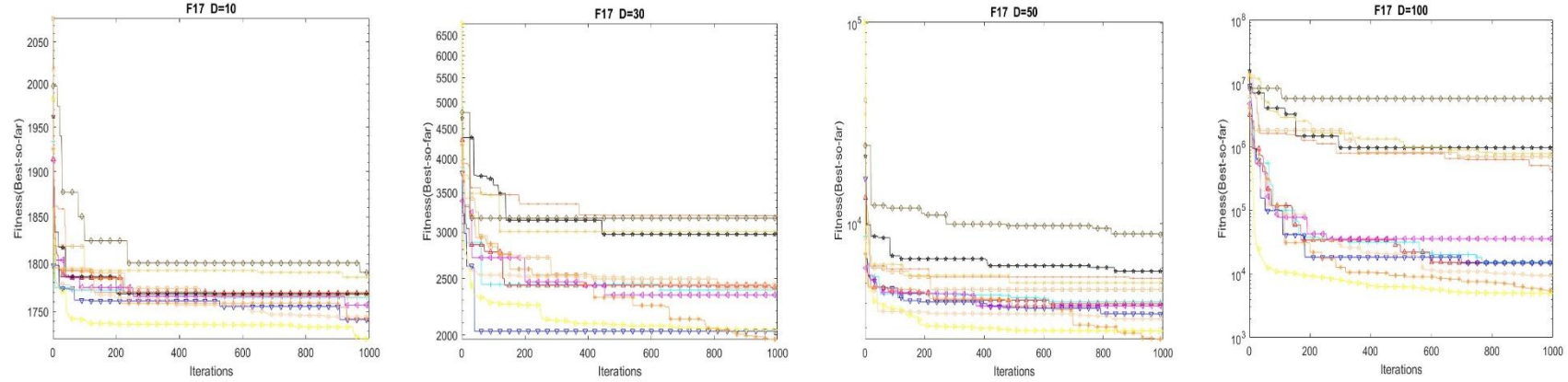


Fig. 6. (Continued)



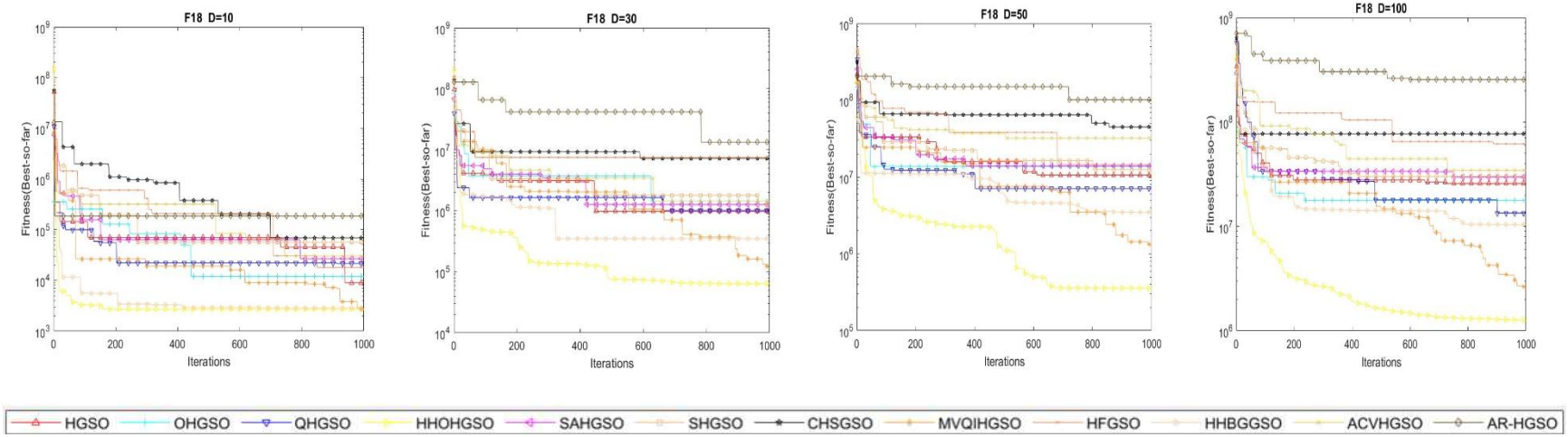
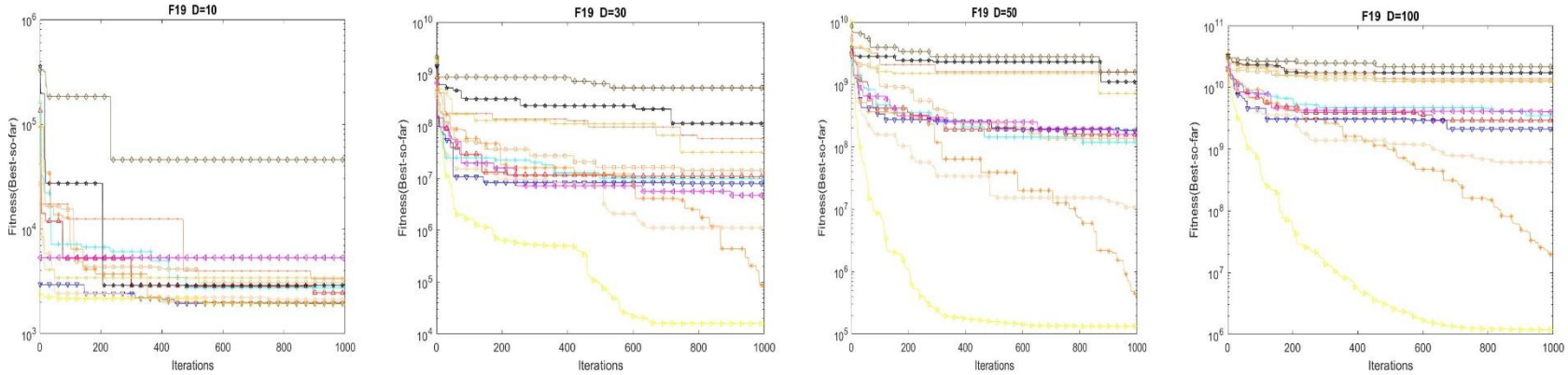


Fig. 6. (Continued)



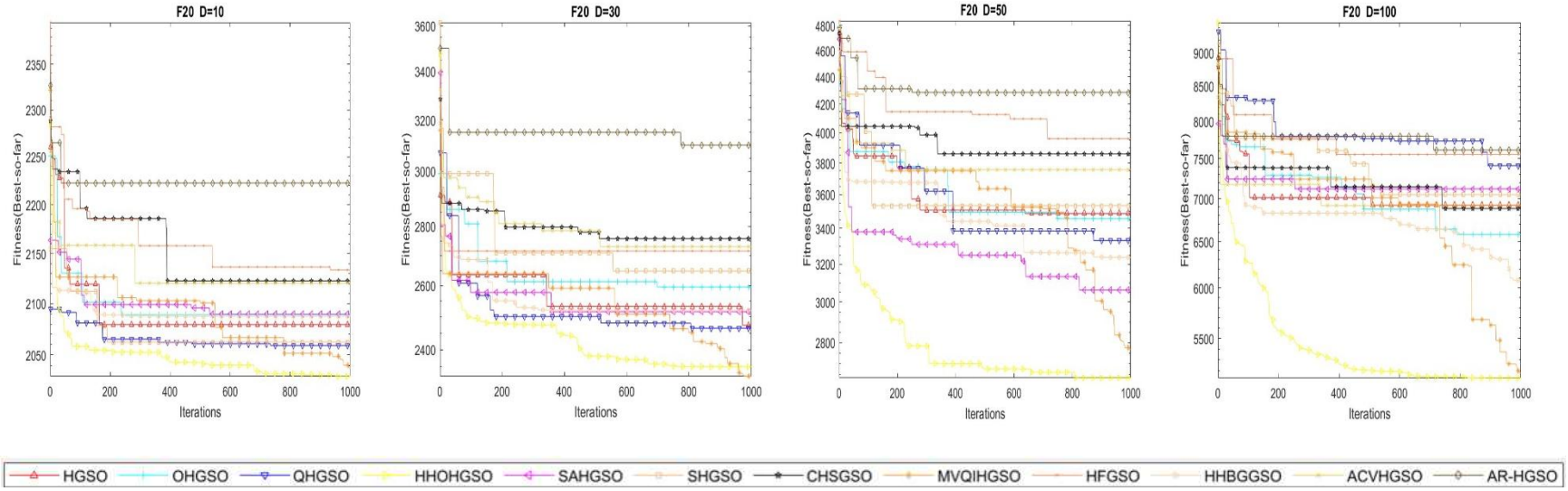
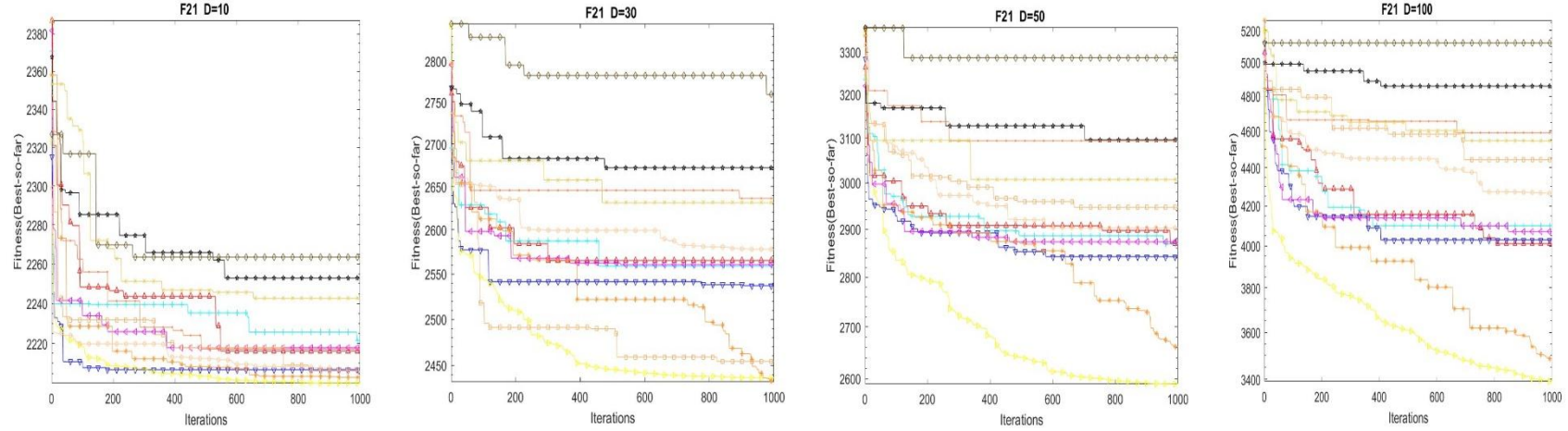


Fig. 6. (Continued)



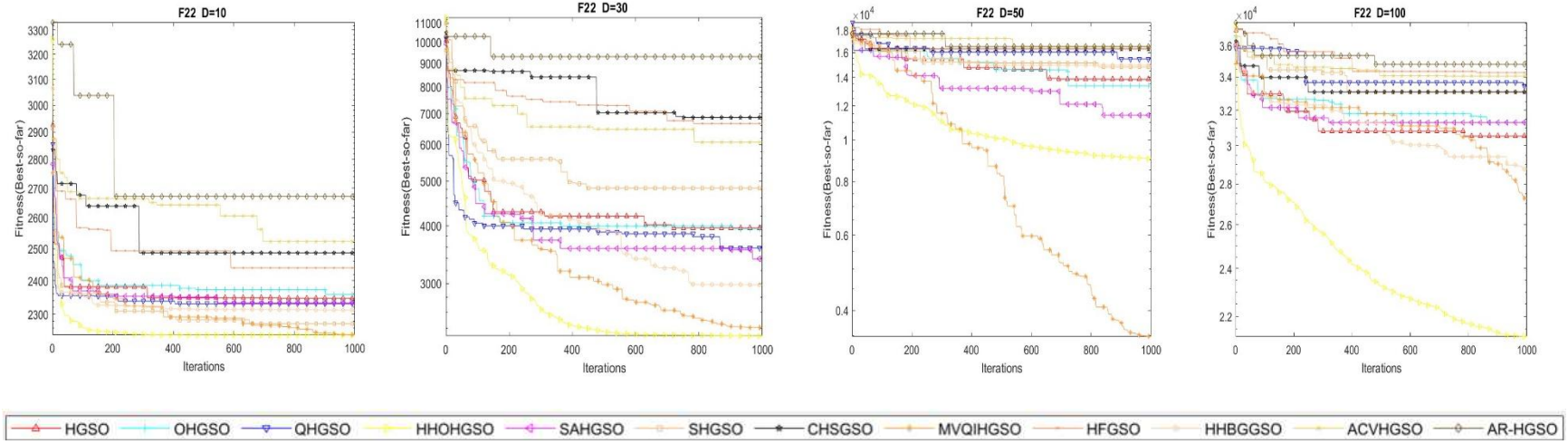


Fig. 7. Comparison of convergence capability of the HGSO along with its variants on the composition test functions

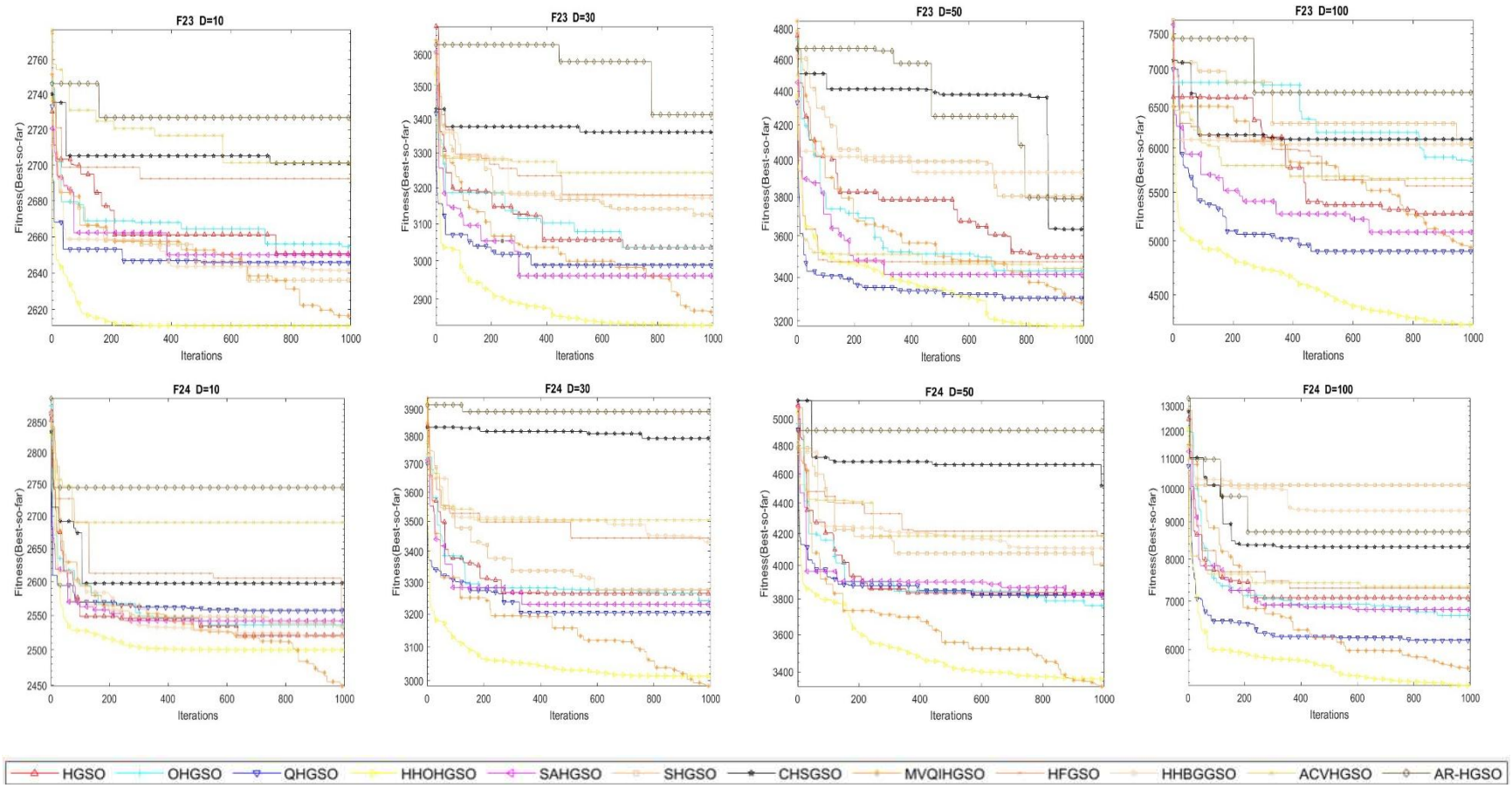


Fig. 7. (Continued)

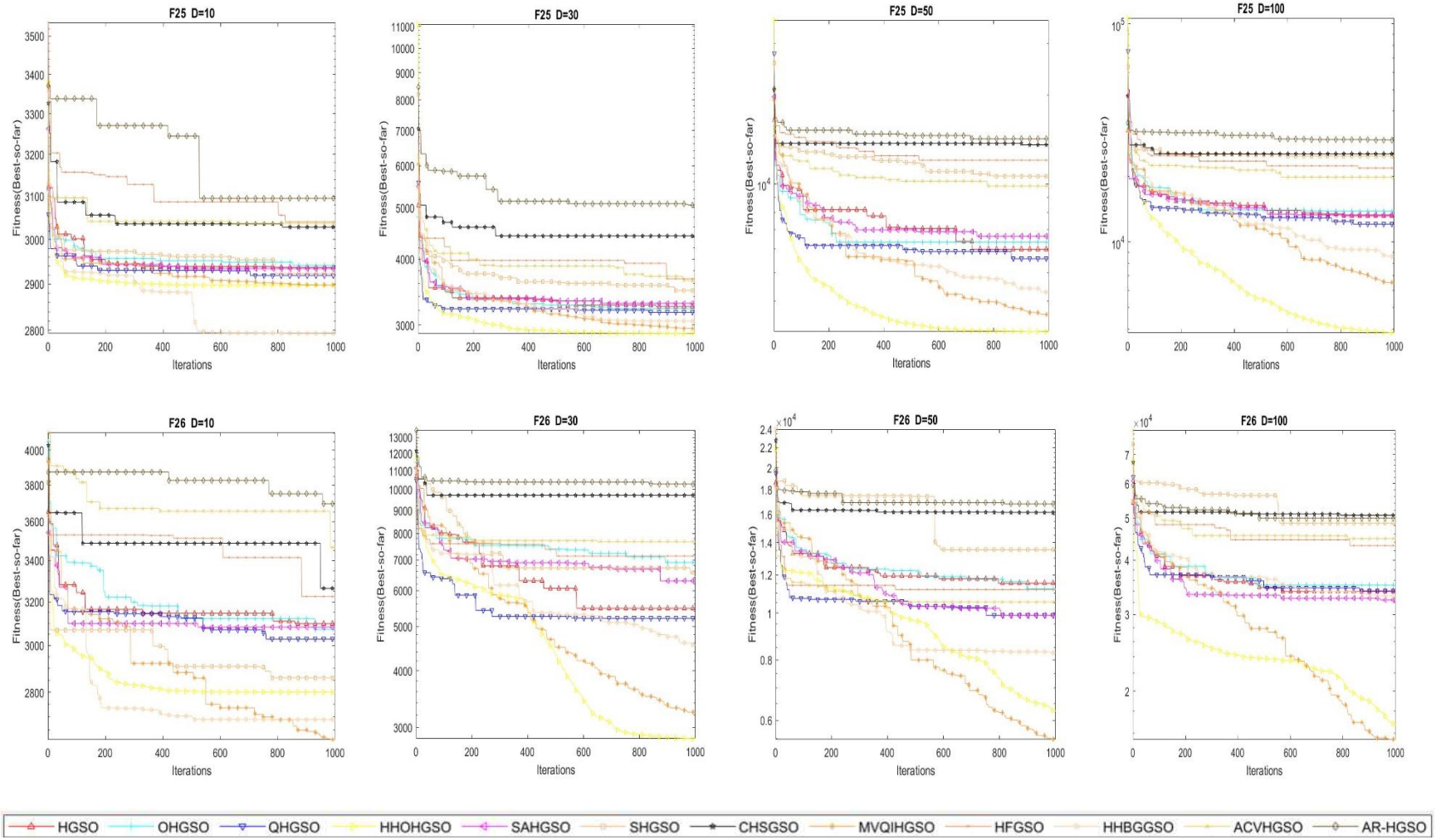


Fig. 7. (Continued)

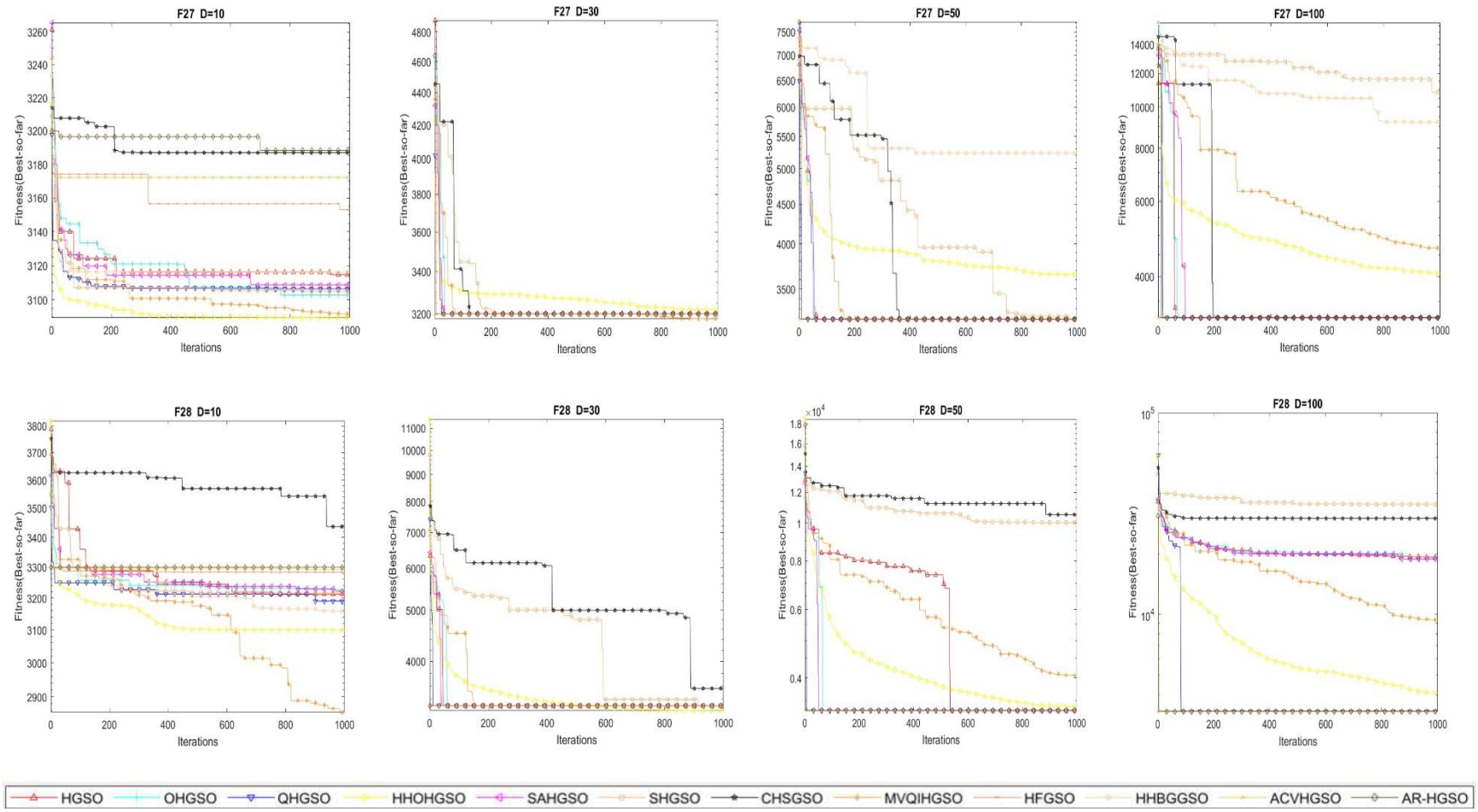


Fig. 7. (Continued)

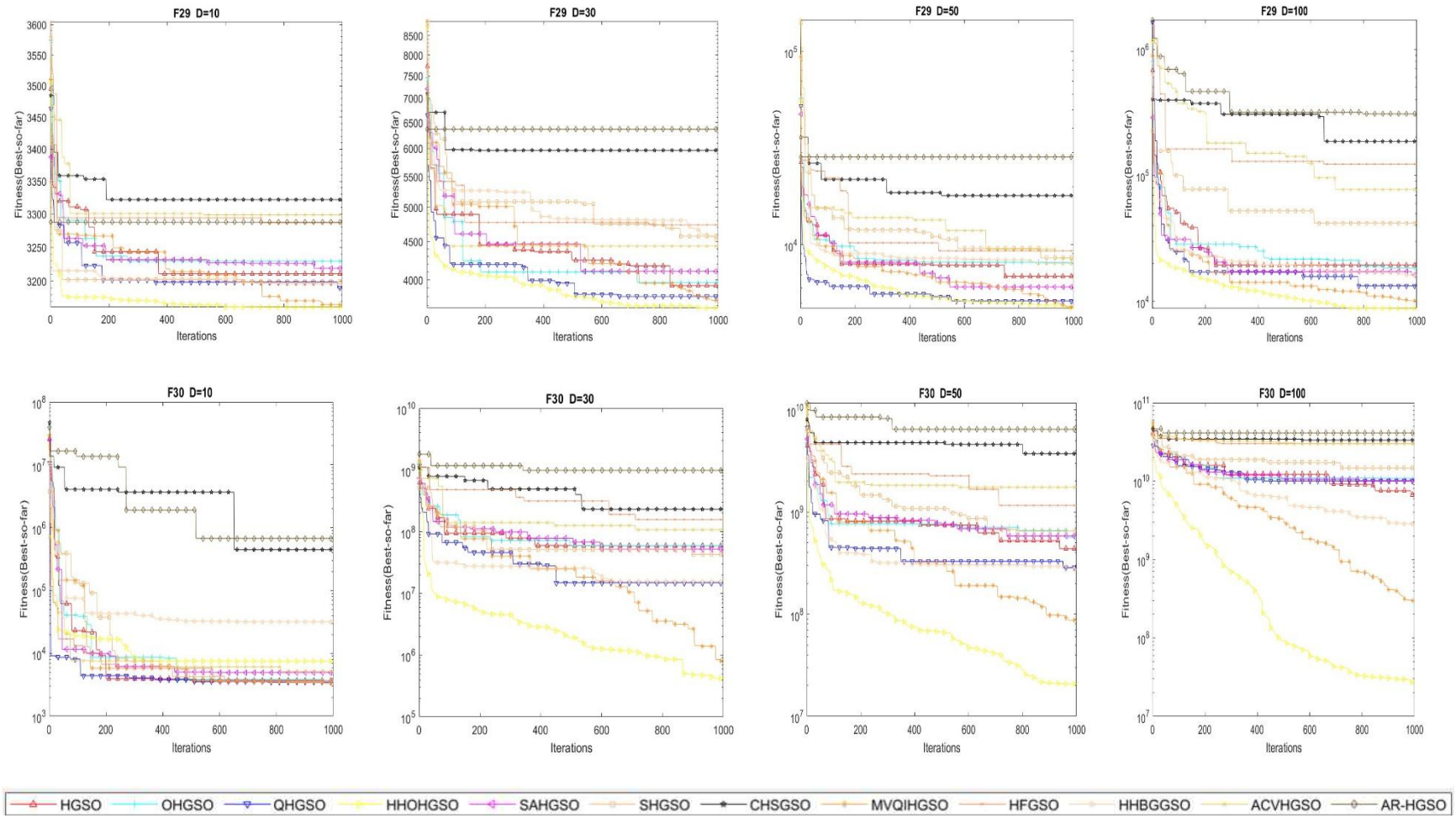


Fig. 7. (Continued)

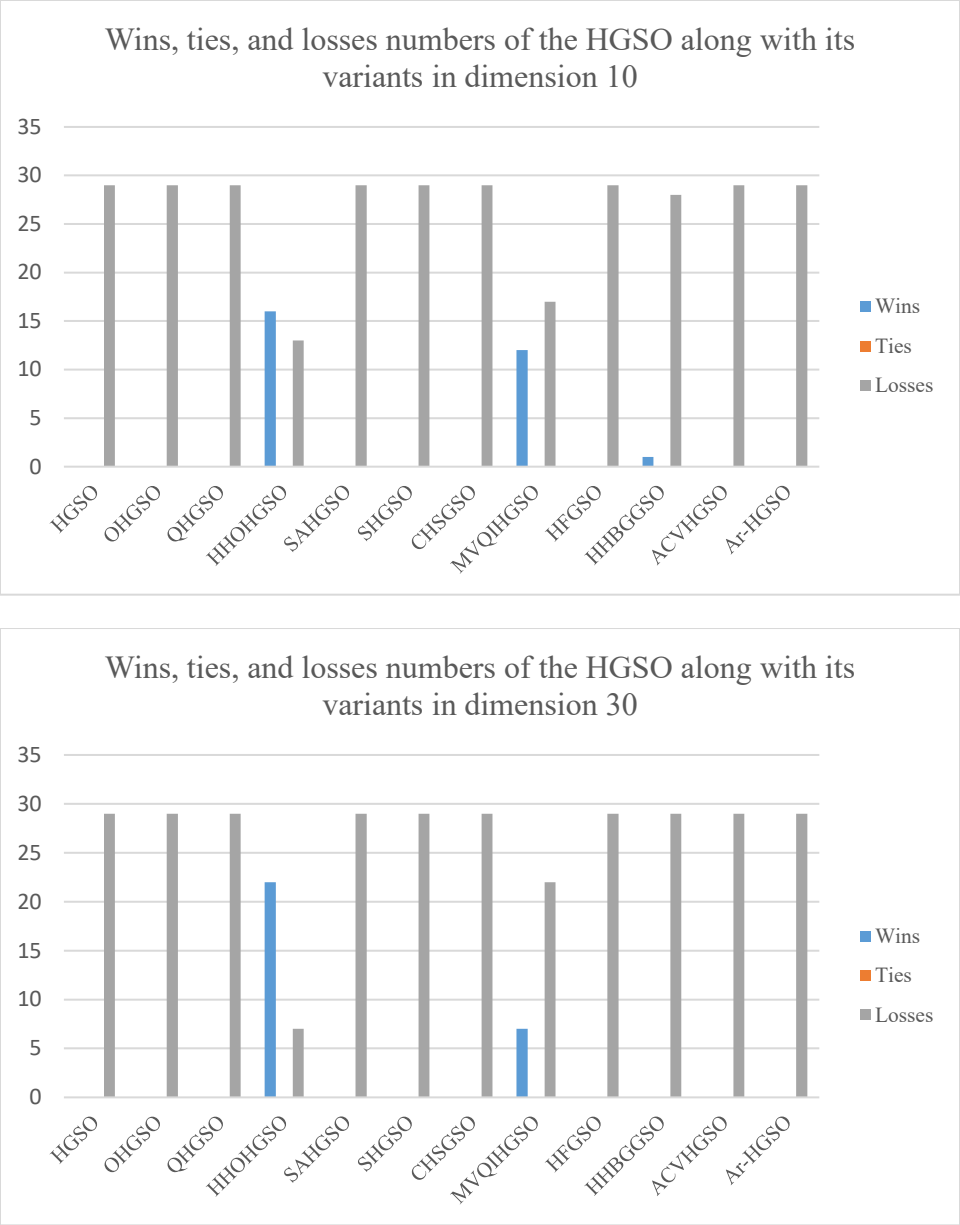
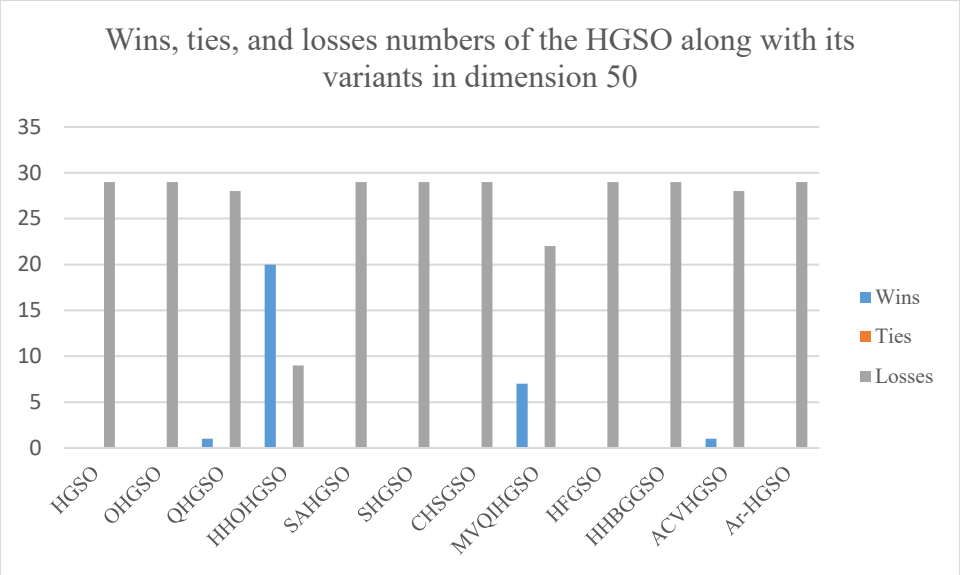


Fig. 8. Wins, ties, and losses numbers of HGSO along with its variants in 10, 30, 50 and 100 dimensions



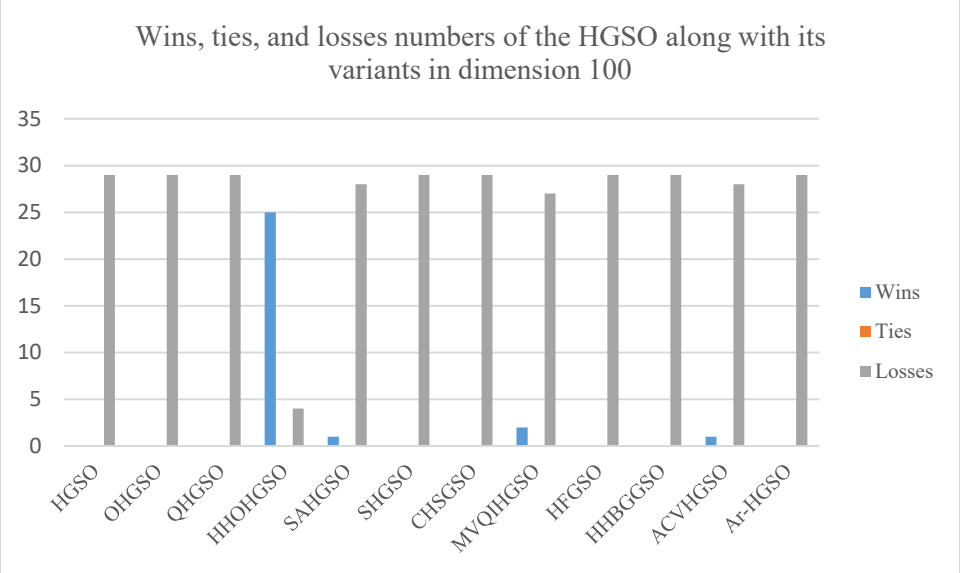


Fig. 8. (Continued)

The authors in [135] proposed a method known as HGSO-based MPTT to collect the optimal solar energy in photovoltaic systems. The effectiveness of the HGSO-based MPTT has been compared with other methods such as FDOA, PSO, perturb and observe (P&O), GHO and CSA considering various weather conditions, partial shading as well as static irradiance. The experimental results approved the superiority of the HGSO-based MPTT over other compared methods regards to oscillation minimization, settling time, power tracking efficiency and tracking time.

4.3. Electrochemical

4.3.1. Proton exchange membrane fuel cells

In [136], the HGSO has been utilized to tackle the parameter extraction problem in the proton exchange membrane fuel cells (PEMFC). The performance of the HGSO has been investigated on 10 benchmark functions along with three PEMFC models (i.e. BCS-500 W FC stack, SR-12 modular PEMFC stack and NedSstack PS-6 PEMFC stack). The experimental results confirmed the supremacy of the HGSO over GWO, PSO, WOA, ABC and ACO algorithms in accomplishing reduced execution time, smallest errors, best quality solutions as well as faster convergence.

4.3.2. Solid oxide fuel cells

In [68], the SAHGSO has been employed to deal with the parameter estimation problem in SOFC. The effectiveness of the SAHGSO has been firstly ascertained on 10 benchmark functions. Subsequently, the presented algorithm has been evaluated on the 96-cell SOFC stack under various pressure and temperature conditions. The experimental outcomes affirmed that the proposed algorithm is able to achieve the best values of the unknown parameters of the SOFC along with MSE in comparison with other competitive algorithms.

4.4. Medical applications

A wide range of medical applications utilizing the HGSO-related algorithms are illustrated in [57, 77, 79, 80, 82, 78, 92, 84, 90, 108, 102, 87, 137, 138, 139, 140, 141, 142].

To address the problem of forecasting the probability for cesarean or C-Section (CS) delivery, the work in [137] proposed a model known as HGSORF which combined the HGSO algorithm with the RF. In the proposed model, the HGSO is employed to optimally adjust the hyper-parameters of RF and thereby preventing local optima points. The effectiveness of the HGSORF model was validated on the Pakistan Demographic and Health Survey (PDHS) datasets (PDHS ’12-13 and PDHS’17-18 datasets) by utilizing different performance metrics including kappa index, precision, recall, MCC, specificity, sensitivity, accuracy, F1-Score, ROC curve, area under the ROC curve (AUC), and precision-recall curve (PRC). In addition, the HGSORF model has been compared with other approaches, namely grid search-based RF (GSRF), Bayesian optimization-based RF (BORF), WOA-based RF (WOARF) and random search-based RF (RSRF). The simulation results showed that the proposed HGSORF model gives better results than other compared methods for the considered problem.

In [138], an image segmentation technique based on HGSO which employed Kapur entropy was presented and investigated on the COVID-19 patient’s CT images. Various evaluation metrics, namely MSE, PSNR, FSIM (Feature Similarity Index Measure) and SSIM have been used in this

study. The simulation results confirmed the supremacy of HGSO over SA, SCA, GWO, MFO and CPSOGSA for optimal image segmentation.

To handle the problem of automatic alcoholism detection for EEG signals, the work in [139] proposed a model based on the HGSO along with feedforward neural network (FFNN). The proposed HGSO-FFNN was investigated on EEG alcoholism dataset known as UCI considering three evaluation metrics, namely accuracy, sensitivity and specificity. The empirical assessment results confirmed the effectiveness of the HGSO-FFNN for alcoholic detection.

In [140], a method known as MAFCNN-SCD (Optimal Multi-Attention Fusion Convolutional Neural Network-based Skin Cancer Diagnosis) has been proposed for detecting the skin cancer in dermoscopic images. The proposed MAFCNN-SCD comprises the initial stage (i.e preprocessing), the feature extraction stage and the final stage (i.e. detecting and classifying the skin cancer). The data are preprocessed through Wiener filter. Then, the HGSO is utilized to determine the hyper-parameters of the MAFNet approach during the feature extraction stage. The final stage is performed by the DBN. The effectiveness of the MAFCNN-SCD method has been ascertained on HAM10000 database and the ISIC 2017 database using various evaluation metrics like sensitivity, accuracy, specificity, MCC and F-score. The simulation results approved the supremacy of the MAFCNN-SCD method over Naïve Bayes, DenseNet169, MobileNet, KELM and MSVM methods in detecting the skin cancer.

To early forecast the pediatric sepsis along with evaluate its survival rate, the authors in [141] presented a SVM-BRF-HGSO model which integrated the SVM and radial basis function (RBF) into the HGSO. In the proposed model, the HGSO was employed to train the SVM-RBF classifier and thereby performing the informative gene selection. The effectiveness of the SVM-BRF-HGSO model was evaluated on the GSE66099 pediatric microarray dataset from the NCBI Gene Expression Omnibus repository employing various evaluation metrics including accuracy, specificity, sensitivity, AUC and precision. The simulation results attested the superiority of the SVM-BRF-HGSO model over other compared models in early detecting the pediatric sepsis.

In [142], the HGSO has been combined with deep learning (DL) to detect and classify the chronic kidney disease (CKD). The presented CKD-HGSODL method firstly employs min-max scaling for input data normalization and HGSO model for optimal feature selection. Subsequently, the classification is performed by an attention-based gated recurrent unit (AGRU) model. Lastly, the optimal hyperparameter selection is achieved by the slime mould algorithm (SMA). The proposed method has been validated on the CKD database using different metrics including precision, recall, accuracy, MCC and Fscore. The experimental outcomes revealed that the proposed technique is promising for CKD classification and detection.

4.5. Engineering Design Problems

Various applications of the HGSO-based algorithms to the engineering design problems are presented in [43, 49, 52, 114, 58, 76, 117].

The authors in [43] firstly proposed the HGSO algorithm and evaluated it on 47 benchmark functions from CEC'17 test suite along with three engineering design problems such as speed reducer, welded beam design and tension/compression spring design problems. The simulation results showed that the HGSO yielded better results than GSA, WOA, GWO, CS, PSA, SA and EHO algorithms for the studied problems.

4.6. Mechanical Engineering

4.6.1. Friction stir welding

In [143], the HGSO is integrated with the Random Vector Functional Link (RVFL) method to forecast the ultimate tensile strength (UTS) of AA6061-T6 friction stir welded (FSW) joints. The welding parameters considered in this study are welding speed, tilt angle, rotational speed as well as pin profile. The performance of the HGSO-RVFL model was tested on the data gathered from [144] and compared with KNN and ANFIS models. The simulation results confirmed the supremacy of the HGSO-RVFL model over KNN and ANFIS models under consideration of different evaluation metrics such as the MAE, RMSE, mean relative estimate error (MRE), coefficient of variance (COV) as well as coefficient of determination (R^2).

4.6.2. Fault Diagnosis

Fault diagnosis applications utilizing the HGSO are shown in [145, 146].

To address the problem of fault diagnosis for aero-engines, the authors in [145] proposed a three-stage framework optimized by both HGSO and HHO algorithms. In the first stage, the multi-domain feature extraction is performed. During the second stage, the HGSO is employed for feature selection and in the third stage, the HHO is utilized to train the ADBN. The effectiveness of the developed framework was tested on the dataset comprising seven types of sensor health conditions. The evaluation criteria used are average accuracy and average computation time. The simulation results approved the robustness of the developed framework in achieving high accuracy and reduced time for aero-engine fault diagnosis.

In [146], the problem of bearing fault diagnosis applied to rotating machines is tackled by a model combining the HGSO with Hilbert Transform (HT), Discrete Wave Transform (DWT) and Artificial Neural Network (ANN). The HT along with DWT are employed to perform the frequency shifting and then the feature extraction is carried out through sliding window.

Afterwards, the selection of the adequate features is accomplished by the HGSO. Ultimately, the ANN model is trained by the obtained optimal attributes so as to categorize various bearing faults. The feasibility of the proposed model was examined considering the constant speed and the speed variation. The experimental results demonstrate that the proposed model is effective to optimally diagnose the bearing faults in rotating machines.

4.7. Civil engineering and environment

Civil engineering and environment applications employing the HGSO are presented as follows:

To tackle a problem concerned with the forecasting of soil shear strength, the authors in [147] proposed a model named as HGSO-ANFIS which combined the HGSO with the ANFIS (adaptive network-based fuzzy inference system). The effectiveness of the proposed HGSO-ANFIS model was ascertained on soil dataset gathered from the Hai Phong-Thai Binh coastal national road project (Vietnam) based on RMSE and R^2 metrics. The simulation outcomes approved that the HGSO-ANFIS models accomplished better accuracy than GA-ANFIS and ICA-ANFIS models.

To predict the landslide susceptibility in mountainous areas, the HGSO has been used in [148] to optimally identify the weights of the deep neural network. The presented model has been investigated on the landslide dataset from a study site in Vietnam considering different performance metrics like MAE, RMSE, Kappa, OA (overall accuracy) and AUC. The simulation results affirmed the supremacy of HGSO over RF, random subspace and bagging.

In [149], the group method of data handling (GMDH) model has been integrated with the HGSO to predict the maximum hydro-suction dredging depth. The HGSO has been employed to optimally find the weights of the GMDH model. The effectiveness of the proposed GMDH-HGSO method has been examined on 100 datasets and compared with GMDH-PSO, LE-PSO, LE-HGSO, NLE-PSO and NLE-HGSO. The simulation results demonstrated that the GMDH-HGSO performed better than other compared methods considering R^2, RMSE, IA (mean index of agreement) and MAE.

To tackle the problem related to forecasting the sediment discharge in free-flushing, two techniques known as GMDH-HGSO and SVR-HGSO have been presented in [150]. The proposed techniques combined the GMDH model and Support Vector Regression (SVR) with the HGSO, respectively. The proposed techniques have been applied on 160 datasets to confirm their feasibility based on RMSE, R^2 (correlation coefficient), MARE (mean absolute relative error) and MAE evaluation metrics. The simulation results revealed that the GMDH-HGSO provided better results than SVR-HGSO, GMDH-EO, SVR-EO, ANFIS, MLP (Multivariate Linear Regression), MLPNN (Multi-Layer Perceptron Neural Network) and GMDH models for the considered problem.

In [151], a HGSO-SVR algorithm has been proposed to forecast the compressive strength of the high-performance concrete. The effectiveness of the HGSO-SVR was ascertained on high-performance concrete dataset having fly ash, superplasticizer and silica fume. The evaluation metrics used in this work are RMSE, MAE, R^2, VAF (variance account factor) and the aggregate statistical parameter of MAE, RMSE and R2 (OBJ). The simulation results confirmed the supremacy of the HGSO-SVR over PSO-SVR in forecasting the compressive strength of the high-performance concrete.

The authors in [152] proposed a hybrid machine learning model to forecast the maximum displacement of reinforced concrete beams subjected to blast loading. In the proposed model, the HGSO was integrated with a hybrid gradient-boosted tree algorithm and utilized to optimally tune the model parameters. The effectiveness of the proposed model was tested on various blast loading datasets considering the coefficient of determination R^2, MAE and the variance explained by cross-validation (VEcv).The simulation results approved the effectiveness of the presented model.

In [153], the authors proposed a SVR-HGSO algorithm to estimate the pile settlement of the Kuala Lampur transportation network considering the land rock properties. The performance measures employed are RMSE, MAE, R^2, VAF and the aggregate statistical parameter of MAE, RMSE and R^2 (OBJ). The simulation results affirmed the effectiveness of the SVR-HGSO over PSO-HGSO in estimating the pile settlement.

In [154], the HGSO has been merged with the SVR technique in order to predict the frost durability of the recycled aggregate concrete (RCA). The proposed HGSO-SVR model was tested on a comprehensive dataset comprising RCA, air-entraining type, water, sand, cement, natural coarse aggregate, fly ash, gravel, RCA treatment method, RCA replacement ratio, and water sorption. The evaluation metrics employed in this study include RMSE, relative absolute error (RAE), root relative square error (RRSE), R^2, MAE, performance index (PI), agreement of forecasting results (AI), as well as comprehensive index (OBJ). The experimental results demonstrate that the HGSO-SVR model outperformed the GWO-SVR and ALO-SVR models.

The HGSO-SVR algorithm has been presented in [155] to estimate the compressive strength of the high-performance concrete (HPC) including flash ash along with blast furnace slag. The simulation showed that of the HGSO-SVR surpassed CSO (cuckoo search optimization)-SVR in terms of RMSE.

In [156], the compressive strength of the concrete mixtures has been successfully predicted by a model combining the HGSO along with radial basis function neural network (HGSO-RBFNN).

The HGSO-RBFNN model has been presented in [157] to forecast the compressive strength of the HPC mixtures. The proposed model was applied on the dataset of 181 HPC mixtures that consist of superplasticizer and fly ash. The proposed model yielded promising results.

4.8. Mining Engineering

In [158], the authors proposed two hybrid techniques based on the HGSO to estimate the copper grade in the porphyry copper deposits (PCD). In this work, the HGSO has been employed to optimally tune the parameters of the multi-layer perceptron (MLP) as well as ANFIS models. The empirical results based on Iju PDC located in the province of Kerman in Iran approved the effectiveness of the ANFIS-HGSO and MLP-HGSO techniques.

The ANFIS-HGSO method has been proposed in [159] for forecasting the mine blast-induced flyrock. In this study, the HGSO has been employed to optimize the ANFIS model. The simulation results approved that the ANFIS-HGSO was effective to forecast flyrock distance induced from mine blasting.

4.9. Communication Engineering

The applications of the HGSO variants in communication engineering are illustrated in [63, 95, 127].

4.10. Nuclear Engineering

A HGSO algorithm has been utilized in [160] to adjust the PID gains for a pressurized water reactor (PWR) of the point kinetics model having six groups of the delayed-neutron precursors. The objective function optimized in this study is the ITSE performance index which is subjected to Lyapunov stability criterion for insuring the controller stability. The results showed that the HGSO-PID outperformed GA-PID and PID approaches in providing better accuracy and the minimum error while adjusting PID controller.

In [161], the PID gains for a PWR of a two-point kinetics model have been optimized by the HGSO taking into account the axial offset (AO) following strategy along with ITAE performance index. Furthermore, the ITAE performance index was constrained to Lyapunov stability criterion to assure the stability of the controller. The simulation results revealed the superiority of HGSO-PID method compared to PSO-PID and conventional PID methods regards to execution time, speed and accuracy to attain optimal solutions.

Table 13

The overall effectiveness of the HGSO and its variants

Function	Dimension	Metrics	HGSO [43]	OHGSO [61]	QHGSO [114]	HHO-HGSO [49]	SAHGSO [68]	SHGSO [99]	CHSGSO [109]	MVQIHGSO [85]	HFGSO [87]	HHBGGSO [89]	ACVHGSO [79]	Ar-HGSO [80]
	10	W/T/L	0/0/29	0/0/29	0/0/29	16/0/13	0/0/29	0/0/29	0/0/29	12/0/17	0/0/29	1/0/28	0/0/29	0/0/29
	30	W/T/L	0/0/29	0/0/29	0/0/29	22/0/7	0/0/29	0/0/29	0/0/29	7/0/22	0/0/29	0/0/29	0/0/29	0/0/29
	50	W/T/L	0/0/29	0/0/29	1/0/28	20/0/9	0/0/29	0/0/29	0/0/29	7/0/22	0/0/29	0/0/29	1/0/28	0/0/29
	100	W/T/L	0/0/29	0/0/29	0/0/29	25/0/4	1/0/28	0/0/29	0/0/29	2/0/27	0/0/29	0/0/29	1/0/28	0/0/29
Total		W/T/L	0/0/116	0/0/116	1/0/115	83/0/33	1/0/115	0/0/116	0/0/116	28/0/88	0/0/116	1/0/115	2/0/114	0/0/116
Overall Effectiveness		%	0	0	0.862	**71.552**	0.862	0	0	24.138	0	0.862	1.724	0

Table 14

Average execution times (in second) required by the HGSO along with its variants to handle the unimodal test functions

Function	Dimension	Metrics	HGSO [43]	OHGSO [61]	QHGSO [114]	HHO-HGSO [49]	SAHGSO [68]	SHGSO [99]	CHSGSO [109]	MVQIHGSO [85]	HFGSO [87]	HHBGGSO [89]	ACVHGSO [79]	Ar-HGSO [80]
Unimodal	10	Avg	3.88435	4.5866	1.8274	2.14105	6.01845	**1.61715**	4.5597	3.61945	26.53295	2.5288	8.9634	4.6007
	30	Avg	8.17405	10.6043	3.4296	3.945	12.35265	7.30055	10.96215	6.54865	59.69495	**3.2134**	20.47925	12.4624
	50	Avg	13.78435	13.93985	6.8029	**4.28755**	18.1416	8.50905	13.18145	8.3156	88.33775	11.73715	20.8593	15.5882
	100	Avg	19.2539	24.4065	13.89385	**8.3368**	29.31865	14.43085	21.1991	16.0502	179.66225	21.35355	51.0912	25.0883

Table 15

Average execution times (in second) required by the HGSO along with its variants to handle the multimodal test functions

Function	Dimension	Metrics	HGSO [43]	OHGSO [61]	QHGSO [114]	HHO-HGSO [49]	SAHGSO [68]	SHGSO [99]	CHSGSO [109]	MVQIHGSO [85]	HFGSO [87]	HHBGGSO [89]	ACVHGSO [79]	Ar-HGSO [80]
Multimodal	10	Avg	4.120442857	3.383728571	**1.993114286**	2.806942857	5.69537143	2.27742857	4.52362857	4.100657143	15.8670286	3.807085714	7.453928571	3.363528571
	30	Avg	8.669128571	8.032557143	3.708414286	**3.6543286**	11.3223429	5.7507	9.43995714	8.157757143	50.0280857	6.621985714	15.78951429	9.429328571
	50	Avg	15.09231429	15.40385714	6.448885714	**5.2683143**	15.5248286	10.2623	13.7720857	10.93544286	80.7522857	7.841842857	27.30911429	15.47918571
	100	Avg	25.21971429	35.86664286	11.2111	**10.389371**	26.3194857	22.4788857	22.9200857	19.08474286	156.481714	15.29798571	44.73925714	27.18278571

Table 16

Average execution times (in second) required by the HGSO along with its variants to handle the hybrid test functions

Function	Dimension	Metrics	HGSO [43]	OHGSO [61]	QHGSO [114]	HHO-HGSO [49]	SAHGSO [68]	SHGSO [99]	CHSGSO [109]	MVQIHGSO [85]	HFGSO [87]	HHBGGSO [89]	ACVHGSO [79]	Ar-HGSO [80]
Hybrid	10	Avg	3.55798	3.81545	**2.02716**	3.0328	5.6363	3.70324	4.83328	3.6583	18.19762	3.25468	7.53851	3.7657
	30	Avg	8.66198	9.08045	4.16026	**3.83472**	11.79789	7.61006	10.3803	7.00104	50.19041	5.62263	18.06019	9.89941
	50	Avg	15.72278	11.52493	7.57917	**4.03651**	15.96827	10.08688	14.82534	11.25537	87.65584	9.42173	27.75308	14.07347
	100	Avg	22.56228	36.26945	10.68776	**7.75257**	25.5696	24.01137	25.21847	19.2434	174.84852	17.25141	48.94589	29.76088

Table 17

Average execution times (in second) required by the HGSO along with its variants to handle the composition test functions

Function	Dimension	Metrics	HGSO [43]	OHGSO [61]	QHGSO [114]	HHO-HGSO [49]	SAHGSO [68]	SHGSO [99]	CHSGSO [109]	MVQIHGSO [85]	HFGSO [87]	HHBGGSO [89]	ACVHGSO [79]	Ar-HGSO [80]
Composition	10	Avg	3.49014	3.44554	**1.94545**	2.70182	6.13863	4.03393	5.12641	4.21291	17.54944	3.3456	7.21058	3.62461
	30	Avg	7.74318	8.31571	**4.12772**	5.02996	12.93183	7.99434	11.14362	8.11263	53.70231	6.17623	18.08991	10.00708
	50	Avg	13.99461	12.99027	**6.51385**	8.66907	18.51593	12.79228	17.10898	15.48908	83.27815	8.76325	26.05387	16.91077
	100	Avg	25.56555	30.73922	**13.37861**	22.93773	32.97679	32.19825	32.83319	30.31949	155.4583	19.2309	48.53375	34.44981

Table 18

Average execution times (in second) required by the HGSO along with its variants to handle all the test functions

Function	Dimension	Metrics	HGSO [43]	OHGSO [61]	QHGSO [114]	HHO-HGSO [49]	SAHGSO [68]	SHGSO [99]	CHSGSO [109]	MVQIHGSO [85]	HFGSO [87]	HHBGGSO [89]	ACVHGSO [79]	Ar-HGSO [80]
All Test	10	Avg	3.692862069	3.636868966	**1.976989655**	2.802651724	5.850131034	3.329241379	4.840748276	3.953641379	17.98640345	3.369310345	7.503282759	3.677558621
Functions	30	Avg	8.313227586	8.6689	**3.989582759**	4.210934483	12.11237586	7.272413793	10.45666207	7.632355172	52.01771379	5.888596552	17.68917586	9.999827586
	50	Avg	14.8409931	13.13305862	6.885455172	**5.948589655**	16.88962069	10.95330345	15.24519655	12.43530345	84.52694483	8.973	26.58454828	15.49562414
	100	Avg	24.01117586	33.44711034	**11.96307241**	13.6655931	28.56336552	25.80379655	27.01225517	22.80422414	164.0608655	17.74538276	47.93633103	30.4332069

4.11. Transportation

The applications of the HGSO-related algorithms to transportation are depicted in [55, 61, 162].

The authors in [162] presented a model named as HGSODL-TFF to forecast the traffic flow in the 6G enabled VANET (vehicular ad hoc networks). In this model, at the beginning, the traffic data are preprocessed by employing z-score normalization method. Moreover, the traffic flow forecasts the DBN model. Ultimately, the hyper-parameters including epoch count, learning rate and batch size are optimally adjusted by HGSO algorithm. The effectiveness of the HGSODL-TFF model was evaluated on data gathered in the 6G assisted vehicular networks. The simulation results demonstrated the superiority of the HGSODL-TFF model over the state-of-the-art models considering mean absolute percentage error (MAPE), MAE and RMSE evaluation metrics.

4.12. Agriculture

The applications of HGSO in agriculture have been mentioned in [59, 71, 110, 163].

In [163], the classification of soil images has been addressed by the HGSO integrating the improved bag of features (BOF) and AlexNet model. The proposed HGSO-BOF method was ascertained on the soil image dataset containing seven soil images such as clay, clayey sand, clayed peat, sandy clay, peat, silty sand and humus clay. The performance measures used to assess the BOF-HGSO are classification accuracy, F1-Score, precision and recall. The simulation results approved the supremacy of the BOF-HGSO over BOF, BOF-GWO, BOF-GOA, BOF-DE and BOF-WOASA methods in classifying soil images.

4.13. E-waste management

The electronic waste (E-waste) management problems have been tackled in [60, 91] through the HGSO variants.

4.14. Meteorology

The authors in [164], employed the HGSO to optimize the parameters of the radial basis function neural network (RABFN). The resulting RABFN-HGSO model has been utilized to predict the rainfall on monthly basis. The experimental results showed that the RABFN-HGSO model yielded better results than RABFN-SSA as well as RABFN-COA models.

In [165], the GRNN-HGSO model has been presented for monthly solar irradiance forecasting on three stations located at Mazandaran in Iran. The HGSO has been employed to optimize the GRNN (generalized regression neural network). The simulation results confirmed the outperformance of

the GRNN-HGSO model over GRNN, GRNN-SSA and GRNN-ANO for solar irradiance prediction.

4.15. Other applications

Some other applications of the HGSO and its variants are illustrated in [51], [54], [166], [103], [50], [86], [106].

To address the problem related to optimal design of a vehicle brake pedal, the authors in [51] proposed a model named as HGSO-RBF. In this study, the Latin hypercube sampling technique has been employed to get the optimization variables. The objective function taken into account in this study was the minimization of the structural mass subjected to stress. The simulation results remarkably confirmed the effectiveness of HGSO-RBF over GA, ALO and SSA in achieving optimal design for vehicle brake pedal.

In [166], the authors proposed a novel framework for solving the object detection and multi-object tracking problem. In the proposed framework, firstly, the input video underwent the video frame extraction in order to get useful information related to an action. Afterwards, the entropy weighting K-means (EWKM) algorithm was employed to segment the objects. Then, the DCNN was trained by the hybridized Jaya-political optimizer (Jaya-PO) algorithm (i.e. hybridizing Jaya optimization along with political optimizer algorithms) to detect the object. Finally, the HGSO was employed to optimize the unscented Kalman filtering (UKF) and thereby perform the multi-object tracking. Both Jaya-PO-based DCNN and HGSO-based UKF models proposed for the novel framework have been validated on the UCSD anomaly detection dataset and MOT17 dataset respectively utilizing various evaluation metrics like accuracy, F1-Score, specificity, sensitivity and MOTP (multi-object tracking precision). The simulation results confirmed the supremacy of both Jaya-PO-based DCNN and HGSO-based UKF models in detecting objects and tracking multiple-objects.

To tackle the problem of trajectory planning for a 9-DOF redundant manipulator, the PI-based HGSO algorithm was proposed in [50]. In this work, the HGSO was employed to find the optimal parameters of the PI controller so as to accomplish the least trajectory planning error. The experimental results approved the supremacy of the PI-HGSO over PI-PSO, PI-ACO, PI-GWO and PI-GA for trajectory planning.

The applications of fabric defect detection using the MHL21-RELM are detailed in [86].

5. Discussion and Critical Analysis of HGSO along with its Variants

5.1. Merits and Demerits of HGSO

The HGSO is an algorithm which has been firstly proposed in 2019 and since then it has proven its supremacy to tackle a variety of problems in multiple research areas owing to its merits including easy implementation, less control parameters, better adjustability, ability to balance exploration and exploitation phases in the searching space, etc. The easiness of the HGSO has encouraged its applications to a large range of domains like computer science, electrical engineering, medical, mechanical engineering, engineering design problems, civil engineering and environment, etc, as portrayed in Table 3. This shows the popularity of the HGSO.

Despite its better merits for some optimization problems, the HGSO presents some demerits as other metaheuristics according to the no-free-lunch theorem that states that no algorithm is able to competently tackle all kinds of optimization problems [167]. Some demerits of the HGSO are its slow convergence speed, being stuck in local optima, etc. The merits and demerits of the HGSO are tabulated in Table 8.

The demerits exhibited by the conventional HGSO have motivated various researches to propose diverse variants to ameliorate its performance. Tables 2, 3, 4, 5 and 6 are illustrating a variety of HGSO variants which are therefore the improved versions of the conventional HGSO. Numerous HGSO variants fall in the category of hybridizations of the HGSO. There is only one binary version of HGSO and three multi-objective HGSO variants.

5.2. Effective assessment and analysis of the HGSO and its variants

This section describes the evaluation and analysis of the HGSO with some of its variants. Twelve algorithms comprising HGSO [43] and eleven HGSO variants such as QHGSO [114], OHGSO [61], HHO-HGSO [49], SHGSO [99], SAHGSO [68], CHSGSO [109], HFGSO [87], MVQIHGSO [85], ACVHGSO [79], HHBGGSO [89], and Ar-HGSO [80], have been assessed on 29 test functions from the CEC 2018 [167] for various dimensions including 10, 30, 50 and 100. This CEC 2018 benchmark suite comprises unimodal test functions (F_1, F_3), multimodal test functions (F_4, F_5, F_6, F_7, F_8, F_9, F_{10}), hybrid test functions (F_{11}, F_{12}, F_{13}, F_{14}, F_{15}, F_{16}, F_{17}, F_{18}, F_{19}, F_{20}) and composition test functions (F_{21}, F_{22}, F_{23}, F_{24}, F_{25}, F_{26}, F_{27}, F_{28}, F_{29}, F_{30}). The objective of this evaluation is to analyze the effectiveness of the HGSO variants in addressing the drawbacks associated with the conventional HGSO. In this study, the parameters settings of the competitive algorithms are kept alike as in the respective references. For each algorithm involved in this comparison, 30 independent runs have been carried out. Furthermore, the values assigned to the size of population (gases number), number of groups (cluster number), and number of maximum iterations are 35, 5, and 1000, respectively.

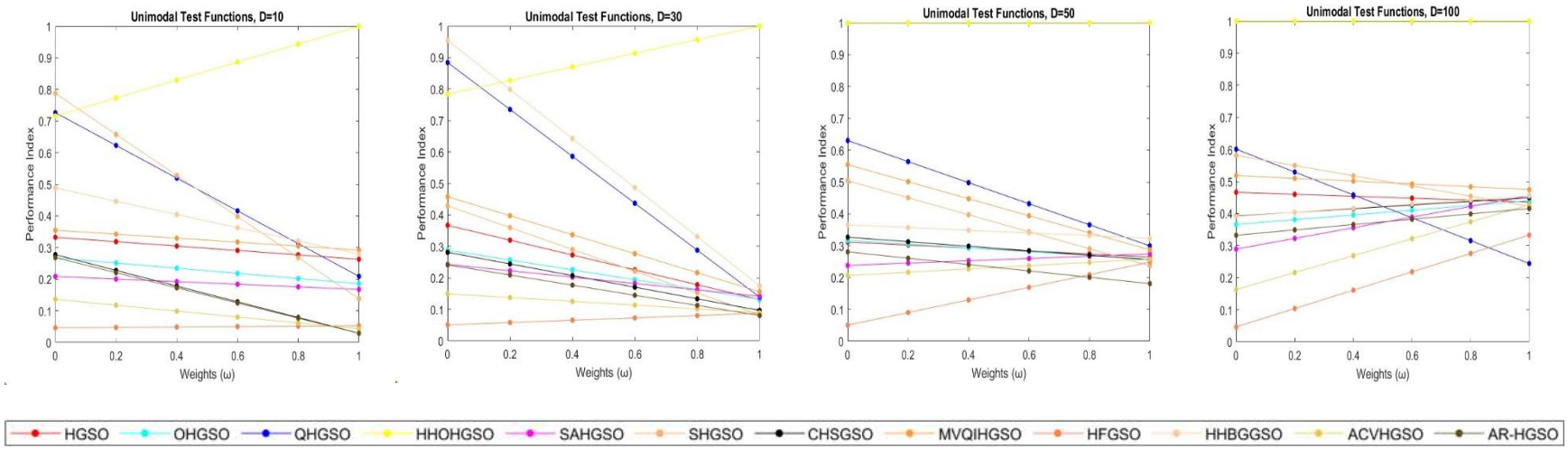


Fig. 9. Comparison of performance index analysis of the HGSO along with its variants on the unimodal test functions

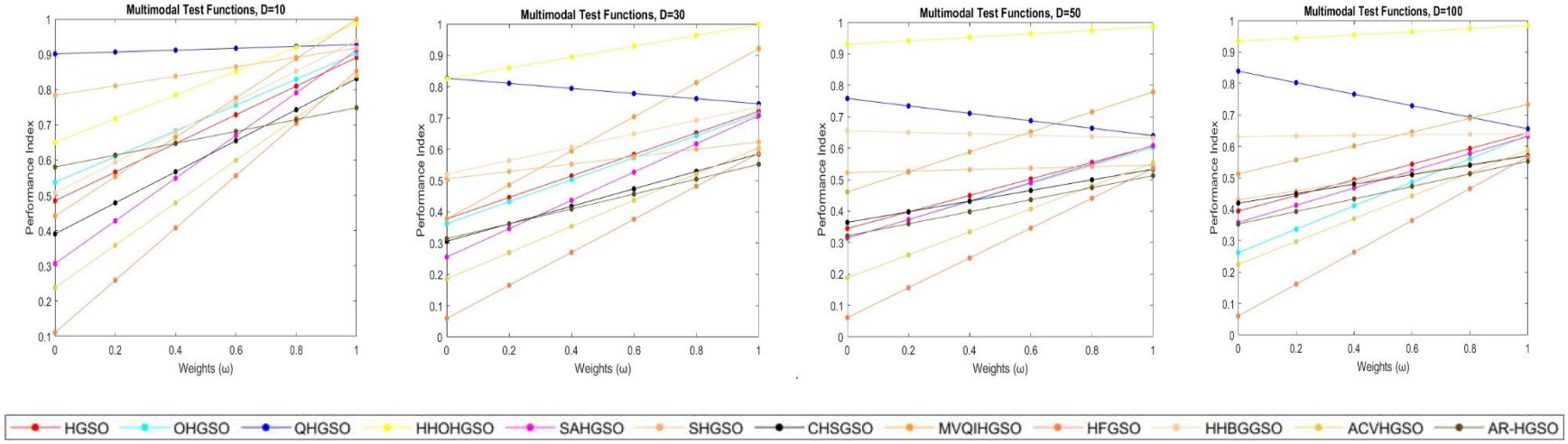


Fig. 10. Comparison of performance index analysis of the HGSO along with its variants on the multimodal test functions

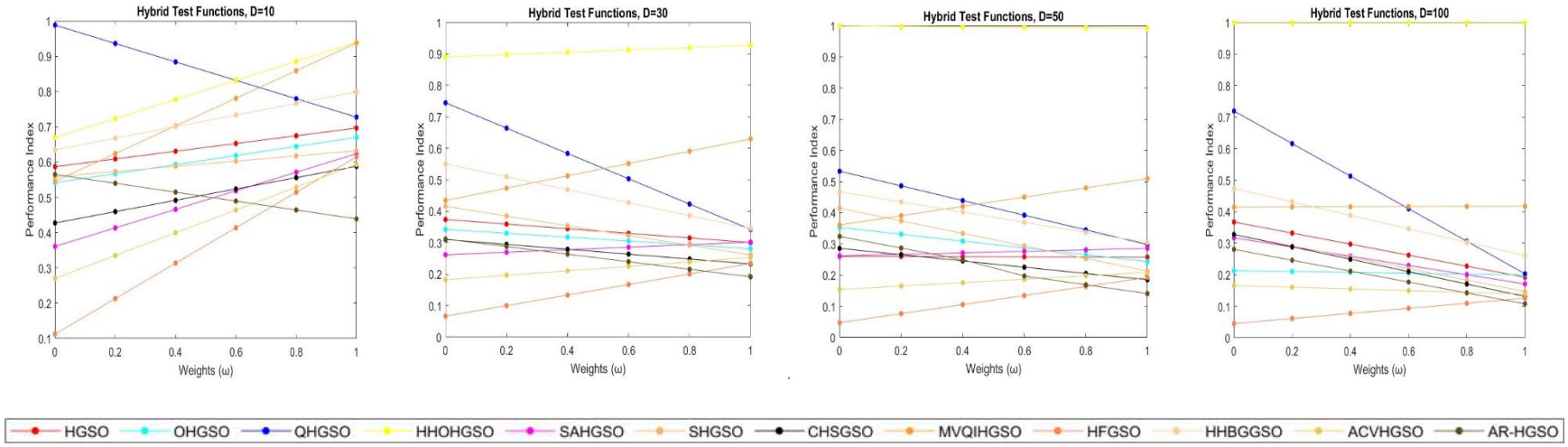


Fig. 11. Comparison of performance index analysis of the HGSO along with its variants on the hybrid test functions

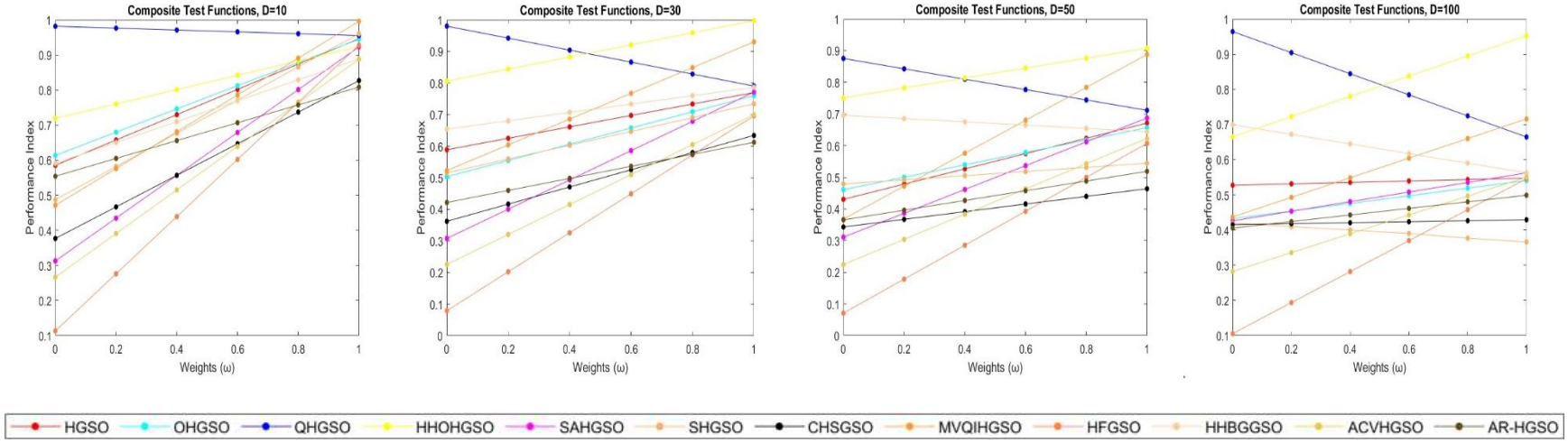


Fig. 12. Comparison of performance index analysis of the HGSO along with its variants on the composition test functions

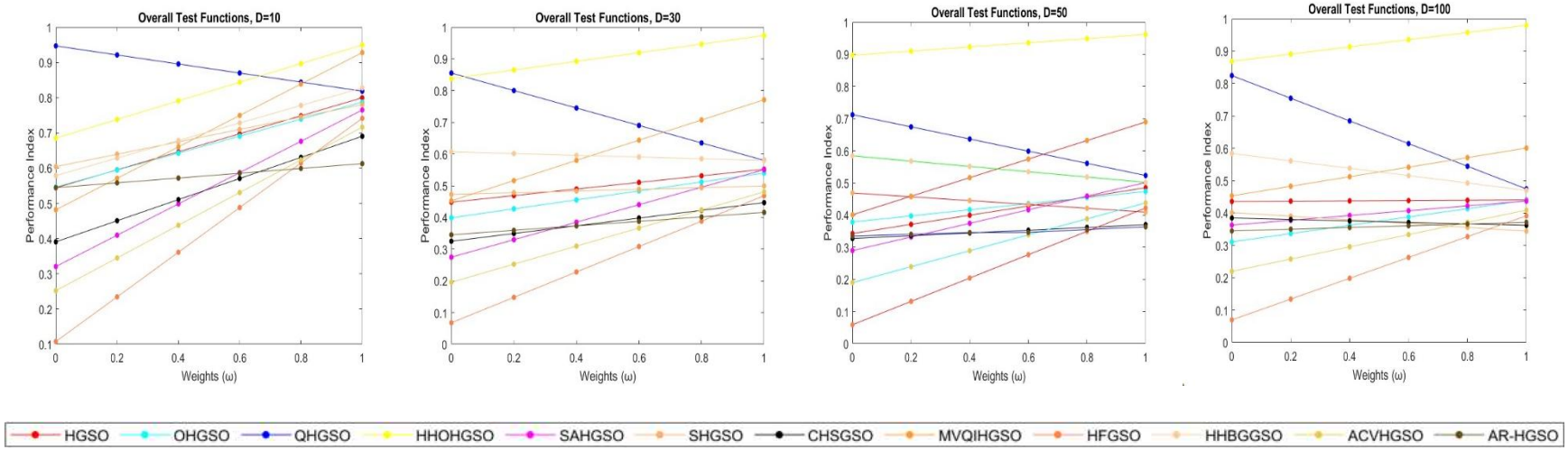


Fig. 13. Comparison of performance index analysis of the HGSO along with its variants on the overall test functions

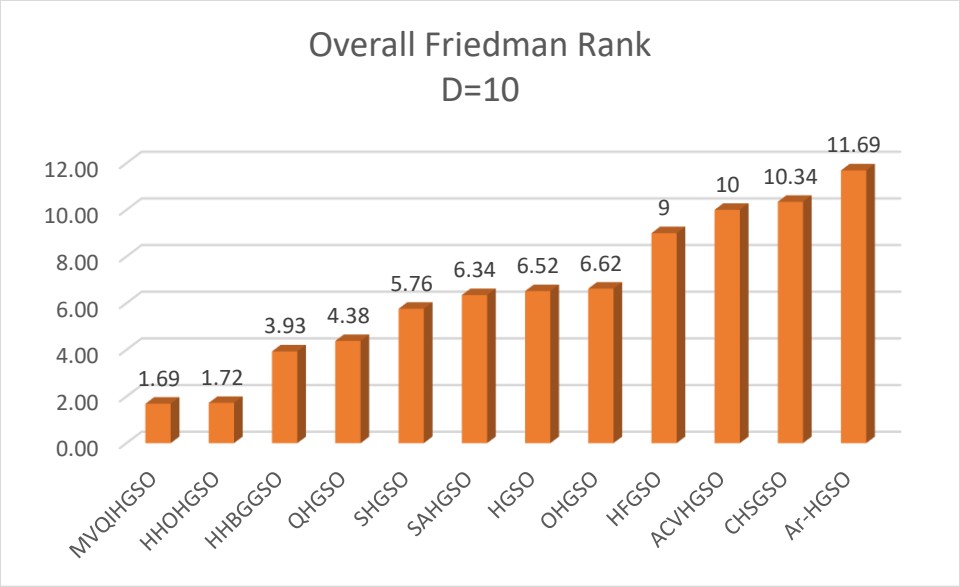
Table 19
MAE test of the HGSO along with its variants in various dimensions on all the test functions

Function	Dimension	Metrics	HGSO[43]	OHGSO [61]	QHGSO [114]	HHO-HGSO [49]	SAHGSO [68]	SHGSO [99]	CHSGSO [109]	MVQIHGSO [85]	HFGSO [87]	HHBGGSO [89]	ACVHGSO [79]	Ar-HGSO [80]
Unimodal	10	MAE	1.55E+08	1.56E+08	1.48E+08	**1.46E+01**	1.86E+08	1.05E+08	1.67E+09	1.46E+05	8.31E+08	6.78E+06	9.01E+08	2.58E+09
Test		Rank	6	7	5	**1**	4	9	12	2	10	3	8	11
Functions	30	MAE	6.19E+09	6.585E+09	5138675686	**7.13E+05**	6799867699	1.1868E+10	1.9853E+10	114867966.7	1.5506E+10	1.249E+09	1.5002E+10	2.279E+10
		Rank	5	6	4	**1**	7	8	11	2	10	3	9	12
	50	MAE	1.85E+10	2.49E+10	1.87E+10	**2.02E+07**	1.93E+10	4.00E+10	4.96E+10	2.63E+09	3.98E+10	5.30E+09	4.11E+10	5.05E+10
		Rank	4	7	5	**1**	6	9	11	2	8	3	10	12
	100	MAE	7.82E+10	8.16E+10	7.57E+10	**7.06E+08**	7.49E+10	1.17E+11	1.34E+11	2.46E+10	1.19E+11	3.68E+10	1.09E+11	1.32E+11
		Rank	6	7	5	**1**	4	9	12	2	10	3	8	11
Multimodal	10	MAE	2.28E+02	1.97E+02	1.56E+02	6.16E+01	1.90E+02	1.60E+02	2.82E+02	**4.66E+01**	2.53E+02	1.36E+02	2.96E+02	4.11E+02
Test		Rank	8	7	4	2	6	5	10	**1**	9	3	11	12
Functions	30	MAE	1.73E+03	1.71E+03	1.69E+03	**8.16E+02**	1.79E+03	2.44E+03	3.75E+03	1.06E+03	3.27E+03	1.84E+03	2.94E+03	4.64E+03
		Rank	5	4	3	**1**	6	8	11	2	10	7	9	12
	50	MAE	6.39E+03	6.81E+03	5.50E+03	**2.23E+03**	6.46E+03	8.39E+03	1.07E+04	4.16E+03	9.98E+03	5.72E+03	8.94E+03	1.30E+04
		Rank	5	7	3	**1**	6	8	11	2	10	4	9	12
	100	MAE	1.78E+04	1.76E+04	1.69E+04	**7.07E+03**	1.79E+04	2.53E+04	2.71E+04	1.31E+04	2.62E+04	1.55E+04	2.43E+04	2.97E+04
		Rank	6	5	4	**1**	7	9	11	2	10	3	8	12
Hybrid	10	MAE	3.17E+05	7.20E+04	8.70E+04	2.29E+03	2.18E+05	1.53E+05	8.00E+05	**1.03E+03**	8.43E+05	1.87E+04	6.55E+05	2.23E+06
Test		Rank	8	4	5	2	7	6	10	**1**	11	3	9	12
Functions	30	MAE	1.90E+08	1.04E+08	8.04E+07	**2.73E+05**	1.61E+08	8.71E+07	1.48E+09	1.06E+06	6.76E+08	1.45E+07	1.10E+09	2.20E+09
		Rank	8	6	4	**1**	7	5	11	2	9	3	10	12
	50	MAE	1.81E+09	1.37E+09	1.28E+09	**2.23E+06**	1.40E+09	3.76E+09	9.03E+09	2.34E+07	7.47E+09	5.24E+08	6.85E+09	1.12E+10
		Rank	7	5	4	**1**	6	8	11	2	10	3	9	12
	100	MAE	8.37E+09	8.46E+09	7.70E+09	**4.23E+07**	6.91E+09	1.73E+10	2.19E+10	7.36E+08	2.28E+10	2.64E+09	2.05E+10	2.70E+10

	Rank	6	7	5	**1**	4	8	10	2	11	3	9	12

Table 19
(Continued)

Function	Dimension	Metrics	HGSO[43]	OHGSO [61]	QHGSO [114]	HHO-HGSO [49]	SAHGSO [68]	SHGSO [99]	CHSGSO [109]	MVQIHGSO [85]	HFGSO [87]	HHBGGSO [89]	ACVHGSO [79]	Ar-HGSO [80]
Composite	10	MAE	3.47E+02	3.51E+02	3.14E+02	6.55E+02	4.73E+02	3.01E+02	4.47E+04	**1.92E+02**	4.05E+02	3.08E+03	5.94E+02	6.77E+04
Test		Rank	4	5	3	9	7	2	11	**1**	6	10	8	12
Functions	30	MAE	5.90E+06	5.93E+06	1.48E+06	**4.17E+04**	5.22E+06	4.30E+06	2.32E+07	7.66E+04	1.57E+07	1.56E+06	1.07E+07	9.87E+07
		Rank	7	8	3	**1**	6	5	11	2	10	4	9	12
	50	MAE	4.38E+07	5.65E+07	2.84E+07	**2.07E+06**	5.84E+07	6.50E+07	3.74E+08	8.68E+06	1.16E+08	2.74E+07	1.75E+08	6.48E+08
		Rank	5	6	4	**1**	7	8	11	2	9	3	10	12
	100	MAE	8.59E+08	9.14E+08	9.42E+08	**3.80E+06**	8.34E+08	1.79E+09	3.51E+09	3.60E+07	3.20E+09	3.03E+08	2.94E+09	4.56E+09
		Rank	5	6	7	**1**	4	8	11	2	10	3	9	12



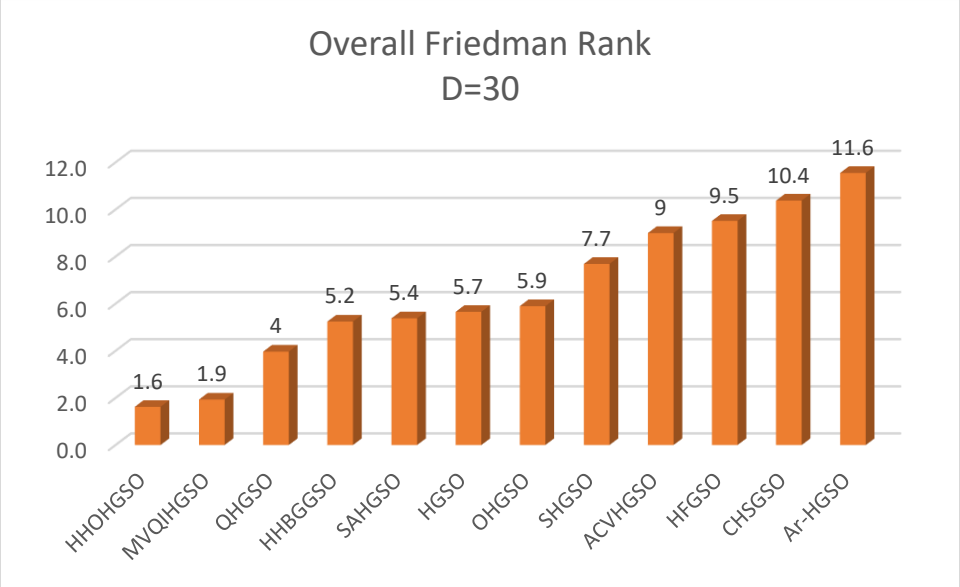
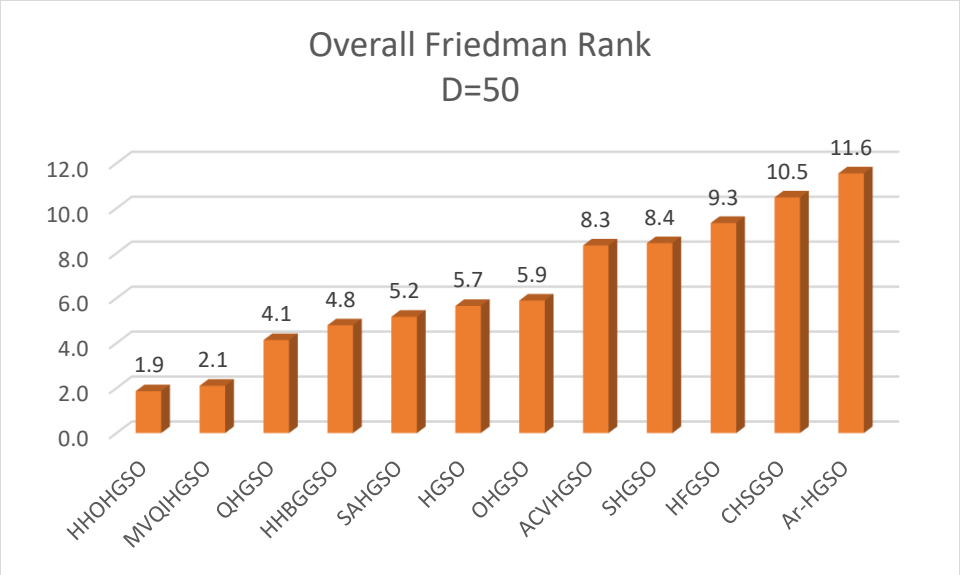


Fig. 14. The overall Friedman rank of the HGSO along with its variants in 10, 30, 50, and 100 dimensions



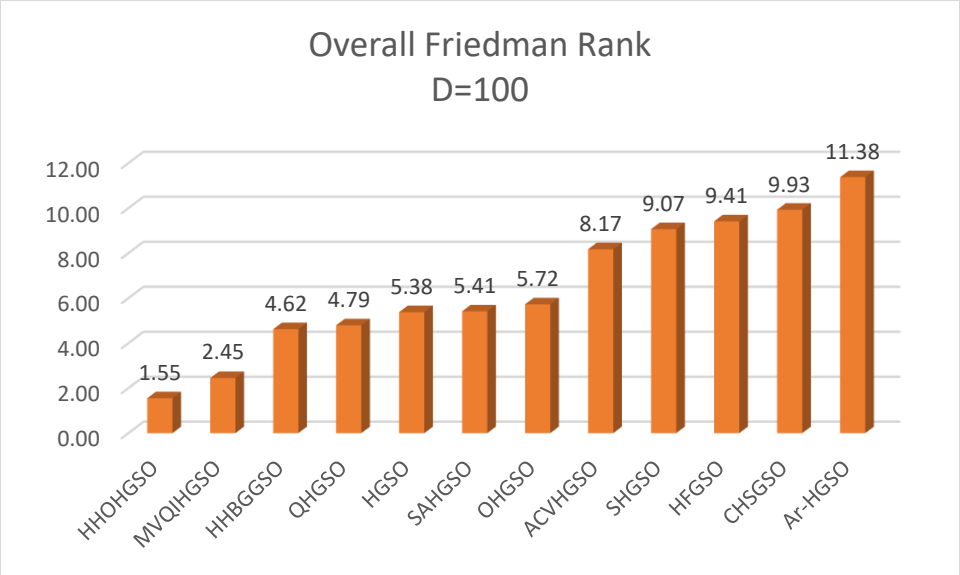


Fig. 14. (Continued)

5.2.1. Analysis of the convergence behavior of the HGSO and its variants

This sub-section presents the comparison of the convergence behaviors for the competitive algorithms considered in this work as portrayed in Fig. 4, 5, 6 and 7 for unimodal, multimodal, hybrid and composition test functions, respectively. Besides, the comparison of the performance results for the competitive algorithms on the CEC 2018 suite with distinct dimensions are tabularized in Table 9, 10, 11 and 12 for unimodal, multimodal, hybrid and composition test functions, respectively. In those tables, different statistical metrics comprising rank, standard

deviation (Std), average (Avg) and minimum (Min) are presented for the sake of performance results comparison.

The experimental outcomes provided in Table 9 clearly approve that the HHO-HGSO [49] outperforms its counterparts and always holds the first ranking for the unimodal test functions in 10, 30, 50 and 100 dimensions. This outperformance is also supported by Fig. 4.

As far as the multimodal test functions are concerned, the HHO-HGSO [49] exhibits also better performance compared with other HGSO variants for most of these functions except for some cases where it is surpassed by the MVQIHGSO [85] as illustrated in both Table 10 and Fig. 5.

Table 11 along with Fig. 6 exemplify the experimental results attained by the HGSO variants on the hybrid test functions. Likewise the multimodal test functions, the HHO-HGSO [49] always offers better results than its counterparts with the exception of few cases where the the MVQIHGSO [85] is ranked first.

The experimental outcomes accomplished by the HGSO variants on the composition functions are illustrated in Table 12 as well as Fig. 7. Similarly, the HHO-HGSO [49] confirms its superiority excluding certain cases where it is outstripped by the MVQIHGSO [85], QHGSO [114], SAHGSO [68], HHBGGSO [89] and ACVHGSO [79].

5.2.2. Analysis of the effectiveness of the HGSO and its variants

Three kinds of effectiveness analysis including overall effectiveness, execution time analysis and performance index (PI) analysis [45, 168] are described in this sub-section and were performed in order to compare the effectiveness of the HGSO variants.

Overall Effectiveness

The general performance of the HGSO variants is illustrated by the overall effectiveness (OE) in Eq. (13) [45, 168] with N being the total number of the benchmark test functions which is the summation of the winning (W), tying (T), and losing (L) benchmark test functions, respectively.

$$OE = \left(\frac{N - L}{N} \right) \times 100 \tag{13}$$

Where $N = \left(W + T + L \right)$ (14)

The results of OE for the HGSO variants are depicted in Table 13 in which the HHO-HGSO [49] surpassed its counterparts with an OE of **71.552%**, followed by MVQIHGSO [85] with 24.138%

of OE . Moreover, the winning, tying and losing numbers for different dimensions are exemplified in Fig. 8.

Execution Time Analysis

The average execution time ($At_{i,j}$) in seconds utilized by the i th algorithm for tackling the j th benchmark test function is expressed as in Eq. (15) [45, 168]:

$$At_{i,j} = \frac{1}{M}\sum_{t=1}^{M} RunTime\left(A\lg orithm_{i,j}^{t}\right) \tag{15}$$

where M is the number of the runs and $RunTime\left(A\lg orithm_{i,j}^{t}\right)$ denotes the execution time needed by the i th algorithm for solving the j th benchmark test function.

The average execution time employed by the i th algorithm to handle all benchmark test functions is given in Eq. (16) [45, 168] by:

$$ExecutionTime_i = \frac{1}{N}\sum_{j=1}^{N} At_{i,j} \tag{16}$$

with N being the number of the benchmark test functions.

Tables 14-18 tabulated the results of the average execution times spent by the HGSO variants to deal with unimodal, multimodal, hybrid, composite and all benchmark test functions, respectively. In these tables, the bolded values show the smallest average execution times accomplished by the algorithm.

For the unimodal test functions, Table 14 shows that the SHGSO [99] exhibits the best average execution time in 10 dimension, HHBGGSO [89] exhibits the best average execution time in 30 dimension and the HHO-HGSO [49] exhibits the best average execution time in 50 and 100 dimensions.

For the multimodal test functions, Table 15 reveals that the QHGSO [114] spends the smallest average execution time in 10 dimension and the HHO-HGSO [49] spends the smallest average execution times in 30, 50 and 100 dimensions.

For the hybrid test functions, Table 16 illustrates that the QHGSO [114] records the best average execution time in 10 dimension and the HHO-HGSO [49] records the best average execution times in 30, 50 and 100 dimensions.

For the composition test functions, Table 17 elucidates that the QHGSO [114] displays the best average execution times in 10, 30, 50 and 100 dimensions.

As far as all benchmark test functions are concerned, Table 18 clarifies that the QHGSO [114] exhibits the smallest average execution times in 10, 30 and 100 dimensions whilst the HHO-HGSO [49] exhibits the smallest execution time in 50 dimension.

Performance Index Analysis

The computational time along with the effectiveness of the algorithm are utilized in order to express the PI analysis as in Eq. (17) [168-170]:

$$PI_i = \frac{1}{N}\sum_{j=1}^{N}\left(\alpha\frac{Mf_j}{Af_{i,j}} + \beta\frac{Mt_j}{At_{i,j}}\right) \tag{17}$$

$$\alpha = \omega,\ \beta = 1-\omega, \text{and}\ \omega = \begin{bmatrix}0 & 0.2 & 0.4 & 0.6 & 0.8 & 1\end{bmatrix}$$

With α being the weights allotted to the error value, β is the computational time, Mf_j designates the smallest average fitness value, Mt_j signifies the smallest average time utilized by the all the algorithms to tackle the j th benchmark test function, $Af_{i,j}$ defines the average fitness value accomplished by the i th algorithm to handle the j th benchmark test function, N represents the number of the benchmark test functions.

The figures resulting from the plotting of the PI analysis for HGSO variants are illustrated in Fig. 9-13 for unimodal, multimodal, hybrid, composition and overall test functions.

For the unimodal test functions, Fig. 9 shows that the HHO-HGSO [49] achieves the best PI values in 10, 30, 50 and 100 dimensions.

For the multimodal test functions, Fig. 10 reveals that the HHO-HGSO [49] accomplishes the best PI values in 10, 30, 50 and 100 dimensions.

For the hybrid test functions, Fig. 11 illustrates that the HHO-HGSO [49] records the best PI values in 10, 30, 50 and 100 dimensions.

For the composition test functions, Fig. 12 elucidates that the MVQIHGSO [85] displays the best PI values in 10 dimension whereas the HHO-HGSO [49] displays the best PI values in 30, 50 and 100 dimensions.

As far as overall test functions are concerned, Fig. 13 clarifies that the HHO-HGSO [49] attains the best PI values in 10, 30, 50 and 100 dimensions.

5.3. Analysis of the statistical results

In this sub-section, two statistical tests including Friedman test and MAE [45, 168], have been utilized in order to analyze and compare the results achieved by the HGSO variants for benchmark test functions in various dimensions.

Friedman test

The ranking of the HGSO variants considering the benchmark test functions in different dimensions has been performed by using the Friedman test which is expressed in Eq. (18) as [45, 168]:

$$\chi_F^2 = \frac{12n}{k(k+1)}\left[\sum_{j=1}^{k} R_j^2 - \frac{k(k+1)^2}{4}\right] \tag{18}$$

with k being the total number of the algorithms involved in the comparison, n indicates the total number of test functions, and R_j signifies the average rank assigned to the j th benchmark test function.

By considering the fitness values, the results of the Friedman test achieved by the HGSO variants are tabulated in Table 9-12. The overall ranking illustrates in Table 12 that the MVQIHGSO [85] is ranked first in 10, 30 and 50 dimensions. On the contrary, the HHO-HGSO [49] accomplished the first rank in 100 dimension. The worst ranking (i.e. 12^{th}) in all dimensions is attributed to the Ar-HGSO [80]. Besides, the overall Friedman test ranking considering all benchmark test functions is depicted in Fig. 14 for different dimensions.

Mean Absolute Error test

The calculation of the average absolute errors existing between the fitness values accomplished by the algorithms and the optimal values on a certain benchmark test function is carried out by using the MAE test as expressed in Eq. (19) [45, 168]:

$$MAE = \frac{1}{N}\sum_{j=1}^{N}\left|Func_j^* - Func_j\right| \tag{19}$$

with $Func_j^*$ being the global optimal solution, $Func_j$ indicates the best solution accomplished by the j th benchmark test function, N is the number of the benchmark test functions. .

The results of the MAE test attained by the HGSO variants for various dimensions are depicted in Table 19. In this table, the bolded values illustrate the best MAE values achieved by the algorithm.

For the unimodal test functions, Table 19 shows that the HHO-HGSO [49] achieves the best MAE values in 10, 30, 50 and 100 dimensions.

For the multimodal test functions, Table 19 reveals that the MVQIHGSO [85] accomplishes the best MAE values in 10 dimension whilst the HHO-HGSO [49] accomplishes the best MAE values in 30, 50 and 100 dimensions.

For the hybrid test functions, Table 19 illustrates that the MVQIHGSO [85] records the best MAE values in 10 dimension while the HHO-HGSO [49] records the best MAE values in 30, 50 and 100 dimensions.

For the composition test functions, Table 19 elucidates that the MVQIHGSO [85] displays the best MAE values in 10 dimension whereas the HHO-HGSO [49] displays the best MAE values in 30, 50 and 100 dimensions.

6. Conclusion and Future Works

The HGSO is a novel metaheuristic algorithm that mimics the gas dissolving behavior in a liquid. This algorithm has attracted many researchers in recent years and it has been applied to tackle numerous optimization problems associated with a vast range of applications from the field of engineering, computer science, medicine, etc. Since its advents in 2019, the HGSO has significantly grown in popularity.

The massive recognition of HGSO is shown in this review where around 118 HGSO-based papers were selected from various well-known journals publishers like Elsevier, Springer, IEEE Xplore, Wiley, Sage, MDPI, Taylor&Francis, etc. The conventional HGSO algorithm has been presented and discussed along with its merits and demerits. Various kinds of HGSO variants and their respective applications have been discussed. Furthermore, the HGSO along with its variants have been tested on the benchmark test functions for the sake of performance comparison through convergence behavior analysis, overall effectiveness analysis, execution time analysis, PI analysis, Friedman test and MAE test. From Table 9-12 and Fig. 2-7, the HHO-HGSO accomplished the

best results in most cases for the convergence behavior. Table 13 shows that the HHO-HGSO outperformed other HGSO variants as it recorded an overall effectiveness of 71.552%. Table 18 illustrates that the QHGSO is the fastest algorithm amidst the HGSO variants in 10, 30 and 100 dimensions, whereas the HHO-HGSO is the quickest algorithm in 50 dimension. Fig. 9-13 demonstrate that the HHO-HGSO achieved better PI values for the most cases. According to Fig. 14, the Friedman test reveals that the HHO-HGSO is ranked first in 30, 50 and 100 dimensions while the MVQIHGSO is ranked first in 10 dimension. Finally, Table 19 confirms that the HHO-HGSO accomplishes better MAE test results in 30, 50 and 100 dimensions while the MVQIHGSO records better MAE test results in 10 dimension.

Although a vast range of variants of the HGSO have been developed and applied effectively to various applications, there are yet some open rooms to be considered in the future:

- Proposing the binary HGSO employing various V-shape and S-shape transfer functions
- Proposing the enhanced versions of the HGSO through different strategies such as comprehensive learning strategy [171], lens-imaging learning strategy [172], variable spiral search strategy [173, 174], elitist learning strategy [175], etc.
- Utilizing the HGSO variants to solve a variety of optimization problems such as knapsack problem, traveling salesman problem, multi-level thresholding image segmentation, optimal power flow, load frequency control for power system, wind power forecasting, etc.

Author Contributions

François Xavier Rugema: Conceptualization, formal analysis, writing-original draft, supervision. Sylvère Mugemanyi: Conceptualization, supervision, data collection. Félicité Pacifique Mutuyimana: Conceptualization, data collection, Writing-review & editing. Emmanuel Mutabazi: Conceptualization, data collection, Writing- review & editing. Providence Habumuremyi: Conceptualization, data collection, Writing – review & editing. Christophe Bananeza: Writing-review & editing. Clarisse Kagaju: Writing-review & editing. Jennifer Batamuliza: Writing-review & editing.

Funding

There is no funding associated with this research.

Data Availability

The authors do not have the permission to share the data.

Declarations

Conflict of interest

On behalf of all authors, the corresponding author states that there is no conflict of interest. The authors declare that they have no conflict of interest.

Ethical Approval

This article does not contain any studies with human participants or animals performed by any of the authors.

Informed Consent

Not applicable.

References

1. Cui Y, Geng Z, Zhu, Q, Han Y (2017) Multi-objective optimization methods and application in energy saving. Energy, 125: 681-704. https://doi.org/10.1016/j.energy.2017.02.174
2. Li J, Wei X, Li B, Zeng Z (2022) A survey on firefly algorithms. Neurocomputing, 500: 662-678. https://doi.org/10.1016/j.neucom.2022.05.100
3. Fesanghary M, Ardehali, MM (2009) A novel meta-heuristic optimization methodology for solving various types of economic dispatch problem. Energy, 34(6):757-766 https://doi.org/10.1016/j.energy.2009.02.007
4. Calvet L, Armas JD, Masip D, Juan AA (2017) Learn heuristics: hybridizing metaheuristics with machine learning for optimization with dynamic inputs. Open Mathematics, 15(1): 261-280. https://doi.org/10.1515/math-2017-0029
5. Heidari AA, Mirjalili S, Faris H, Aljarah I, Mafarja M, Chen, H (2019) Harris hawks optimization: Algorithm and applications. Future generation computer systems, 97: 849-872. https://doi.org/10.1016/j.future.2019.02.028
6. Talbi, EG (2009) Metaheuristics: from design to implementation. vol. 74, John Wiley & Sons. https://doi.org/10.1002/9780470496916
7. Gogna A, Tayal A. (2013). Metaheuristics: review and application. Journal of Experimental & Theoretical Artificial Intelligence, *25*(4): 503-526. https://doi.org/10.1080/0952813X.2013.782347
8. Walters DC, Sheble GB (1993) Genetic algorithm solution of economic dispatch with valve point loading. IEEE transactions on Power Systems, 8(3): 1325-1332. https://doi.org/10.1109/59.260861

9. Eberhart R, Kennedy J (1995) Particle swarm optimization. In Proceedings of the IEEE international conference on neural networks, 4: 1942-1948
10. Mahor A, Prasad V, Rangnekar S (2009) Economic dispatch using particle swarm optimization: A review. Renewable and sustainable energy reviews, 13(8): 2134-2141. https://doi.org/10.1016/j.rser.2009.03.007
11. Nguyen TT, Vo DN, Dinh BH (2016). Cuckoo search algorithm for combined heat and power economic dispatch. International Journal of Electrical Power & Energy Systems, 81: 204-214. https://doi.org/10.1016/j.ijepes.2016.02.026
12. Gendreau M, Potvin JY (2005) Tabu search. Search methodologies: introductory tutorials in optimization and decision support techniques, 165-186. https://doi.org/10.1007/0-387-28356-0_6
13. Hansen P, Mladenović N, Moreno Perez JA (2010) Variable neighbourhood search: methods and applications. Annals of Operations Research, 175: 367-407. https://doi.org/10.1007/s10479-009-0657-6
14. Kirkpatrick, S., Gelatt Jr, C. D., & Vecchi, M. P. (1983). Optimization by simulated annealing. Science, 220(4598): 671-680. https://doi.org/10.1126/science.220.4598.671.
15. Doğan B, Ölmez T (2015) A new metaheuristic for numerical function optimization: vortex search algorithm. Information sciences, 293: 125-145. https://doi.org/10.1016/j.ins.2014.08.053
16. Nematollahi AF, Rahiminejad A, Vahidi B (2017) A novel physical based meta-heuristic optimization method known as lightning attachment procedure optimization. Applied Soft Computing, 59: 596-621. https://doi.org/10.1016/j.asoc.2017.06.033
17. Mousavirad SJ, Ebrahimpour-Komleh H (2017) Human mental search: a new population-based metaheuristic optimization algorithm. Applied Intelligence, 47: 850-887. https://doi.org/10.1007/s10489-017-0903-6
18. Vikhar PA (2016) Evolutionary algorithms: A critical review and its future prospects. In 2016 International conference on global trends in signal processing, information computing and communication (ICGTSPICC) (pp. 261-265). IEEE. https://doi.org/10.1109/ICGTSPICC.2016.7955308
19. Whitley D (2001) An overview of evolutionary algorithms: practical issues and common pitfalls. Information and software technology, 43(14): 817-831. https://doi.org/10.1016/S0950-5849(01)00188-4
20. Ma H, Simon D, Siarry P, Yang Z, Fei M (2017) Biogeography-based optimization: a 10-year review. IEEE Transactions on Emerging Topics in Computational Intelligence, 1(5): 391-407. https://doi.org/10.1109/TETCI.2017.2739124
21. Hansen N, Arnold DV, Auger A (2015) Evolution strategies. Springer handbook of computational intelligence, 871-898. https://doi.org/10.1007/978-3-662-43505-2_44

22. Pant M, Zaheer H, Garcia-Hernandez L, Abraham A (2020) Differential evolution: A review of more than two decades of research. Engineering Applications of Artificial Intelligence, 90, 103479. https://doi.org/10.1016/j.engappai.2020.103479Yao X, Liu Y, Lin G (1999) Evolutionary programming made faster. IEEE Transactions on Evolutionary computation, 3(2): 82-102. https://doi.org/10.1109/4235.771163
23. Yao X, Liu Y, Lin G (1999) Evolutionary programming made faster. IEEE Transactions on Evolutionary computation, 3(2): 82-102. https://doi.org/10.1109/4235.771163
24. Biswas A, Mishra KK, Tiwari S, Misra AK (2013) Physics-inspired optimization algorithms: a survey. Journal of Optimization. https://doi.org/10.1155/2013/438152
25. Can Ü, Alataş B (2015) Physics based metaheuristic algorithms for global optimization. American Journal of Information Science and Computer Engineering, 1(3): 94-106
26. Birbil, Şİ, Fang, SC (2003) An electromagnetism-like mechanism for global optimization. Journal of global optimization, 25: 263-282. https://doi.org/10.1023/A:1022452626305
27. Rashedi, E, Rashedi, E, & Nezamabadi-Pour, H (2018) A comprehensive survey on gravitational search algorithm. Swarm and evolutionary computation, 41: 141-158. https://doi.org/10.1016/j.swevo.2018.02.018
28. Kaveh, A (2017) Charged system search algorithm. In: Advances in Metaheuristic Algorithms for Optimal Design of Structures. Springer, Cham. https://doi.org/10.1007/978-3-319-46173-1_3
29. Formato, RA (2009) Central force optimization: A new deterministic gradient-like optimization metaheuristic. Opsearch, 46(1): 25-51. https://doi.org/10.1007/s12597-009-0003-4
30. Mousavirad, SJ, Ebrahimpour-Komleh, H, Schaefer, G (2020) Automatic clustering using a local search-based human mental search algorithm for image segmentation. Applied Soft Computing, 96: 106604. https://doi.org/10.1016/j.asoc.2020.106604
31. Hosseini, S, Al Khaled, A (2014) A survey on the imperialist competitive algorithm metaheuristic: implementation in engineering domain and directions for future research. Applied Soft Computing, 24: 1078-1094. https://doi.org/10.1016/j.asoc.2014.08.024
32. Shao, W, Pi, D, Shao, Z (2017) An extended teaching-learning based optimization algorithm for solving no-wait flow shop scheduling problem. Applied Soft Computing, 61: 193-210. https://doi.org/10.1016/j.asoc.2017.08.020
33. Dehghani, M, Trojovská, E, Zuščák, T (2022) A new human-inspired metaheuristic algorithm for solving optimization problems based on mimicking sewing training. Scientific Reports, 12(1): 17387. https://doi.org/10.1038/s41598-022-22458-9
34. Ruiz-Vanoye, JA, Díaz-Parra, O, Cocón, F, Soto, A, Arias, MDLÁB, Verduzco-Reyes, G, Alberto-Lira, R (2012) Meta-heuristics algorithms based on the grouping of animals by social

behavior for the traveling salesman problem. International Journal of Combinatorial Optimization Problems and Informatics, 3(3): 104-123
35. Shehab, M, Abu-Hashem, MA, Shambour, MKY, Alsalibi, AI, Alomari, OA, Gupta, JND, Alsoud AR, Abuhaija B, Abualigah, L (2023) A comprehensive review of bat inspired algorithm: Variants, applications, and hybridization. Archives of Computational Methods in Engineering, 30(2): 765-797. https://doi.org/10.1007/s11831-022-09817-5
36. Mirjalili, S, Mirjalili, SM, Lewis, A (2014) Grey wolf optimizer. Advances in engineering software, 69: 46-61. https://doi.org/10.1016/j.advengsoft.2013.12.007
37. Karaboga, D, Gorkemli, B, Ozturk, C, Karaboga, N (2014) A comprehensive survey: artificial bee colony (ABC) algorithm and applications. Artificial intelligence review, 42: 21-57. https://doi.org/10.1007/s10462-012-9328-0
38. Meraihi, Y, Gabis, AB, Ramdane-Cherif, A, Acheli, D (2021) A comprehensive survey of crow search algorithm and its applications. Artificial Intelligence Review, 54(4): 2669-2716. https://doi.org/10.1007/s10462-020-09911-9
39. Dorigo, M, Stützle, T (2019) Ant colony optimization: overview and recent advances, 272: 311-351. Springer International Publishing. https://doi.org/10.1007/978-3-319-91086-4_10
40. Xu, J, & Zhang, J (2014) Exploration-exploitation tradeoffs in metaheuristics: Survey and analysis. In Proceedings of the 33rd Chinese control conference. IEEE, pp. 8633-8638. https://doi.org/10.1109/ChiCC.2014.6896450
41. Yang, XS, Deb, S, Fong, S (2014) Metaheuristic algorithms: optimal balance of intensification and diversification. Applied Mathematics & Information Sciences, 8(3): 977-983. http://dx.doi.org/10.12785/amis/080306
42. Boussaïd, I, Lepagnot, J, Siarry, P (2013) A survey on optimization metaheuristics. Information sciences, 237: 82-117. https://doi.org/10.1016/j.ins.2013.02.041
43. Hashim, FA, Houssein, EH, Mabrouk, MS, Al-Atabany, W, Mirjalili, S (2019) Henry gas solubility optimization: A novel physics-based algorithm. Future Generation Computer Systems, 101: 646-667. https://doi.org/10.1016/j.future.2019.07.015
44. Mugemanyi, S, Qu, Z, Rugema, FX, Dong, Y, Wang, L, Bananeza, C, Nshimiyimana, A, Mutabazi, E (2023) Marine predators algorithm: a comprehensive review. Machine Learning with Applications 12: 100471. https://doi.org/10.1016/j.mlwa.2023.100471
45. Mugemanyi, S, Qu, Z, Rugema, FX, Dong, Y, Wang L, Mutuyimana, FP, Mutabazi, E, Habumuremyi, P, Mutabazi, RC, Muhirwa, A, Bananeza, C, Nshimiyimana, A, Clarisse Kagaju, C, Nsengumuremyi, J (2025) Atom search optimization: a systematic review of current variants and applications. Knowledge and Information Systems, 1-102. Springer, https://doi.org/10.1007/s10115-025-02389-3
46. Kitchenham, B, Brereton, OP, Budgen, D, Turner, M, Bailey, J, Linkman, S (2009) Systematic literature reviews in software engineering-a systematic literature review. Information Software Technology, 51(1): 7-15

47. Kitchenham, BA, Charters, S (2007) Guidelines for performing systematic literature reviews in software engineering. Technical report EBSE-2007-01, School of Computer Science and Mathematics, Keele University
48. Li, Y, Zhang, W, Wang, L, Zhao, F, Han, W, Chen, G (2017) Henry's law and accumulation of weak source for crust-derived helium: a case study of Weihe Basin, China. Journal of Natural Gas Geoscience, 2(5-6): 333-339. https://doi.org/10.1016/j.jnggs.2018.02.001
49. Xie, W, Xing, C, Wang, J, Guo, S, Guo, MW, Zhu, LF (2020) Hybrid Henry gas solubility optimization algorithm based on the harris hawk optimization. IEEE Access, 8: 144665-144692. https://doi.org/10.1109/ACCESS.2020.3014309
50. Liu, M, Liu, T, Zhu, M, Chen, L (2022) A PI control method with HGSO parameter regulator for trajectory planning of 9-DOF redundant manipulator. Sensors, 22 (18): 6860. https://doi.org/10.3390/s22186860
51. Yildiz, BS, Yildiz, AR, Pholdee, N, Bureerat, S, Sait, SM, Patel, V (2020) The Henry gas solubility optimization algorithm for optimum structural design of automobile brake components. Materials Testing, 62(3): 261-264. https://doi.org/10.3139/120.111479
52. Yildiz, BS, Pholdee, N, Panagant, N, Bureerat, S, Yildiz, AR, Sait, SM (2022) A novel chaotic Henry gas solubility optimization algorithm for solving real-world engineering problems. Engineering with Computers, 38 (Suppl 2): S871–S883. https://doi.org/10.1007/s00366-020-01268-5
53. Yadav, NK, Saraswat, M (2024). A new feature selection approach with binary exponential henry gas solubility optimization and hybrid data transformation methods. MethodsX, 102770. https://doi.org/10.1016/j.mex.2024.102770
54. Hashim, FA, Houssein, EH, Hussain, K, Mabrouk, MS, Al-Atabany, W (2020) A modified Henry gas solubility optimization for solving motif discovery problem. Neural Computing and Applications, 32: 10759-10771. https://doi.org/10.1007/s00521-019-04611-0
55. Utama, DM, Farida, BNI, Fitriani, U, Ibrahim, MF, Widodo, DS (2021) Hybrid Henry gas solubility optimization: An effective algorithm for fuel consumption vehicle routing problem. Jurnal Ilmiah Teknik Industri, 20(2): 141-152. https://doi.org/10.23917/jiti.v20i2.15640
56. Yadav, NK, Saraswat, M (2022) A novel fuzzy clustering based method for image segmentation in RGB-D images. Engineering Applications of Artificial Intelligence, 111: 104709. https://doi.org/10.1016/j.engappai.2022.104709
57. Jaffino, G, Sundaram, M, Jose, JP (2022) Weighted 1D-local binary pattern features and Taylor-Henry gas solubility optimization based deep maxout network for discovering epileptic seizure using EEG. Digital Signal Processing, 122: 103349. https://doi.org/10.1016/j.dsp.2021.103349.

58. Li, S, Wang, JS, Xie, W, Li, XL (2022) An improved Henry gas solubility optimization algorithm based on Lévy flight and Brown motion. Applied Intelligence, 52(11): 12584-12608. https://doi.org/10.1007/s10489-021-02811-7
59. Nandhini, S, Ashokkumar, K (2022) An automatic plant leaf disease identification using DenseNet-121 architecture with a mutation-based Henry gas solubility optimization algorithm. Neural Computing and Applications, 1-22. https://doi.org/10.1007/s00521-021-06714-z
60. Ramya, P, Ramya, V, Rao, MB (2023) Optimized deep learning-based E-waste management in IoT application via energy-aware routing. Cybernetics and Systems, 1-30. https://doi.org/10.1080/01969722.2023.2175119
61. Ravikumar, S, Kavitha, D (2021) CNN-OHGS: CNN-oppositional-based Henry gas solubility optimization model for autonomous vehicle control system. Journal of Field Robotics, 38(7): 967-979. https://doi.org/10.1002/rob.22020
62. Ekinci, S, Hekimoğlu, B, Izci, D (2021) Opposition based Henry gas solubility optimization as a novel algorithm for PID control of DC motor. Engineering Science and Technology, an International Journal, 24(2): 331-342. https://doi.org/10.1016/j.jestch.2020.08.011
63. Jeyalakshmi, S, Sekar, S, Ravikumar, S, & Kavitha, D (2022) Random forest-based oppositional Henry gas solubility optimization model for service attack improvement in WSN. Journal of the Institution of Engineers (India): Series B, 103(3): 939-950. https://doi.org/ 10.1007/s40031-021-00702-6
64. Ahamed, F, Sukhi, Y (2023) Modeling of hybrid Henry gas solubility optimization algorithm with deep learning based LED driver system. https://doi.org/10.21203/rs.3.rs-2449840/v1
65. Ninu, SB (2023) An intrusion detection system using exponential Henry gas solubility optimization based deep neuro fuzzy network in MANET. Engineering Applications of Artificial Intelligence, 123: 105969. https://doi.org/10.1016/j.engappai.2023.105969
66. Zhang, M, Wang, JS, Liu, Y, Wang, M, Li, XD, Guo, FJ (2023) Feature selection method based on stochastic fractal search henry gas solubility optimization algorithm. Journal of Intelligent & Fuzzy Systems, 44(3): 5377-5406. https://doi.org/10.3233/JIFS-221036
67. ELgazzar, S., Mohamed, H., & Haroun, A. (2024, May). A Hybrid Feature Selection Approach: β-Hill Climbing and Henry Gas Optimization. In 2024 International Conference on Machine Intelligence and Smart Innovation (ICMISI) (pp. 262-265). IEEE. https://doi.org/10.1109/ICMISI61517.2024.10580620
68. Xu, H, Razmjooy, N (2024) Self-adaptive henry gas solubility optimizer for identification of solid oxide fuel cell. Evolving Systems 15, 133-151. https://doi.org/10.1007/s12530-023-09517-w
69. Saranya, S, Saravanan, B (2020) Effect of emission in SMES based unit commitment using modified Henry gas solubility optimization. Journal of Energy Storage, 29: 101380. https://doi.org/10.1016/j.est.2020.101380

70. Abdel-Mawgoud, H, Kamel, S, Khasanov, M, Khurshaid, T (2021) A strategy for PV and BESS allocation considering uncertainty based on a modified Henry gas solubility optimizer. Electric Power Systems Research, 191: 106886. https://doi.org/10.1016/j.epsr.2020.106886
71. Daniya, T, Vigneshwari, S (2022) Exponential rider-Henry gas solubility optimization-based deep learning for rice plant disease detection. International Journal of Information Technology, 1-11. https://doi.org/10.1007/s41870-022-01022-8
72. Zamli, KZ, Kader, MA, Azad, S, Ahmed, BS (2021) Hybrid Henry gas solubility optimization algorithm with dynamic cluster-to-algorithm mapping. Neural Computing and Applications, 33: 8389-8416. https://doi.org/10.1007/s00521-020-05594-z
73. Chen, Y, Gou, L, Li, H (2022) A differential evolution based Henry gas solubility optimizer for dynamic performance optimization problems of PRO system. Applied Soft Computing, 125: 109097. https://doi.org/10.1016/j.asoc.2022.109097
74. Abd Elaziz, M, Attiya, I (2021) An improved Henry gas solubility optimization algorithm for task scheduling in cloud computing. Artificial Intelligence Review, 54: 3599-3637. https://doi.org/10.1007/s10462-020-09933-3
75. Abd Elaziz, M, Yousri, D (2021) Automatic selection of heavy-tailed distributions-based synergy Henry gas solubility and Harris hawk optimizer for feature selection: case study drug design and discovery. Artificial Intelligence Review, 54(6): 4685-4730. https://doi.org/10.1007/s10462-021-10009-z
76. Bi, J, Zhang, Y (2022) An improved Henry gas solubility optimization for optimization tasks. Applied Intelligence, 52(6): 5966-6006. https://doi.org/10.1007/s10489-021-02670-2
77. Patra, R, Khuntia, B, Panda, DC (2022a) Fractional rider gradient descent applied u-net based segmentation with optimal deep maxout network for lung cancer classification using histopathological images. Research on Biomedical Engineering, 38(2): 599-615. https://doi.org/10.1007/s42600-022-00211-5
78. Kalpana, G, Durga, AK, Karuna, G (2022) CNN features and optimized General Adversarial Network for COVID-19 detection from chest X-ray images. Critical Reviews in Biomedical Engineering, 50(3): 1-17. https://doi.org/10.1615/CritRevBiomedEng.2022042286
79. Ramkumar, MP, Mano Paul, PD, Maram, B, Ananth, JP (2022) Deep maxout network for lung cancer detection using optimization algorithm in smart Internet of Things. Concurrency and Computation: Practice and Experience, 34(25): e7264. https://doi.org/10.1002/cpe.7264
80. Elwin, JGR, Mandala, J, Maram, B, Kumar, RR (2022) Ar-HGSO: Autoregressive-Henry Gas Sailfish Optimization enabled deep learning model for diabetic retinopathy detection and severity level classification. Biomedical Signal Processing and Control, 77: 103712. https://doi.org/10.1016/j.bspc.2022.103712

81. Boopathi, M (2022) Henry MaxNet: tversky index based feature selection and competitive swarm henry gas solubility optimization integrated deep maxout network for intrusion detection in IoT. International Journal of Intelligent Robotics and Applications, 6(2): 365-383. https://doi.org/10.1007/s41315-022-00234-2
82. Patra, R, Khuntia, B, Panda, DC (2022b) Hybrid optimization-based structural design of deep Q network with feature selection algorithm for medical data classification. International Journal of Swarm Intelligence Research (IJSIR), 13(1): 1-20. https://doi.org/10.4018/IJSIR.304722
83. Kumar, BM, Ainapure, BS, Singh, SP, Vyas, S (2022) Feature extraction based deep indexing by deep fuzzy clustering for image retrieval using Jaro Winkler distance. The Computer Journal. https://doi.org/10.1093/comjnl/bxac070
84. Mosa, DT, Mahmoud, A, Zaki, J, Sorour, SE, El-Sappagh, S, Abuhmed, T (2023) Henry gas solubility optimization double machine learning classifier for neurosurgical patients. Plos one, 18(5): e0285455. https://doi.org/10.1371/journal.pone.0285455
85. Qiu, H, Hu, T, Zhang, S, Xiao, Y (2023) Deriving operating rules of hydropower reservoirs using multi-strategy ensemble Henry gas solubility optimization-driven support vector machine. Water, 15(3): 437. https://doi.org/10.3390/w15030437
86. Zhou, Z, Yang, X, Ji, J, Wang, Y, Zhu, Z (2023) Classifying fabric defects with evolving inception v3 by improved L2, 1-norm regularized extreme learning machine. Textile Research Journal, 93(3-4): 936-956. https://doi.org/10.1177/00405175221114633
87. Reddy, S. K., & Kathirvelu, K. (2024). Prostate cancer detection using Henry firefly gas solubility optimization-based deep residual network. Multimedia Tools and Applications, 83(10), 29331-29352. https://doi.org/10.1007/s11042-023-16655-5
88. Singh, G, Nagpal, A (2023) HFCVO-DMN: Henry fuzzy competitive verse optimizer-integrated deep maxout network for incremental text classification. Computation, 11(1): 13. https://doi.org/10.3390/computation11010013
89. Parashivamurthy, SPT, Rajashekararadhya, SV (2023) Recognition of Kannada character scripts using hybrid feature extraction and ensemble learning approaches. Cybernetics and Systems, 1-36. https://doi.org/10.1080/01969722.2023.2175145
90. Rethikumari Amma, KN, Ranjana, P (2023) Pivotal region and optimized deep neuro fuzzy network for autism spectrum disorder detection. Biomedical Signal Processing and Control, 83: 104634. https://doi.org/10.1016/j.bspc.2023.104634
91. Ramya, P, Ramya, V (2023) E-waste management using hybrid optimization-enabled deep learning in IoT-cloud platform. Advances in Engineering Software, 176: 103353. https://doi.org/10.1016/j.advengsoft.2022.103353
92. Omana, SP, Dar, JA, Kumar, TR, Sampath, AK, Sharma, S (2023) Henry gas bird swarm optimization algorithm-based deep learning for brain tumor classification using magnetic

resonance imaging. Concurrency and Computation: Practice and Experience, 35(4): e7541. https://doi.org/10.1002/cpe.7541
93. Kulkarni, YR, Jagdale, B, Sugave, SR (2023) Optimized key generation-based privacy preserving data mining model for secure data publishing. Advances in Engineering Software, 175: 103332. https://doi.org/10.1016/j.advengsoft.2022.103332
94. Arumugasamy, M, Arokiasamy, A (2023) Tunicate Henry gas solubility optimization-based deep residual network for fruit ripeness classification. Concurrency and Computation: Practice and Experience, e7490. https://doi.org/10.1002/cpe.7490
95. Tamizharasi, S, Arunadevi, B, Deepa, S N (2023) Bio-inspired deep residual neural network learning model for QoS routing enhancement in mobile ad-hoc networks. Wireless Networks, 1-25. https://doi.org/10.1007/s11276-023-03424-3
96. Deepa, SN, Rasi, D (2023) FHGSO: Flower Henry gas solubility optimization integrated deep convolutional neural network for image classification. Applied Intelligence, 53(6): 7278-7297. https://doi.org/10.1007/s10489-022-03834-4
97. Mahanta, A, Nur, MOB, Islam, R, Azad, S, Wadith, S, Mahmud, M, Kaiser, MS (2023, December) EHHGSO: Enhancing hybrid Hugo gas solubility optimization algorithm using backtracking technique. In 2023 5th International Conference on Sustainable Technologies for Industry 5.0 (STI) (pp. 1-6). IEEE. https://doi.org/10.1109/STI59863.2023.10464490
98. Daniya, T, Vigneshwari, S (2023) Rice plant leaf disease detection and classification using optimization enabled deep learning. Journal of Environmental Informatics, 42(1). https://doi.org/10.3808/jei.202300492
99. Nirmala Priya, G, Suresh Kumar, K, Suganthi, N, Muppidi, S (2024) Squirrel Henry gas solubility optimization driven deep maxout network with multi-texture feature descriptors for digital image forgery detection. Concurrency and Computation: Practice and Experience, 36(8), e7965. https://doi.org/10.1002/cpe.7965
100. Ramachandran, M, Sundaram, A, Ridha, HM, Mirjalili, S (2024) Estimation of photovoltaic models using an enhanced Henry gas solubility optimization algorithm with first-order adaptive damping Berndt-Hall-Hall-Hausman method. Energy Conversion and Management, 299, 117831. https://doi.org/10.1016/j.enconman.2023.117831
101. Legoui, KZ, Maza, S, Attia, A, Houssein, EH (2024) Hybrid Henry gas solubility optimization and the equilibrium optimizer for feature selection: real cases with Twitter spam detection. Knowledge and Information Systems, 66(5), 3055-3084. https://doi.org/10.1007/s10115-023-02054-7
102. Kavitha Nair, R, & Ranjana, P (2024) Hybrid optimization enabled functional connectivity-based pivotal region extraction and transfer learning for autism spectrum disorder detection. Biomedical Engineering: Applications, Basis and Communications, 36(04), 2450018. https://doi.org/10.4015/S1016237224500182

103. Karasu, S, Altan, A (2022) Crude oil time series prediction model based on LSTM network with chaotic Henry gas solubility optimization. Energy, 242: 122964. https://doi.org/10.1016/j.energy.2021.122964
104. Kanagasabai, L (2022) Opposition-based chaotic Henry's law-soluble gas, hybridization of chelonioidea with anthoathecata and vaporization of liquid optimization algorithms for power loss diminution. Soft Computing, 26(4): 1563-1585. https://doi.org/10.1007/s00500-021-06710-4
105. Tripathi, KN, Sharma, SC (2023) An optimal trust and secure model using deep metric learning for fog-based VANET. Transactions on Emerging Telecommunications Technologies, e4805. https://doi.org/10.1002/ett.4805
106. Arivalahan, R, Tamilarasan, P, Kamalakannan, M (2023) Liquid level control in two tanks spherical interacting system with fractional order proportional integral derivative controller using hybrid technique: a hybrid technique. Advances in Engineering Software, 175: 103316. https://doi.org/10.1016/j.advengsoft.2022.103316
107. Ghadimi, N, Sedaghat, M, Azar, KK, Arandian, B, Fathi, G, Ghadamyari, M (2023) An innovative technique for optimization and sensitivity analysis of a PV/DG/BESS based on converged Henry gas solubility optimizer: a case study. IET Generation, Transmission & Distribution. https://doi.org/10.1049/gtd2.12773
108. Loganathan, S, Chellaian, G, Nazaren, AR, Fernandez, MHF (2023) Autism spectrum disorder detection and classification using chaotic optimization based Bi-GRU network: An weighted average ensemble model. Expert Systems with Applications, 120613. https://doi.org/10.1016/j.eswa.2023.120613
109. Hussien, RM, Abohany, AA, Moustafa, N, Sallam, KM (2023) An improved Henry gas optimization algorithm for joint mining decision and resource allocation in a MEC-enabled blockchain networks. Neural Computing and Applications, 35(25), 18665-18680. https://doi.org/10.1007/s00521-023-08695-7
110. Agarwal, R, Shekhawat, NS, Luhach, AK (2021) Automated classification of soil images using chaotic Henry's gas solubility optimization: Smart agricultural system. Microprocessors and Microsystems, 103854. https://doi.org/10.1016/j.micpro.2021.103854
111. Kishor YN, Saraswat, M (2021) Chaotic Henry gas solubility optimization algorithm. In Intelligent Learning for Computer Vision: Proceedings of Congress on Intelligent Systems 2020 (247-257). Springer Singapore. https://doi.org/10.1007/978-981-33-4582-9_20
112. Karthika, J, Rajkumar, M, Vishnupriyan, J (2023) A hybrid control technique for small signal stability analysis for microgrids under uncertainty. Journal of Intelligent & Fuzzy Systems, 44 (1) 625-645. https://doi: 10.3233/JIFS-221425
113. Sarıkaya, MS, Hamida El Naser, Y, Kaçar, S, Yazıcı, İ, Derdiyok, A (2024) Chaotic-based improved Henry gas solubility optimization algorithm: Application to electric motor control. Symmetry, 16(11), 1435. https://doi.org/10.3390/ sym16111435

114. Mohammadi, D, Abd Elaziz, M, Moghdani, R, Demir, E, Mirjalili, S (2022) Quantum Henry gas solubility optimization algorithm for global optimization. Engineering with Computers 38 (Suppl 3): 2329-2348. Springer. https://doi.org/10.1007/s00366-021-01347-1
115. Sukpancharoen, S, & Prasartkaew, B (2021) Combined heat and power plant using a multi-objective Henry gas solubility optimization algorithm: a thermodynamic investigation of energy, exergy, and economic (3E) analysis. Heliyon, 7(9): e08003. https://doi.org/10.1016/j.heliyon.2021.e08003
116. Haider, HT, Muhsen, DH, Al-Nidawi, YM, Khatib, T, See, OH (2022) A novel approach for multi-objective cost-peak optimization for demand response of a residential area in smart grids. Energy, 254: 124360. https://doi.org/10.1016/j.energy.2022.124360
117. Kahloul, S, Zouache, D, Brahmi, B, Got, A (2022) A multi-external archive-guided Henry Gas Solubility Optimization algorithm for solving multi-objective optimization problems. Engineering Applications of Artificial Intelligence, 109: 104588. https://doi.org/10.1016/j.engappai.2021.104588
118. Neggaz, N, Houssein, EH, Hussain, K (2020) An efficient Henry gas solubility optimization for feature selection. Expert Systems with Applications, 152: 113364. https://doi.org/10.1016/j.eswa.2020.113364
119. Legoui, KZ, Maza, S, Attia, A (2022) Equilibrium optimizer and Henry gas solubility optimization algorithms for feature selection: Comparison study. In 2022 5th International Symposium on Informatics and its Applications (ISIA). IEEE, (pp. 1-6). https://doi.org/10.1109/ISIA55826.2022.9993543
120. Alrayes, FS, Alshuqayran, N, Nour, MK, Al Duhayyim, M, Mohamed, A, Mohammed, A AA, Mohammed, AAA, Mohammed, GP, Yaseen, I (2023) Optimal fuzzy logic enabled intrusion detection for secure IoT-cloud environment. CMC-Computers Materials & Continua, 74(3): 6737-6753. https://doi.org/10.32604/cmc.2023.032591
121. Wang, Y (2022) The performance of artificial intelligence translation App in Japanese language education guided by deep learning. Computational Intelligence and Neuroscience, 2022. https://doi.org/10.1155/2022/7962722
122. Roy, D, Dutta, M (2023). An intelligent group recommender system using Henry gas solubility optimization algorithm-based adaptive deep belief network. In 2023 4th International Conference on Computing and Communication Systems (I3CS). IEEE, (pp. 1-6). https://doi.org/10.1109/I3CS58314.2023.10127394
123. Lakshmanan, S, Maheswari Gnaniyan Ponnusamy, U, Andi, S (2023) An efficient DDoS attack detection using chaos Henry gas solubility optimization weight initialization based rectified linear unit. Cybernetics and Systems, 1-28. https://doi.org/10.1080/01969722.2023.2175140

124. Hussain, K, Talpur, N, Aftab, MU, Zakria (2020) A novel metaheuristic approach to optimization of neuro-fuzzy system for students' performance prediction. Journal of Soft Computing and Data Mining, 1(1): 1-9. https://doi.org/10.30880/jscdm.2020.01.01.001
125. Aleisa, HN, Alrowais, F, Negm, N, Almalki, N, Khalid, M, Marzouk, R, AlnifIai, MM, Mohammed, GP, Alneil, AA (2023) Henry gas solubility optimization with deep learning based facial emotion recognition for human computer interface, IEEE Access, 11: 62233-62241. https://doi: 10.1109/ACCESS.2023.3284457
126. Cao, W, Liu, X, Ni, J (2020) Parameter optimization of support vector regression using henry gas solubility optimization algorithm. IEEE Access, 8: 88633-88642. https://doi.org/10.1109/ACCESS.2020.2993267
127. Kumar, DP, Kumar, PG (2025) Implementation of optimal routing in heterogeneous wireless sensor network with multi-channel media access control protocol using enhanced Henry gas solubility optimizer. International Journal of Communication Systems, 38(1), e5980. https://doi.org/10.1002/dac.5980
128. Kanagasabai, L (2021) Reduction of power loss by Henry's law-based soluble gas, mobula alfredi and balanced condition optimization algorithms. COMPEL-The international journal for computation and mathematics in electrical and electronic engineering, 40(3): 689-721. https://doi.org/10.1108/COMPEL-02-2021-0031
129. Selim, A, Kamel, S, Abdelkader, M, Jurado, F (2022) Optimal placement of PMUs using Henry gas solubility optimization for state estimation of power system. In 2022 IEEE International Conference on Automation/XXV Congress of the Chilean Association of Automatic Control (ICA-ACCA). IEEE, (pp. 1-6). https://doi.org/10.1109/ICA-ACCA56767.2022.10006122
130. Hemeida, AM, Rashwan, A, Hasanien, HM, Senjyu, T (2023) Voltage and angle stability assessment of power systems based optimizated FACTS devices. In 2023 IEEE Conference on Power Electronics and Renewable Energy (CPERE). IEEE, (pp. 1-6). https://doi.org/10.1109/CPERE56564.2023.10119616
131. Ekinci, S, İzci, D, & Hekimoğlu, B (2021) Implementing the Henry gas solubility optimization algorithm for optimal power system stabilizer design. Electrica, 21(2), 250-258. https://doi.org/10.5152/electrica.2021.20088
132. Ebrahim, MA, Fattah, RMA, Saied, EM, Maksoud, SMA, El Khashab, H (2021) An islanded microgrid droop control using Henry gas solubility optimization, International Journal of Innovative Technology and Exploring Engineering (IJITEE) 10(3): 43-48. https://doi.org/10.35940/ijitee.C8365.0110321
133. Idir, A, Khettab, K, Bensafia, Y (2022) Design of an optimally tuned fractionalized PID controller for dc motor speed control via a Henry gas solubility optimization algorithm. International Journal of Intelligent Engineering and Systems, 15(3): 59-69. https://doi.org/10.22266/ijies2022.0630.06

134. Ekinci, S, Izci, D, Hekimoğlu, B (2020) Henry gas solubility optimization algorithm based FOPID controller design for automatic voltage regulator. In 2020 International Conference on Electrical, Communication, and Computer Engineering (ICECCE) Istanbul, Turkey, 2020. IEEE, (pp. 1-6).. https://doi.org/10.1109/ICECCE49384.2020.9179406
135. Mirza, AF, Mansoor, M, Ling, Q (2020) A novel MPPT technique based on Henry gas solubility optimization. Energy Conversion and Management, 225: 113409. https://doi.org/10.1016/j.enconman.2020.113409
136. Singh, P, Sandhu, A (2022) Optimal parameter extraction of proton exchange membrane fuel cell using Henry gas solubility optimization. International Journal of Energy Research, 46(13): 18212-18224. https://doi.org/10.1002/er.8437
137. Islam, MS, Awal, MA, Laboni, JN, Pinki, FT, Karmokar, S, Mumenin, KM, Al-Ahmadi, S, Rahman MA, Hossain MS, Mirjalili, S (2022) HGSORF: Henry gas solubility optimization-based random forest for C-section prediction and XAI-based cause analysis. Computers in Biology and Medicine, 147: 105671. https://doi.org/10.1016/j.compbiomed.2022.105671
138. Mishra, SK, Pal, R (2022) An optimal image segmentation method based on HGSO for CT Images. In 2022 8th International Conference on Signal Processing and Communication (ICSC). IEEE, (pp. 289-293). https://doi.org/10.1109/ICSC56524.2022.10009328
139. Sadiq, MT, Akbari, H, Siuly, S, Li, Y, Wen, P (2022) Alcoholic EEG signals recognition based on phase space dynamic and geometrical features. Chaos, Solitons & Fractals, 158: 112036. https://doi.org/10.1016/j.chaos.2022.112036
140. Obayya, M, Alhebri, A, Maashi, M, Salama, SA, Hilal, MA, Alsaid, MI, Osman, AE, Alneil, AA (2023) Henry gas solubility optimization algorithm based feature extraction in dermoscopic images analysis of skin cancer. Cancers, 15(2146): 1-20. https://doi.org/10.3390/cancers15072146
141. Elden, RH, Ghonim, VF, Hadhoud, MM, Al-Atabany, W (2023) Transcriptomic marker screening for evaluating the mortality rate of pediatric sepsis based on Henry gas solubility optimization. Alexandria Engineering Journal, 68: 693-707. https://doi.org/10.1016/j.aej.2022.12.027
142. Gokiladevi, M., & Santhoshkumar, S. (2024). Henry Gas Optimization Algorithm with Deep Learning based Chronic Kidney Disease Detection and Classification Model. International Journal of Intelligent Engineering & Systems, 17(2). https://doi.org/10.22266/ijies2024.0430.52
143. Shehabeldeen, TA, Abd Elaziz, M, Elsheikh, AH, Hassan, OF, Yin, Y, Ji, X, Shen, X, Zhou, J (2020) A novel method for predicting tensile strength of friction stir welded AA6061 aluminium alloy joints based on hybrid random vector functional link and henry gas solubility optimization. IEEE Access, 8: 79896-79907. https://doi.org/10.1109/ACCESS.2020.2990137

144. Safeen, W, Hussain, S, Wasim, A, Jahanzaib, M, Aziz, H, Abdalla, H (2016) Predicting the tensile strength, impact toughness, and hardness of friction stir-welded AA6061-T6 using response surface methodology. The International Journal of Advanced Manufacturing Technology, 87(5-8): 1765-1781
145. Li, H, Gou, L, Chen, Y, Li, H (2022) Fault diagnosis of aeroengine control system sensor based on optimized and fused multidomain feature. IEEE Access, 10: 96967-96983. https://doi.org/10.1109/ACCESS.2022.3205105
146. Mishra, RK, Choudhary, A, Mohanty, AR, Fatima, S (2022) An intelligent bearing fault diagnosis based on hybrid signal processing and Henry gas solubility optimization. Proceedings of the Institution of Mechanical Engineers, Part C: Journal of Mechanical Engineering Science, 236(19): 10378-10391. https://doi.org/10.1177/09544062221101737
147. Ding, W, Nguyen, MD, Mohammed, AS, Armaghani, DJ, Hasanipanah, M, Van Bui, L, Pham, BT (2021) A new development of ANFIS-Based Henry gas solubility optimization technique for prediction of soil shear strength. Transportation Geotechnics, 29: 100579. https://doi.org/10.1016/j.trgeo.2021.100579
148. Nguyen, QH, Chou, TY, Yeh, ML, Hoang, TV, Nguyen, HD, Bui, QT (2021) Henry's gas solubility optimization algorithm in formulating deep neural network for landslide susceptibility assessment in mountainous areas. Environmental Earth Sciences, 80(11): 414. https://doi.org/10.1007/s12665-021-09711-6
149. Mahdavi-Meymand, A, Zounemat-Kermani, M, Qaderi, K (2021) Prediction of hydro-suction dredging depth using data-driven methods. Frontiers of Structural and Civil Engineering, 15(3): 652-664. https://doi.org/10.1007/s11709-021-0719-7
150. Javadi, F, Qaderi, K, Ahmadi, MM, Rahimpour, M, Madadi, MR, Mahdavi-Meymand, A (2022) Application of classical and novel integrated machine learning models to predict sediment discharge during free-flow flushing. Scientific Reports, 12(1): 19390. https://doi.org/10.1038/s41598-022-23781-x
151. Chen, L, Liu, F, Wu, F (2022) Novel hybrid HGSO optimized supervised machine learning approaches to predict the compressive strength of admixed concrete containing fly ash and micro-silica. Engineering Research Express, 4(2): 025022. https://doi.org/10.1088/2631-8695/ac6d49
152. Almustafa, MK, Nehdi, ML (2022) Novel hybrid machine learning approach for predicting structural response of RC beams under blast loading. Structures, 39: 1092-1106. https://doi.org/10.1016/j.istruc.2022.04.007
153. Kumar, S, Robinson, S (2023) Estimating the pile settlement using a machine learning technique optimized by Henry's gas solubility optimization and particle swarm optimization. Advances in Engineering and Intelligence Systems, 1(04). https://doi.org/10.22034/AEIS.2022.368689.1051

154. Esmaeili-Falak, M, Sarkhani Benemaran, R (2024) Application of optimization-based regression analysis for evaluation of frost durability of recycled aggregate concrete. Structural Concrete, 25(1), 716-737. https://doi.org/10.1002/suco.202300566
155. Wu, C, Yang, L (2023) Estimation of the improved high-performance concrete's mechanical characteristics using unique regression methods. Journal of Intelligent & Fuzzy Systems, 44(4) 5759-5772. https://doi.org/10.3233/JIFS-222348
156. Li, H. (2023) Prediction of high-performance concrete compressive strength through novel structured neural network. Journal of Intelligent & Fuzzy Systems, 45(1), 1791-1803. https://doi.org/10.3233/JIFS-221342
157. Li, W, Wang, R, Ai, Q, Liu, Q, Lu, SX (2023) Estimation of compressive strength and slump of HPC concrete using neural network coupling with metaheuristic algorithms. Journal of Intelligent & Fuzzy Systems, 45(1), 577-591. https://doi.org/10.3233/JIFS-23000
158. Abbaszadeh, M, Ehteram, M, Ahmed, AN, Singh, VP, Elshafie, A (2021) The copper grade estimation of porphyry deposits using machine learning algorithms and Henry gas solubility optimization. Earth Science Informatics, 14: 2049-2075. https://doi.org/10.1007/s12145-021-00667-6
159. Ye, J, He, X (2023) A novel hybrid of ANFIS-based models using optimisation approaches to predict mine blast-induced flyrock. International Journal of Environmental Science and Technology, 20(4): 3673-3686. https://doi.org/10.1007/s13762-022-04170-3
160. Mousakazemi, SMH (2022) Henry gas solubility optimization for control of a nuclear reactor: a case study. Nuclear Engineering and Technology, 54(3): 940-947. https://doi.org/10.1016/j.net.2021.09.029
161. Mousakazemi, SMH (2023) A meta-heuristic algorithm based on Henry's law for the load-following of a two-point PWR model. Progress in Nuclear Energy, 155: 104520. https://doi.org/ 10.1016/j.pnucene.2022.104520
162. Escorcia-Gutierrez, J, Torres-Torres, M, Madera, N, Soto, C (2023) Henry gas solubility optimization with deep learning enabled traffic flow forecasting in 6G enabled vehicular networks. AI-Enabled 6G Networks and Applications, 35-53. https://doi.org/10.1002/9781119812722.ch3
163. Agarwal, R, Shekhawat, NS (2022) Enhanced bag of features using AlexNet and Henry gas solubility optimization for soil image classification. In Proceedings of International Conference on Data Science and Applications: ICDSA 2021, 2:493-503. Springer Singapore. https://doi.org/10.1007/978-981-16-5348-3_39
164. Ehteram, M, Seifi, A, Banadkooki, FB (2022) Predicting rainfall using inclusive multiple model and radial basis function neural network. In Hellenic Conference on Artificial Intelligence (101-115). Singapore: Springer Nature Singapore. https://doi.org/10.1007/978-981-19-9733-4_12

165. Ehteram, M, Seifi, A, Banadkooki, FB (2023) Predicting solar radiation using optimized generalized regression neural network. In Application of Machine Learning Models in Agricultural and Meteorological Sciences (163-174). Singapore: Springer Nature Singapore. https://doi.org/10.1007/978-981-19-9733-4_16
166. Jaganathan, T, Panneerselvam, A, Kumaraswamy, SK (2022) Object detection and multi-object tracking based on optimized deep convolutional neural network and unscented Kalman filtering. Concurrency and Computation: Practice and Experience, 34(25): e7245. https://doi.org/10.1002/cpe.7245
167. Wolpert, D, Macready, W (1997) No free lunch theorems for optimization. IEEE Transactions on Evolutionary Computation, 1(1): 67-82
168. Zamani, H., Nadimi-Shahraki, M. H., Mirjalili, S., Soleimanian Gharehchopogh, F., & Oliva, D. (2024). A critical review of moth-flame optimization algorithm and its variants: structural reviewing, performance evaluation, and statistical analysis. Archives of Computational Methods in Engineering, 1-49. doi:10.1007/s11831-023-10037-8
169. Deep K, Thakur M (2007) A new mutation operator for real coded genetic algorithms. Appl Math Comput 193:211-230. https://doi.org/10.1016/j.amc.2007.03.046
170. Gupta S, Deep K (2019) A novel random walk grey wolf optimizer. Swarm Evol Comput 44:101-112. https://doi.org/10.1016/j.swevo.2018.01.001
171. Liang, JJ, Qin, AK, Suganthan, PN, Baskar, S (2006) Comprehensive learning particle swarm optimizer for global optimization of multimodal functions, in IEEE Transactions on Evolutionary Computation, 10(3): 281-295, https://doi: 10.1109/TEVC.2005.857610
172. Wen, L, Wu, T, Tang, M, Xu, M, Cai, S (2020) Gray wolf optimization algorithm based on lens imaging learning strategy. Acta Automatica Sinica, 46(10): 2148-2164
173. Ouyang, C, Qiu, Y, Zhu, D (2021) Adaptive spiral flying sparrow search algorithm. Scientific Programming, 2021: 1-16. https://doi.org/10.1155/2021/6505253
174. Ouyang, C, Zhu, D, Qiu, Y (2021) Lens learning sparrow search algorithm. Mathematical Problems in Engineering, 2021: 1-17. https://doi.org/10.1155/2021/9935090
175. Lim, WH, Isa, NAM (2014) An adaptive two-layer particle swarm optimization with elitist learning strategy. Information Sciences, 273: 49-72. https://doi.org/10.1016/j.ins.2014.03.031
176. Saadi, AA, Taleb, SM, Yahia, S, Dogan, M, Yasin, ET, Meraihi, Y, Koklu, M, Mirjalili, S, Ramdane Cherif, A (2026) A Comprehensive Survey of Henry Gas Solubility Optimization Algorithm with its Theory, Variants, and Applications. *Arch Computat Methods Eng* **33**, 81–138. https://doi.org/10.1007/s11831-025-10304-w
177. El-Shorbagy MA, Bouaouda A, Nabwey HA, Abualigah L, Hashim FA (2024) Advances in henry gas solubility optimiza tion: a physics-inspired metaheuristic algorithm with its variants and applications. IEEE Access 12:26062–26095 115. https://doi.org/10.1109/ACCESS.2024.3365700.

178. Abualigah L, Al-Hilo G, Raza A, Ezugwu AE, Al Nasar MR, Mughaid A, AlZubi S, Aldiabat K, Al-diabat M (2024) A review of henry gas solubility optimization algorithm: a robust optimizer and applications. Metaheuristic Optim Algorithms. Elsevier, Amsterdam, pp 177–192. https://doi.org/10.1016/B978-0-443-13925-3.00013-3.